Synthesis and Characterization of Pyridine and Quinoline Derivatives for Non-linear Optics Applications

Pumsak Ruanwas

A Thesis Submitted in Partial Fulfillment of the Requirements for the Degree of
Master of Science in Inorganic Chemistry
Prince of Songkla University
2008

Thesis Title	Synthesis and Characterization of Pyridine and Quinoline Derivatives for Non-linear Optics Applications
Author	Mr. Pumsak Ruanwas
Major Program	Inorganic Chemistry

Major Advisor:

……
(Assoc. Prof. Dr. Suchada Chantrapromma)

Co-Advisor:

…….....
(Assoc. Prof. Dr. Chatchanok Karalai)

Examining Committee :

……
(Prof. Dr. Supot Hannongbua)

……
(Assoc. Prof. Dr. Suchada Chantrapromma)

…….....
(Assoc. Prof. Dr. Chatchanok Karalai)

…….....
(Dr. Paradorn Pakdeevanich)

The Graduate School, Prince of Songkla University, has approved this thesis as partial fulfillment of the requirements for the Master of Science Degree in Inorganic Chemistry

……..
(Assoc. Prof. Dr. Krerkchai Thongnoo)
Dean of Graduate School

ชื่อวิทยานิพนธ์	การสังเคราะห์และหาโครงสร้างสารอนุพันธ์ของ pyridine และ quinoline เพื่อประยุกต์ใช้ด้านวัสดุทางทัศนศาสตร์
ผู้เขียน	นายภูมิศักดิ์ เรือนวาส
สาขาวิชา	เคมีอนินทรีย์
ปีการศึกษา	2551

บทคัดย่อ

การสังเคราะห์สารอนุพันธ์ของ pyridine **(PM-C1Me PM-C1OMe PM-C1Cl** และ **PM-C1Br)** และสารอนุพันธ์ของ quinoline **(PM-C2Me PM-C2OMe PM-C2Cl PM-C2Br PM-C3Zn PM-C4Zn PM-C5Zn** และ **PM-C6Zn)** 12 ชนิด เพื่อหาสารที่มีสมบัติทาง ทัศนศาสตร์แบบไม่เชิงเส้น การหาโครงสร้างสารประกอบที่สังเคราะห์ได้ใช้เทคนิคทางสเปกโทรสโกปีและสารประกอบ **PM-C1Me PM-C1Cl PM-C2Cl** และ **PM-C3Zn** สามารถหาโครงสร้างได้จากเทคนิคการเลี้ยวเบนของรังสีเอ็กซ์บนผลึกเดี่ยวอีกด้วย พบว่าโครงสร้างของสารประกอบ **PM-C1Me PM-C1Cl** และ **PM-C3Zn** ตกผลึกในหมู่ปริภูมิที่มีจุดศูนย์กลางสมมาตร (centrosymmetric) ในขณะที่สารประกอบ **PM-C2Cl** ตกผลึกในหมู่ปริภูมิที่ไม่มีจุดศูนย์กลางสมมาตร (non-centrosymmetric space group) และโครงสร้างโมเลกุลของแคตไอออนของ **PM-C2Cl** มีลักษณะแบนราบซึ่งส่งผลให้การถ่ายเทของ π อิเล็กตรอนเกิดได้ดีจึงทำให้สภาพความเป็นขั้วของโมเลกุลมีค่ามากขึ้น ในขณะที่โครงสร้างโมเลกุลของแคตไอออนของ **PM-C1Me PM-C1Cl** และ **PM-C3Zn** มีลักษณะไม่แบนราบทำให้การถ่ายเทของ π อิเล็กตรอนเกิดได้ดีไม่เท่ากับเมื่อมีลักษณะแบนราบส่งผลให้สภาพความเป็นขั้วของโมเลกุลมีค่าน้อยกว่า ซึ่งผลดังกล่าวอาจส่งผลให้สารประกอบ **PM-C2Cl** แสดงสมบัติทางทัศนศาสตร์แบบไม่เชิงเส้นอันดับสอง (second-order nonlinear optical properties) ในขณะที่ **PM-C1Me PM-C1Cl** และ **PM-C3Zn** ไม่แสดงสมบัติทางทัศนศาสตร์แบบไม่เชิงเส้นอันดับสอง

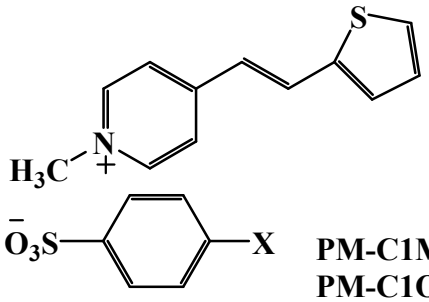

PM-C1Me : X = CH_3
PM-C1OMe : X = OCH_3
PM-C1Cl : X = Cl
PM-C1Br : X = Br

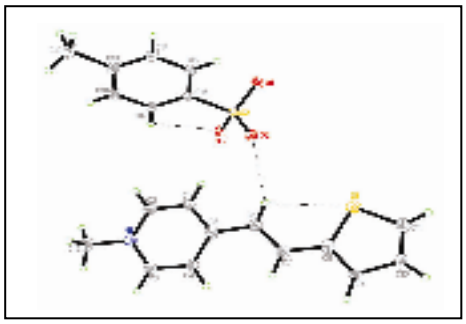

PM-C1Me

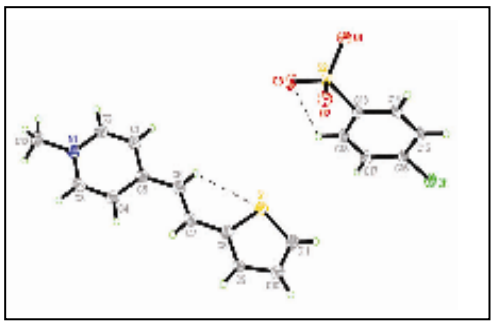

PM-C1Cl

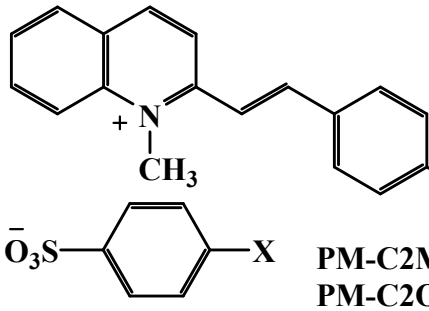

PM-C2Me : X = CH_3
PM-C2OMe : X = OCH_3
PM-C2Cl : X = Cl
PM-C2Br : X = Br

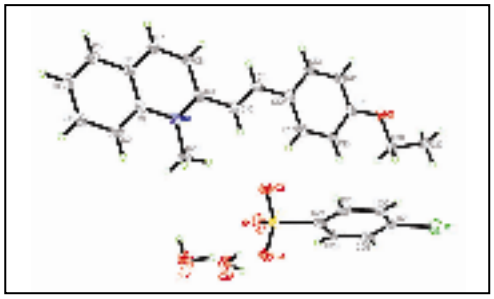

PM-C2Cl

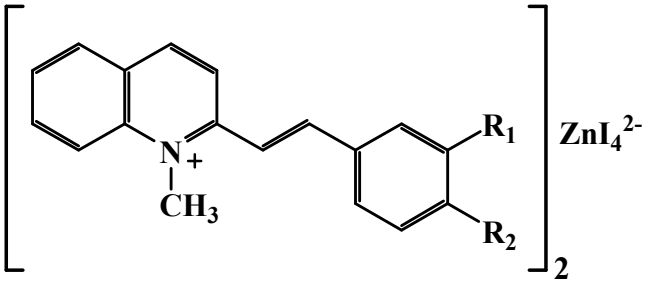

PM-C3Zn:R1 = OH **R2 = OCH_3**
PM-C4Zn:R1 = OCH_3 **R2 = OH**
PM-C5Zn:R1 = H **R2 = OH**
PM-C6Zn:R1 = H **R2 = OCH_3**

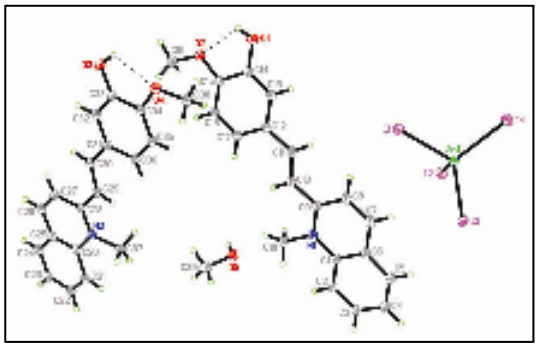

PM-C3Zn

Thesis Title	Synthesis and Characterization of Pyridine and Quinoline Derivatives for Non-linear Optics Applications
Author	Mr. Pumsak Ruanwas
Major Program	Inorganic Chemistry
Academic Year	2551

Abstract

The twelve derivatives of pyridine **(PM-C1Me, PM-C1OMe, PM-C1Cl** and **PM-C1Br)** and quinoline **(PM-C2Me, PM-C2OMe, PM-C2Cl, PM-C2Br, PM-C3Zn, PM-C4Zn, PM-C5Zn** and **PM-C6Zn)** were synthesized, aimed to search for nonlinear optical materials. All synthetic compounds were characterized by spectroscopic techniques. Compounds **PM-C1Me, PM-C1Cl, PM-C2Cl** and **PM-C3Zn** were also determined by the single crystal X-ray crystallography. Compounds **PM-C1Me, PM-C1Cl** and **PM-C3Zn** crystallized out in the centrosymmetric space group whereas compound **PM-C2Cl** crystallized out in the non-centrosymmetric space group. Moreover, in the molecular structure of **PM-C2Cl**, the cation is essentially planar therefore π electron can be better delocalized compare to the non-planar structures of the cations in **PM-C1Me, PM-C1Cl** and **PM-C3Zn**. These effects may contribute to the second-harmonic generation (SHG) property of the compound **PM-C2Cl** whereas compounds **PM-C1Me, PM-C1Cl** and **PM-C3Zn** do not exhibit the SHG properties.

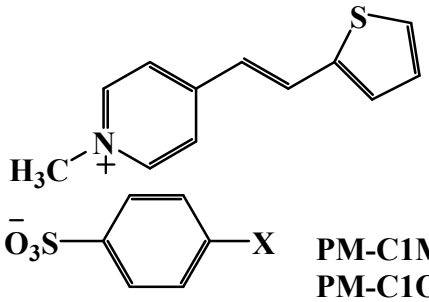

PM-C1Me : X = CH_3
PM-C1OMe : X = OCH_3
PM-C1Cl : X = Cl
PM-C1Br : X = Br

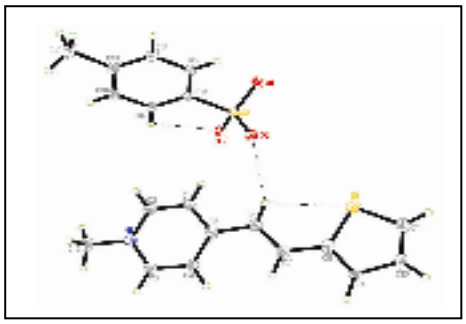

PM-C1Me

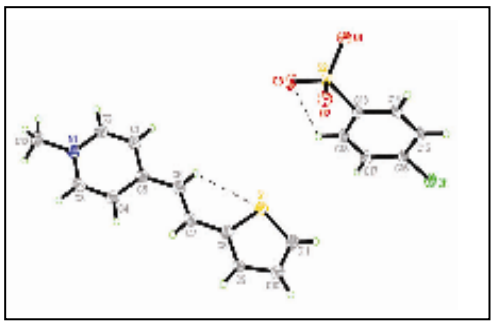

PM-C1Cl

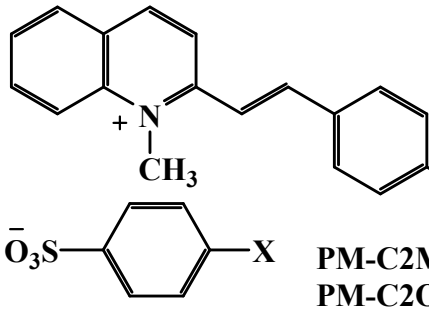

PM-C2Me : X = CH_3
PM-C2OMe : X = OCH_3
PM-C2Cl : X = Cl
PM-C2Br : X = Br

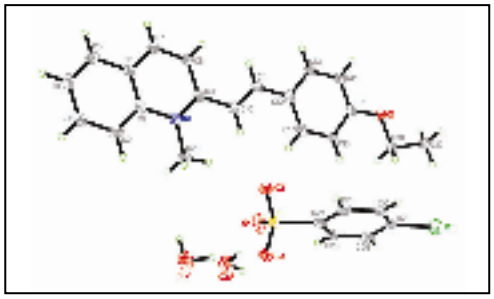

PM-C2Cl

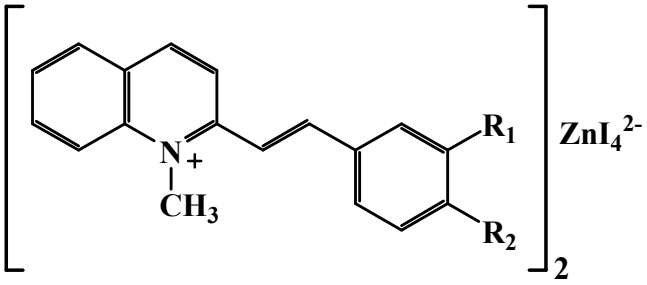

PM-C3Zn:R1 = OH **R2 = OCH_3**
PM-C4Zn:R1 = OCH_3 **R2 = OH**
PM-C5Zn:R1 = H **R2 = OH**
PM-C6Zn:R1 = H **R2 = OCH_3**

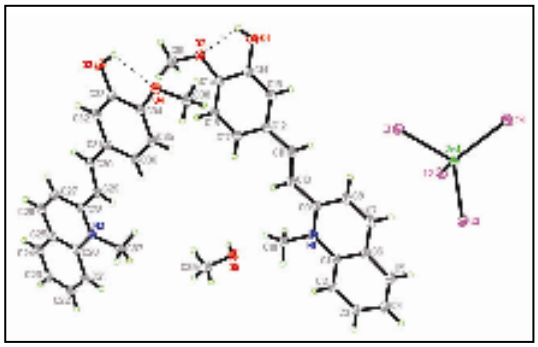

PM-C3Zn

ACKNOWLEDGEMENT

I wish to express my deepest and sincere gratitude to my supervisor, Associate Professor Dr. Suchada Chantrapromma, for her valuable instructions, expert guidance, excellent suggestions and kindness.

My sincere thank is expressed to Associate Professor Dr. Chatchanok Karalai my co-advisor for his kind help and suggestions. Special thanks are addressed to Professor Dr. Hoong-Kun Fun, X-ray Crystallography Unit, School of Physics, Universiti Sains Malaysia, Malaysia for X-ray data collections. I also would like to thank Professor Dr. Supot Hannongbua, Department of Chemistry, Faculty of Science, Chulalongkorn University and Dr. Paradorn Pakdeevanich, Department of Physics, Faculty of Science, Prince of Songkla University for the valuable suggestions.

Appreciately thank to Center of Excellence for Innovation in Chemistry (PERCH-CIC) funded by Commission on Higher Education, Ministry of Education and Prince of Songkla University through Crystal Materials Research Unit (CMRU) and Graduate School for financial supports.

I also would like to thank Department of Chemistry for making available the facilities used in this research. Dr. Yaowapa Sukpondma is highly acknowledged for recording NMR spectral data

I am very grateful to M.Sc and Ph.D students, Crystal Materials Research Unit (CMRU) for their kind help and assistance during my study and research activities. Finally, none of this would have been possible without love and encouragement of my family.

Pumsak Ruanwas

THE RELEVANCE OF THE RESEARCH WORK TO THAILAND

The relevance of this research are listed below:-

1) Twelve new compounds with four pyridinium derivatives and eight quinolinium derivatives were successfully synthesized.

2) Four single crystals of 4-[(*E*)-2-(2-Thienyl)ethenyl]-1-methylpyridinium 4-methylbenzenesulfonate **(PM-C1Me)**,

4-[(*E*)-2-(2-Thienyl)ethenyl]-1-methylpyridinium 4-chlorobenzenesulfonate **(PM-C1Cl)**,

2-[(*E*)-2-(4-Ethoxyphenyl)ethenyl]-1-methylquinolinium 4-cholrobenzene-sulfonate **(PM-C2Cl)** and

Bis[(*E*)-2-(3-hydroxy-4-methoxyphenyl)ethenyl]-1-methylquinolinium tetraiodidozincate(II) **(PM-C3Zn)** were successfully growth and determined their structures by single crystal X-ray structure determinations.

3) It was found that **PM-C1Me**, **PM-C1Cl** and **PM-C3Zn** crystallized out in centrosymmetric space group whereas compounds **PM-C2Cl** crystallized out in non-centrosymmetric space group and exhibit nonlinear optical (NLO) properties.

CONTENTS

CONTENTS (Continued)

CONTENTS (Continued)

CONTENTS (Continued)

CONTENTS (Continued)

LIST OF TABLES

LIST OF TABLES (Continued)

LIST OF ILLUSTRATIONS

LIST OF ILLUSTRATIONS (Continued)

LIST OF ILLUSTRATIONS (Continued)

ABBREVIATIONS AND SYMBOLS

s	=	singlet
d	=	doublet
t	=	triplet
q	=	quartet
m	=	multiplet
dd	=	doublet of doublet
dt	=	doublet of triplet
br d	=	broad doublet
g	=	gram
nm	=	nanometer
ml	=	milliliter
mp.	=	melting point
cm^{-1}	=	reciprocal centimeter (wave number)
δ	=	chemical shift relative to TMS
J	=	coupling constant
λ_{max}	=	maximum wavelength
ν	=	absorption frequencies
ε	=	molar extinction frequencies
°C	=	degree celcius
MHz	=	Megahertz
Hz	=	Hertz
ppm	=	part per million
NLO	=	Nonlinear optics
SHG	=	Second Harmonic Generation
HRS	=	hyper-Rayleigh scattering
ICT	=	intramolecular charge-transfer
Å	=	Angstrom
hr	=	hour
*p*NA	=	*p*-nitroaniline

ABBREVIATIONS AND SYMBOLS (Continued)

KDP	=	potassium dihydrogenphosphate
POM	=	3-methyl 4-nitropyridine 1-oxide
DAST	=	1-methyl-4-(2-(4-(dimethylamino)phenyl)ethenyl) pyridinium *p*-toluenesulfonate
MBST	=	4-methoxybenzaldehyde-*N*-methyl-4-stilbazolium tosylate
HBST	=	4-hydroxybenzaldehyde-*N*-methyl-4-stilbazolium tosylate
HOST	=	(*N*-(4-hydroxyphenyl)ethenyl)pyridinium *p*-toluenesulfonate
DANS	=	4-(*N*,*N*-dimethylamino)-4′-nitrostilbene
DMAEPI	=	4-(dimethylamino)-1-ethylpyridinium iodide
EFISHG	=	Electric Field Induced Second Harmonic Generation
XRD	=	X-ray diffraction
Fig.	=	Figure
IR	=	Infrared
UV-Vis	=	Ultraviolet-Visible
NMR	=	Nuclear magnetic resonance
TMS	=	tetramethylsilane
$CDCl_3$	=	deuterochloroform
DMSO-d_6	=	hexadeutero-dimethyl sulphoxide

CHAPTER 1
INTRODUCTION

1.1 Non-linear optics

Nonlinear optics is a studied that deals mainly with various new optical effects and novel phenomena arising from the interactions of intense coherent optical radiation with mater. In the first nonlinear-optical experiment of the laser era, performed by Franken *et al.* in 1961 (Franken, 1961), a ruby laser radiation with a wavelength of 694.2 nm was used to generate the second harmonic in a quartz crystal at the wavelength of 347.1 nm. This seminal work was followed by the discovery of a rich diversity of nonlinear-optical effects, including sum-frequency generation, stimulated Raman scattering, self-focusing, optical rectification, four-wavemixing, andmany others. While in the pioneering work by Franken the efficiency of second-harmonic generation (SHG) was on the order of 10^{-8}, optical frequency doublers created by early 1963 provided 20%–30% efficiency of frequency conversion (Terhune, 1963). Interest in this field has grown continuously since it has significant impact on optical storage technology and integrated optics technology (Bass, 1962 and Williams, 1984).

Non-linear optics (NLO) is concerned with the interaction of electromagnetic fields (light) in various media to produce new fields altered in phase, frequency, amplitude or other propagation characteristics from the incident fields. The media in which these effects occur are becoming the subject of intense interest, due to their complement properties, such as stability, ease of preparation, compatibility with microelectronic processing methods, mechanical and other properties, as well as their nonlinear optical properties will extremely determine the technological utility of the effect (Williams, 1984). A major advantage of the use of photonics instead of electronics is the possibility to increase the speed of information processes such as photonic switching and optical computing. Typically, only laser light is sufficiently intense to modify the optical properties of a material system. One of the most intensively studied nonlinear optical phenomena is SHG, in which incident light at one

frequency (ω) is converted into light at twice that frequency (2ω). The resulting wavelength is half the incident wavelength and hence it is possible to store information with a higher density. Second-order NLO properties can only be observed in materials lacking a center of symmetry since the second-order NLO coefficient is a third-order tensor which in centrosymmetric system all the tensor components equal zero. So, an important point in designing new organic materials for SHG is to introduce non-centrosymmetry in crystal structures. Electro-optic modulators have traditionally employed ferroelectric inorganic crystals, such as lithium niobate ($LiNbO_3$) or potassium dihydrogenphosphate (KDP), which are formed at high temperatures. However, organic NLO materials offer better several advantages in performance, such as higher nonlinear susceptibilities, higher modulation rates, ultrafast response times, lower dielectric constants, better processability characteristics and a remarkable resistance to optical damage, when compared to the inorganic materials (Nie, 1993). The theory of nonlinear optics has been described thoroughly by Chemla and Zyss (Chemla and Zyss, 1987) and by Williams (Williams, 1984) and will be shortly summarized.

1.1.1 Theory of nonlinear optics

A number of nonlinear optical phenomena can be described as frequency-mixing processes. If the induced dipole moments of the material respond instantaneously to an applied electric field, the dielectric polarization (dipole moment per unit volume) $P(t)$ at time t in a medium can be written as a power series in the electrical field:

$$P(t) \propto \chi^{(1)} E(t) + \chi^{(2)} E^2(t) + \chi^{(3)} E^3(t) + \ldots. \qquad (1.1)$$

Here, the coefficients $\chi^{(n)}$ are the n-th order susceptibilities of the medium. For any three-wave mixing process, the second-order term is crucial; it is only nonzero in media that have no inversion symmetry. If we write

$$E(t) = E_1 e^{i\omega_1 t} + E_1 e^{i\omega_2 t} + \text{c.c.}, \qquad (1.2)$$

where c.c. denotes the complex conjugate (E_1 and E_2 being the incident beams of interest), the second-order term in the above expansion will write

$$P^{(2)}(t) \propto \Sigma\, \chi^{(2)} n_0 E_1^{n_1} E_2^{n_2} e^{i(m1\omega 1 + m2\omega 2)t} + \text{c.c.}, \tag{1.3}$$

where the summation is over

$$(n_0, n_1, n_2, m_1, m_2) = (1, 2, 0, 2, 0), (1, 0, 2, 0, 2), (2, 2, 0, 0, 0), (2, 0, 2, 0, 0), (2, 1, 1, 1, -1), (2, 1, 1, 1, 1) \tag{1.4}$$

.

The six combinations (n_x,m_x) correspond, respectively, to the second harmonic of E_1, the second harmonic of E_2, the optically rectified signals of E_1 and E_2, the difference frequency, and the sum frequency. A medium that is thus pumped by the fields E_1 and E_2 will radiate a field E_3 with an angular frequency $\omega_3 = m_1\omega_1 + m_2\omega_2$.

Note: in this description, $\chi^{(2)}$ is a scalar. In reality, $\chi^{(2)}$ is a tensor whose components depend on the combination of frequencies.

1.1.2 Second-Order Nonlinear Optical Properties

In second-harmonic generation, a pump wave with a frequency of ω generates a signal at the frequency 2ω as it propagates through a medium with a quadratic nonlinearity (**Fig. 1a**). Since all even-order nonlinear susceptibilities $\chi^{(n)}$ vanish in centrosymmetric media, SHG can occur only in media with no inversion symmetry. Two incident photons are converted into one emerging photon with exactly twice the energy (half wavelength). No excitation of molecules take place so all energy is conserved. Second harmonics can be generated by nonlinear optical materials with a non-centrocymmetric molecular organisation. SHG signals characterize by a given value of quadratic hyperpolarizability value β or of the second-order electrical susceptibility $\chi^{(2)}$, to produce a new wave with frequency 2ω as shown in **Fig. 1b**.

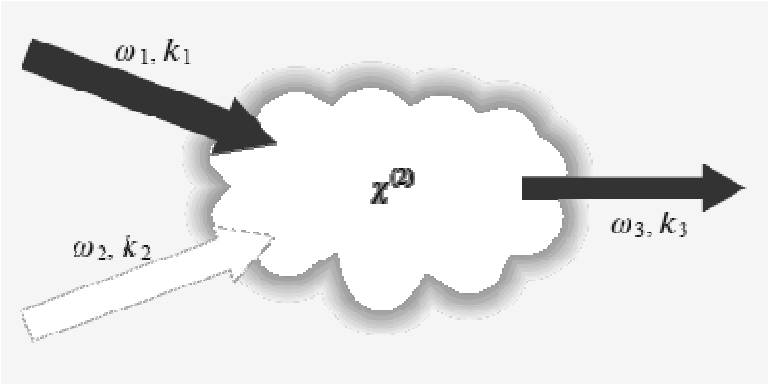

1a

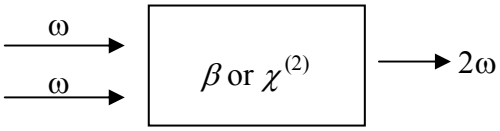

1b

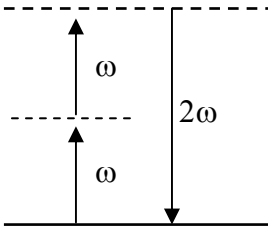

1c

Figure 1a Sum-frequency generation $\omega_1 + \omega_2 = \omega_3$ in a medium with a quadratic nonlinearity. The case of $\omega_1 = \omega_2$ corresponds to second-harmonic generation.

1b Second Harmonic Generation (SHG).

1c Energy-level diagram describing second-harmonic generation.

The SHG can also represent by considering the interaction of an electron in molecule and a photon from incoming light. This process visualized in Fig. 1b, an electron absorbs a photon from the incident light and makes a transition to the next higher unoccupied allowed state, then the excited electron absorbs another photon of the same frequency and makes a transition to yet another allowed state at higher energy. This electron when falling back to its original state emits a photon of a frequency which is two times that of the incident light. This results in the frequency doubling in the output.

The SHG of crystalline materials depends both on the magnitude of the molecular hyperpolarizability β (microscopic non-linearity) and on the orientation

of the molecules in the crystal lattice. In 1977, Oudar and Chemla (Oudar and Chemla, 1977) produced a theoretical interpretation of the electronic origin of β and providing a simple model for the design of second-order NLO molecular materials. NLO properties are concerned to the polarizability of the electrons with electric field E of the light, second-order NLO properties are dependent on electronic transition with high charge-transfer character. Oudar and Chemla assumed that in asymmetric 1D organic NLO chromophores the second-order NLO response is dominated mainly by one major charge-transfer process, so that it is possible to assume that:

$$\beta_{zzz} = \frac{3}{2h^2c^2} \frac{v_{eg}^2 r_{eg}^2 \Delta\mu_{eg}}{(v_{eg}^2 - v_L^2)(v_{eg}^2 - 4v_L^2)} \qquad (1.5)$$

This equation represents the so-called "two level" models, z is the direction of the charge-transfer, $v_{eg}(cm^{-1})$ the frequency of the charge-transfer transition, r_{eg} its transition dipole moment, $\Delta\mu_{eg}$ its difference between the excited state and ground state molecular dipole moment (μ_e-μ_g) and v_L is the frequency of the incident radiation.

For obtaining the materials with large macroscopic second-order NLO susceptibilities (χ^2), optimization of both the molecular first hyperpolarizabilities (β) and their orientation in the bulk are required. It must be non-centrosymmetric, according to the useful guideline of two-level model, should have a large difference in dipole moment of molecule between the ground state and excited state, large $\Delta\mu_{eg}$ and $v_{eg,}$ and a small band-gap energy (charge-transfer transitions). In synthesis, these can be achieved in a linear organic chromophore by attaching strong donor and acceptor group through a π-conjugated polarizable spacer and/or elongation of the π-conjugated electron system, as it occur in classical 1D organic dipolar so called push-pull system (**Fig. 2**).

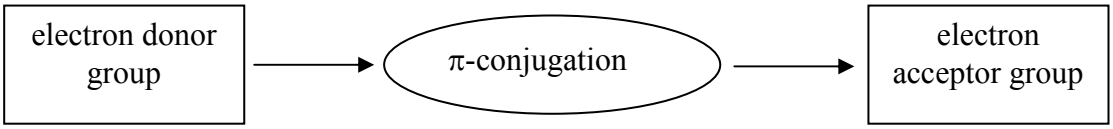

Figure 2 Scheme of a push-pull chromophore.

Nevertheless in such system, molecules with large ground-state dipoles tend to pack in an antiparallel (centric) manner due to intermolecular head-to-tail interactions. For this reason, much effort has been employed to overcome this problem such as the use of supramolecular strategies (Desiraju, 1995), co-crystallization or salt formation strategies (Duan, 2000), inclusion formation with inorganic zeolites strategies (Cox, 1988), etc.

1.1.3 Structural requirements

Organic molecules that exhibit second-order nonlinear optical properties usually consist of a frame with a delocalized π-system, end-capped with either a donor (D) or acceptor (A) substituent or both. This asymmetry results in a high degree of intramolecular charge-transfer (ICT) interaction from the donor to acceptor, which seems to be a prerequisite for a large second-order nonlinearity (Oudar and Chemla, 1977). Extensively studied classes of NLO-chromophores of this type are 1,4-disubstituted benzenes and stilbenes, from which *p*-nitroaniline (*p*NA) and 4-(*N*,*N*-dimethylamino)-4′-nitrostilbene (DANS) are prototypical examples (**Fig. 3**) (Levine, 1975):

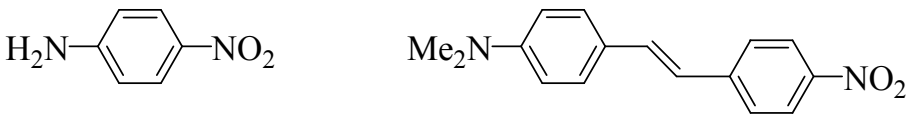

*p*NA DANS

Figure 3 Prototypical examples of nonlinear optical molecules.

The second-order nonlinearity can be enhanced by using stronger donor and acceptor substituents to increase the electronic asymmetry or by increasing

the conjugation length between the substituents. Dulcic and Sauteret (Dulcic and Sauteret, 1978) were the first group to study the substituent effect in *p*-disubstituted benzene derivatives and Oudar and Le Person reported about the effect of the conjugation length by using a stilbene instead of a benzene π-system (Oudar and Le Person,1975). The *p*,*p*-disubstituted molecules possessed largest β values are obtained when the molecule contains substituents that lead to low-lying charge-transfer resonance states (**Fig. 4**) (Williams, 1984).

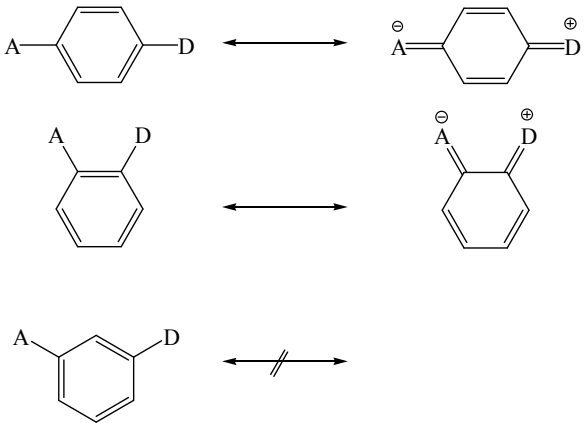

Figure 4 Ground-state and lowest energy polar resonance forms for *para*- and *ortho*-substitution. Resonance is forbidden in the case of *meta*-substitution.

The polarization occurred from contributions of the substituent-induced asymmetry of the π cloud and the σ skeleton of the molecule, as well as from field-induced mixing of the excited state (polar character) into the ground electronic configuration.

Organic crystals were the first bulk organic materials to be investigated for their nonlinear optical properties (Marder and Perry, 1993). About 75% of all organic molecules tend to crystallize in a centrosymmetric space group, which is a serious disadvantage of this approach. Meredith (Williams, 1984) first reported ionic organic NLO (**Fig. 5**).

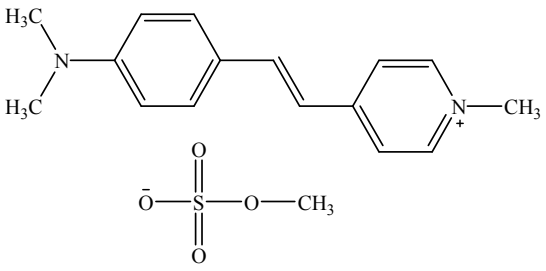

Figure 5 An ionic organic with high SHG efficiency.

This salt had SHG efficiency about 220 times that of urea. Crystallization of organic ionic salts is interesting because they exhibit large β values at molecular level, e.g., the β values of 4-(dimethylamino)pyridinium cation are about $35*10^{-30}$ esu, which is twice larger than that of *p*NA (Anwar, 1997). Moreover, crystals of hydroxyl-substituted stilbazoliums with *p*-toluenesulfonate, MC-PTS, (Okada, 1990) exhibit extremely large $\chi^{(2)}$ more than ten times of inorganic materials such as $LiNbO_3$. In addition, ionic organic NLO crystals possess high values for hardness and have high melting points. Their crystal structures can also be controlled by changing the counter-ions (Nogi, 2000). Benzenesulfonate is most frequently used to co-crystallize with cations to form compounds which are expected to have second-order nonlinear optical properties.

1.2 Nonlinear optic materials

In order to exhibit second-order nonlinearity, a bulk organic material has to possess a non-centrosymmetric alignment of the (di)polar molecules which it consists of. There are several ways to achieve a parallel orientation of NLO-chromophores; those most frequently used are:

(1) Non-centrosymmetric crystals;

(2) Langmuir-Blodgett films;

(3) Poled polymers.

In this study, only the non-centrosymmetric crystals used will be discussed.

Non-centrosymmetric crystals

Organic molecules containing conjugate systems are highly polar in their ground state, tend to set up antiparallel arrangements leading to centrosymmetric structure in the solid state which vanish all components of $\chi^{(2)}$, or although they achieve noncentrosymmetric structure, the orientation of their molecular dipole moments in the crystalline solid with respect to the polar crystal axes are not optimum for maximizing second-order NLO response (Anwar, 2000). Furthermore, it is difficult to direct the crystallization of an organic compound towards a crystal of the required size, processability, environmental stability and transparency for a typical application. Strategies to favour non-centrosymmetric crystallization are incorporation of chiral substituents in the molecular structure (Zyss *et al*., 1984), organic salts (Marder *et al*., 1989) or designing molecules with specific intermolecular interaction such as hydrogen bonding (Etter and Frankenbach, 1989).

1.3 Review of Literatures

Chou *et al*. (1996) studied, UV-VIS absorption spectrum, thermal stability and second-order nonlinear optical properties of a series of new thiophene-containing chromophores (**1-4**) with methylsulfonyl and phenylsulfonyl acceptors.

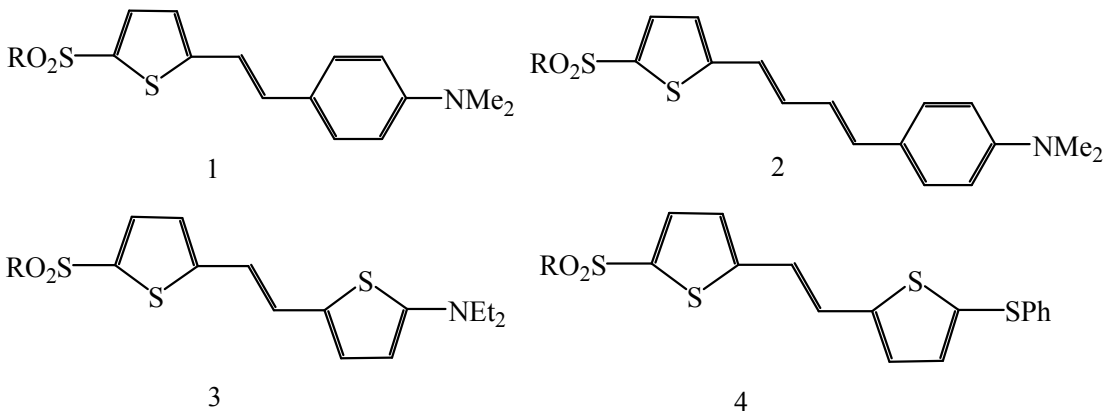

1-4 : a, R = CH_3;b, R = Ph

Anwar *et al*. (1997) studied second-order hyperpolarizability of pyridinium cations (**5, 6**).

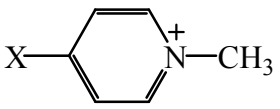

5

X = H, CH_3, C_2H_5, NH_2, $N(CH_3)_2$ $CONH_2$, $COOCH_3$, CN

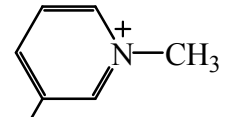

6

X = $CONH_2$, $COOCH_3$, Cl

Huang *et al.* (1997) synthesized phenol-pyridine and nitrophenol-pyridine co-crystals for second harmonic generation. Since organic molecules possess large β-values and usually accompanied by high molecular dipole moments, they tend to form pairs aligned in an anti-parallel fashion and thus tend to crystallize in centrosymmetric space groups. They proposed strategy employed to encourage non-centrosymmetric crystallization of these molecules by make use of ionic and hydrogen-bonding interaction in a system to form ionic co-crystals from proton transfer between organic acid and organic base, as illustrated in below equation.

$$\mathbf{A\text{-}H} + \mathbf{B} \xrightarrow{\text{co-crystallization}} \mathbf{A^-\cdots H\text{-}B^+}$$

A-H is organic acid; **B** is organic base and $\mathbf{A^-\cdots H\text{-}B^+}$ is the resulting ionic co-crystal, which involves in both ionic attractions and hydrogen-bonding interactions.

Anwar *et al.* (1998) studied hyperpolarizability of benzoate anions (**7a-j**) and ester (**8a-j**).

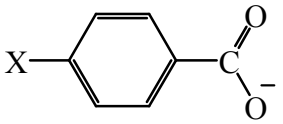

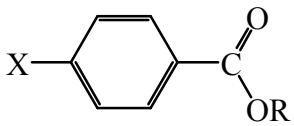

7a : X = $N(CH_3)_2$ **7b** : X = NH_2
7c : X = OH **7d** : X = OCH_3
7e : X = CH_3 **7f** : X = H
7g : X = Cl **7h** : X = Br
7i : X = CN **7j** : X = NO_2

8a : R = C_2H_5
8b-j : R = CH_3

Anwar *et al.* (1999) synthesized substituted pyridinium benzenesulfonate (**9a-h, 10f, 10g, 10i**) crystals for NLO properties.

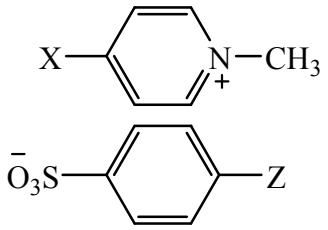

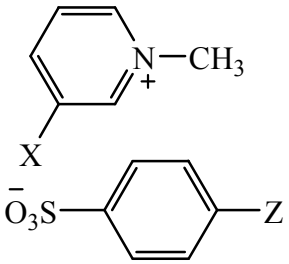

9a : X = H
9b : X = CH_3
9c : X = C_2H_5
9d : X = NH_2
9e : X = $N(CH_3)_2$
9f : X = $CONH_2$
9g : X = $COOCH_3$
9h : X = CN

10f : X = $CONH_2$
10g : X = $COOCH_3$
10i : X = Cl

Z = H, CH_3, OH, OCH_3, NH_2, $NHCOCH_3$, Cl, Br

Anwar *et al*. (1999) synthesized 4-carbamoylpyridinium benzene-sulfonate (**11**) salts for NLO properties.

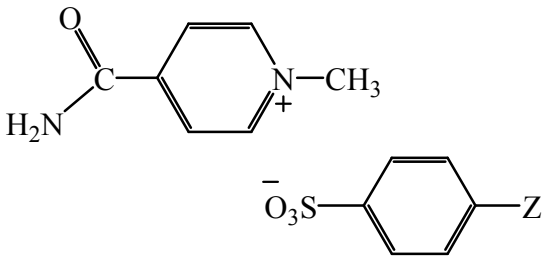

Z = OH, OCH_3, Br

11

Zelichenok *et al*. (1999) reported synthesis, characterization which used X-ray diffraction (XRD), NMR and FTIR, and optical spectroscopy measurements of derivatives of donor-acceptor substituted quinolinium iodide (**12**).

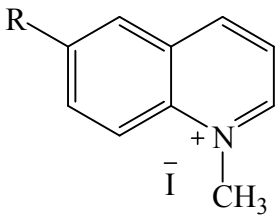

R = OCH_3, CH_3, H, Cl, NO_2

12

These quinolinium derivatives are transparency in the blue and this property is practical importance for NLO usage.

Anwar *et al*. (2000) synthesized 4-amino-1-methylpyridinium benzenesulfonate salts (**13**) for second-order NLO properties.

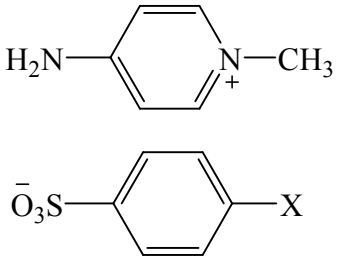

X = OH, OCH_3, CH_3, Cl, Br

13

Nogi *et al*. (2000) synthesized 1-methyl-4-(2-(4-(dimethlyamino) phenyl)ethenyl)pyridinium *p*-toluenesulfonate (DAST) analogues (**14**) with increased double bond number between pyridinium and (dimethylamino)phenyl ring.

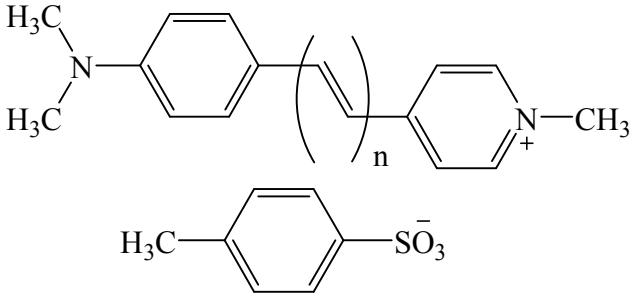

n = 1, 2, 3, 4, 5

14

Umezawa *et al.* (2000) synthesized compounds based on stilbazolium structure with extended π-conjugation by increasing conjugated double-bond number between two aromatic rings and/or using a fused ring system like naphthalene instead of phenylene for NLO materials.

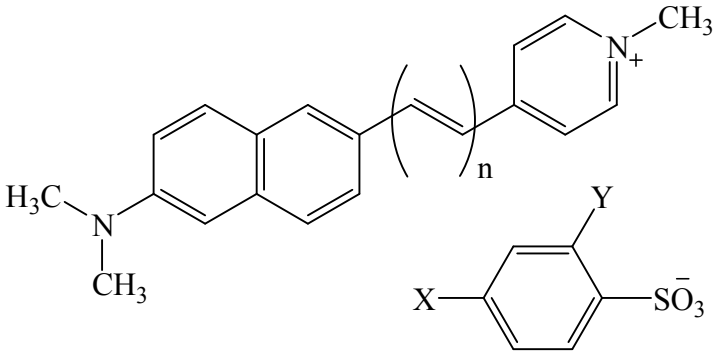

a : X = CH_3, Y = H
b : X = Cl, Y = H
c : X = NO_2, Y = H
d : X = NH_2, Y = H
e : X = Y = H
f : X = Y = NO_2

15a-f : n = 1
16a-f : n = 2

Anwar *et al*. (2001) synthesized 4-(dimethylamino)-1-ethylpyridinium iodide (DMAEPI) (**17**) for use in second-order NLO.

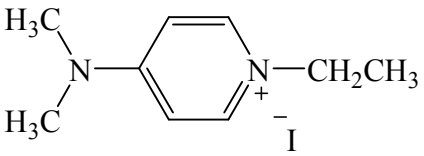

17

Bourgogne *et al.* (2001) reported the synthesis, modeling of μ and β, and hyper-Rayleigh scattering (HRS) hyperpolarizability measurements of 4′-nitro-4-stilbazole-*N*-oxide (**18**) and it azo analogue (**19**). These molecules present an intramolecular donor/acceptor charge transfer (ICT) leading to high β

hyperpolarizability, but its exhibit a vanishing dipole moment μ which was confirmed by Hartree-Fock calculations.

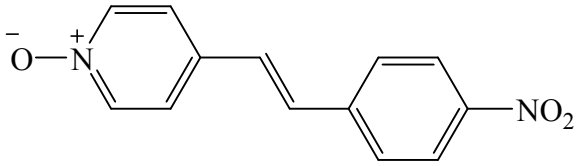

18

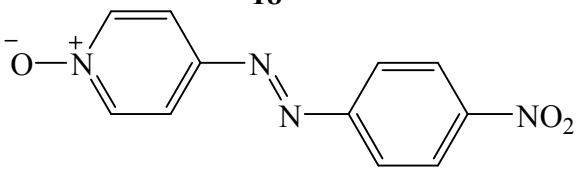

19

Lakshmanaperumal *et al.* (2002) synthesized a new organic nonlinear optical material of 4-methoxybenzaldehyde-*N*-methyl-4-stilbazolium tosylate (MBST) (**20**). Single crystals of MBST were grown by slow cooling solution growth technique. The growth crystals were characterized by IR, NMR and powder XRD techniques. The SHG studies were done with Kurtz powder technique.

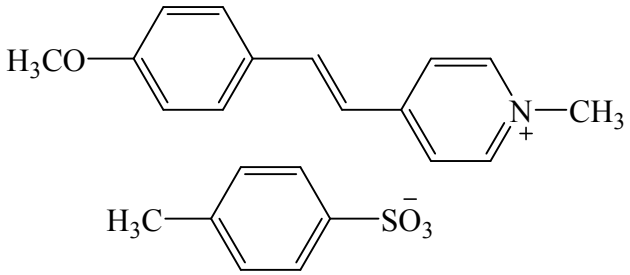

20

Boomadevi *et al.* (2004) grew organic NLO crystals of 3-methyl 4-nitropyridine 1-oxide (POM) (**21**). Growth technique used was the slow evaporation technique. Second harmonic generation was observed by using Q-switched Nd:YAG laser. Laser damage threshold value has been determined using Q-switched Nd:YAG laser. It was found to be 10.5 GW/cm^2 for single shot and 9.3 GW/cm^2 for multiple shots, indicating POM had potential for high power laser application.

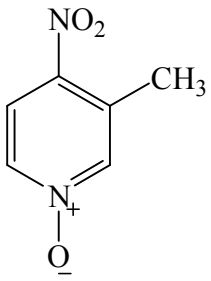

21

Crasta *et al*. (2004) synthesized new chalcone derivative, 1-(4-methyl-phenyl)-3-(4-methoxyphenyl)-2-propen-1-one (**22**). The crystal of chalcone derivative was grown with low temperature solution growth technique. These crystals were characterized using powder X-ray diffraction, FT-IR, UV-Vis and powder SHG studies.

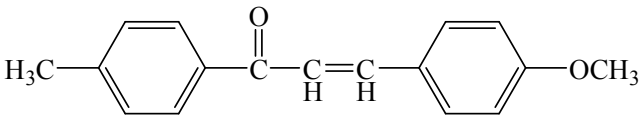

22

Glavcheva *et al*. (2004) synthesized pyridinium-metal iodide complexes (**23a-f, 24a-f and 25a-f**) for SHG materials.

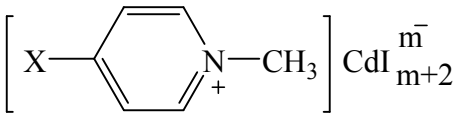

23a : m = 1
23b-f : m = 2

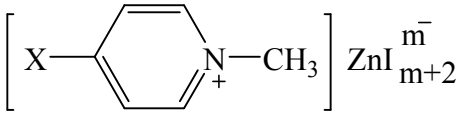

24a-f : m = 2

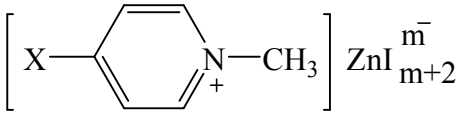

25a-f : m = 1

X = CH_3 X = NH_2
X = CN X = CO_2CH_3
X = $CONH_2$ X = $N(CH_3)_2$

Lakshmanaperumal *et al.* (2004) synthesized new NLO material of 4-hydroxy benzaldehyde-*N*-methyl-4-stilbazolium tosylate (HBST) (**26**). Single crystals of HBST were grown using solution growth technique. The growth crystals were characterized by UV-Vis, IR, NMR and powder XRD techniques. The SHG studies were done with Kurtz powder technique.

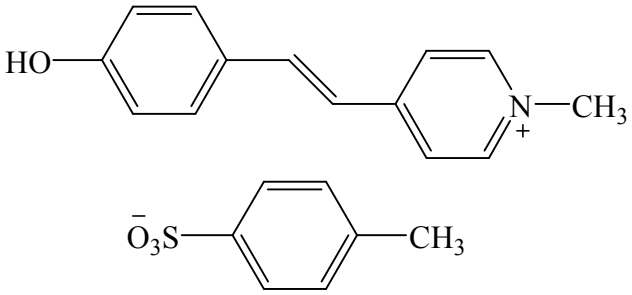

26

Crasta *et al*. (2005) synthesized new chalcone derivative, 1-(4-chloro-phenyl)-3-(4-chlorophenyl)-2-propen-1-one (**27**). The chalcone derivative was grown with low temperature solution growth technique. These crystals were characterized using single crystal X-ray diffraction (XRD), FT-IR, UV-Vis and powder SHG studies.

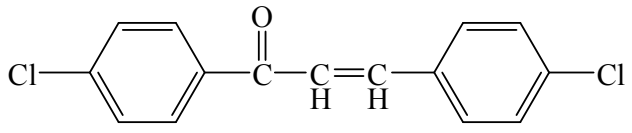

27

Chantrapromma *et al.* (2005) synthesized new NLO material of 2-[(*E*)-2-(3-Hydroxy-4-methoxyphenyl)ethenyl]-1-methyl-quinolinium 4-chloro-

benzenesulfonate (**28**). The SHG efficiency of the compound is about 0.85 times that of urea.

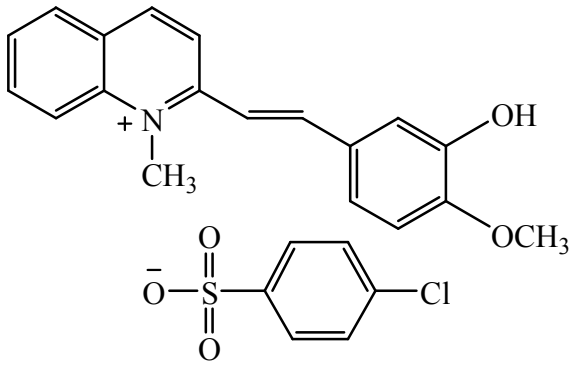

28

Chantrapromma *et al.* (2007) synthesized new NLO material of 2-[(*E*)-2-(4-Hydroxy-3-methoxyphenyl)ethenyl]-1-methyl-quinolinium 4-chloro-benzenesulfonate (**29**). The SHG efficiency of the compound is about 0.5 times that of urea.

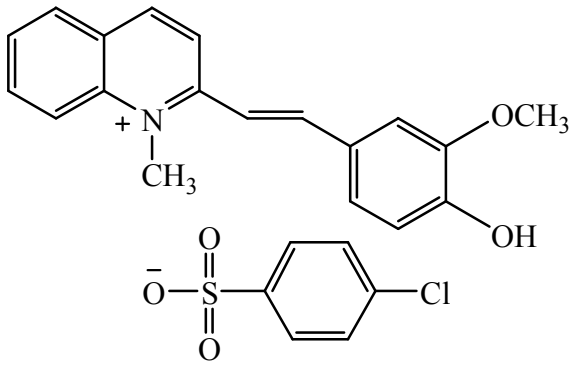

29

1.4 Objective and outline of this study

The objectives of this study are:

1. To synthesize pyridinium and quinolinium derivatives.
2. To determine the structure of pyridinium and quinolinium derivatives by spectroscopic techniques and X-ray diffraction method.

.

Much attention has been given to NLO materials because their promising applications including telecommunication, optical data storage and difference frequency doubling of lasers. In this thesis, the twelve novel compounds of pyridinium and quinolinium derivatives which are expected to exhibit NLO property were designed and synthesized. Their structures were elucidated by spectroscopy techniques. Single crystal X-ray structure determination was also be studied for those compounds which can be crystallized out in order to study for their structures, crystal packing and NLO properties.

The twelve compounds were designed base on introduction of an oxochromes, such as OH, OCH_3, OCH_2CH_3 in ring **B** or modification of ring **B** with thiophene ring or modification of ring **A** with quinolinium unit in the stilbazolium cation which was expected to increase π-conjugation system.

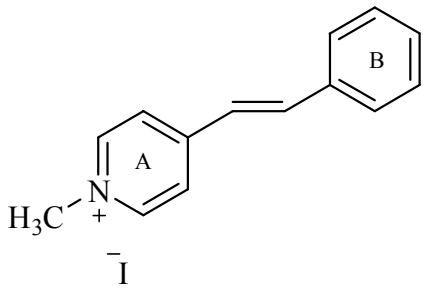

The synthesized compounds were shown in **Figure 6**.

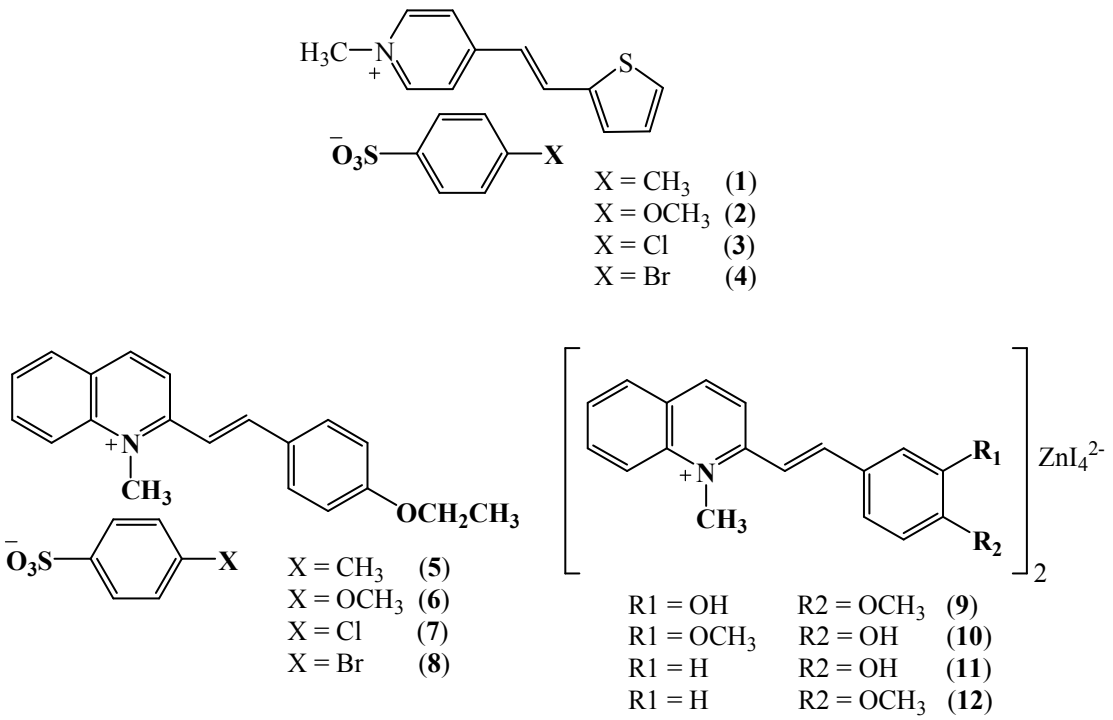

Figure 6 Derivatives of pyridinium and quinolinium.

In this study, focus shall be on the adducts of derivatives of pyridinium and quinolinium (**Fig. 6**) which are expected to exhibit the NLO property. Crystals of a size and quality suitable for single crystal X-ray diffraction studies are grown with the objective to study their structure in solid state.

This thesis is divided into four parts, namely introduction, experimental, results and discussion, and conclusion.

2. EXPERIMENT

2.1 Instruments and chemicals

2.1.1 Instruments

Melting point was recorded in °C and was measured using an Electrothermal melting point apparatus. Proton nuclear magnetic resonance spectra were recorded on FT-NMR Bruker Ultra Shield^{TM} 300 MHz. Spectra were recorded in deuterochloroform mixed with hexadeutero-dimethyl sulphoxide solution and were recorded as δ value in ppm downfield from TMS (internal standard δ 0.00). Infrared spectra were recorded by using FTS 165 FT-IR spectrophotometer. Major bands (ν) were recorded in wave numbers (cm^{-1}). Ultraviolet (UV) absorption spectra were recorded using a SPECORD S 100 (Analytikjena) and principle bands (λ_{max}) were recorded as wavelengths (nm) and log ε in methanol solution. Single crystal X-ray diffraction measurements were collected using a Bruker Apex2 CCD diffractometer with a graphite monochromated MoK_{∞} radiation. (λ = 0.71073 Å) at a detector distance of 5 cm and with APEX2 software. The collected data were reduced using *SAINT* (Bruker, 2005) program, and the empirical absorption corrections were performed using *SADABS* program. The structures were solved by direct methods and refined by least-squares using the *SHELXTL* (Sheldrick, 2008) software package. The SHG measurements were done at Department of studies in Physics, Mangalore University, Mangalagangotri, Mangalore, India. The yields were reported as percentage of crude products.

2.1.2 Chemicals

All chemicals used in this study are AR grade and were used without further purification.

1) 4-Picoline from Fluka Chemica, Switzerland
2) 2-Methylquinoline from Fluka Chemica, Switzerland
3) Piperidine from Fluka Chemica, Switzerland
4) Thiophene-2-carboxaldehyde from Fluka Chemica, Switzerland
5) 3-Hydroxy-4-methoxybenzaldehyde (isovanillin) from Sigma Chemica, USA
6) 4-Hydroxy-3-methoxybenzaldehyde (vanillin) from Sigma Chemica, USA
7) 4-Hydroxybenzaldehtde from Fluka Chemica, Switzerland
8) 4-Methoxybenzaldehyde from Fluka Chemica, Switzerland
9) 4-Ethoxybenzaldehyde from Fluka Chemica, Switzerland
10) *p*-Toluenesulfonic acid monohydrate from Fluka Chemica, Switzerland
11) 4-Methoxybenzenesulfonyl chloride from Fluka Chemica, Switzerland
12) 4-Chlorobenzenesulfonyl chloride from Fluka Chemica, Switzerland
13) 4-Bromobenzenesulfonyl chloride from Fluka Chemica, Switzerland
14) Methyl iodide from Riedel-de Haën, Germany
15) Silver nitrate from Merck, Germany
16) Sodium hydroxide from Lab-Scan, Ireland
17) Zinc iodide from Fluka Chemica, Switzerland
18) Dichloromethane (AR grade) from Merck, Germany
19) Diethyl ether (AR grade) from Merck, Germany
20) Methanol (AR grade) from Merck, Germany
21) Ethanol (AR grade) from Merck, Germany
22) Acetone (AR grade) from Merck, Germany

2.2 *Synthesis of the starting materials*

2.2.1 1,4-Dimethylpyridinium iodide (PM-S1)

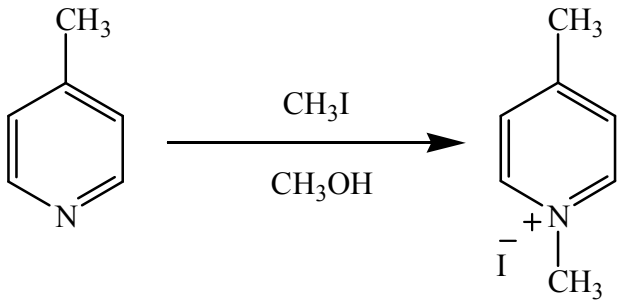

PM1A **PM-S1**

1,4-dimethylpyridinium iodide **(PM-S1)** and 1,2-dimethylquinolinium iodide **(PM-S2)** were prepared to be employed as starting material for the syntheses of related products. Methyl iodide (6.45 ml, 0.10 mol) was added dropwise to a stirred solution of 4-picoline **(PM1A)** (10.00 ml, 0.10 mol) in cold methanol (15 ml) at 5 °C under nitrogen atmosphere for 1 hr and then refluxing for 1 hr. The mixture was cooled in an ice bath and the obtained crystalline solid was filtered, washed with cold methanol and dried in vacuum to give a pale yellow solid of 1,4-dimethylpyridinium iodide **(PM-S1)** (15.50 g, 66%), mp. 140-142 °C, UV-Vis (CH_3OH) λ_{max} (nm) (log ε): 219.7 (3.78), 255.3 (3.16), FT-IR (KBr) $\nu(cm^{-1})$: 1600-1500 (C=C stretching), ^1H NMR ($CDCl_3$ + DMSO-d_6) (δ ppm) (300 MHz): 9.13 (2H, *d*, *J* = 6.3 Hz), 7.88 (2H, *d*, *J* = 6.3 Hz), 4.62 (3H, *s*), 2.69 (3H, *s*).

2.2.2 1,2-Dimethylquinolinium iodide (PM-S2)

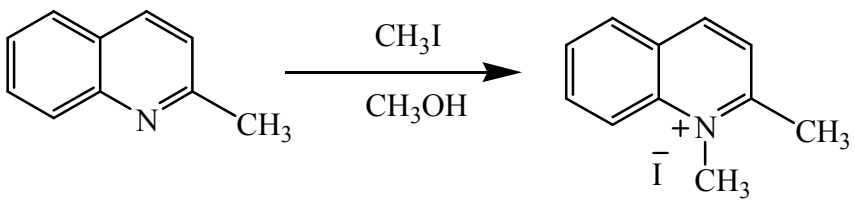

PM1B **PM-S2**

Methyl iodide (4.65 ml, 0.07 mol) was added dropwise to a stirred solution of quinaldine **(PM1B)** (10.00ml, 0.07 mol) in cold methanol (15 ml) at 5 °C under nitrogen atmosphere for 1 hr and then refluxing for 2 hrs. The mixture was cooled and the precipitated solid was filtered, washed with cold methanol and dried in vacuum to give yellow solid of 1,2-dimethylquinoliinium iodide **(PM-S2)** (14.00 g, 66%), mp. 182-184 °C, UV-Vis (CH_3OH) λ_{max} (nm) (log ε): 234.5 (3.47), 316.7 (2.90), FT-IR (KBr) $\nu(cm^{-1})$: 1600-1500 (C=C stretching), ^1H NMR ($CDCl_3$ + DMSO-d_6) (δ ppm) (300 MHz): 9.07 (1H, *d*, *J* = 8.7 Hz), 8.55 (1H, *d*, *J* = 8.1 Hz), 8.39 (1H, *dd*, *J* = 1.5, 8.1 Hz), 8.23 (1H, *dt*, *J* = 1.5, 8.1 Hz), 8.09 (1H, *d*, *J* = 8.7 Hz), 7.98 (1H, *t*, *J* = 8.1 Hz), 4.57 (3H, *s*), 3.20 (3H, *s*).

2.3 Synthesis of the cation parts

2.3.1 4-[(*E*)-2-(2-Thienyl)ethenyl]-1-methylpyridinium iodide (PM-C1)

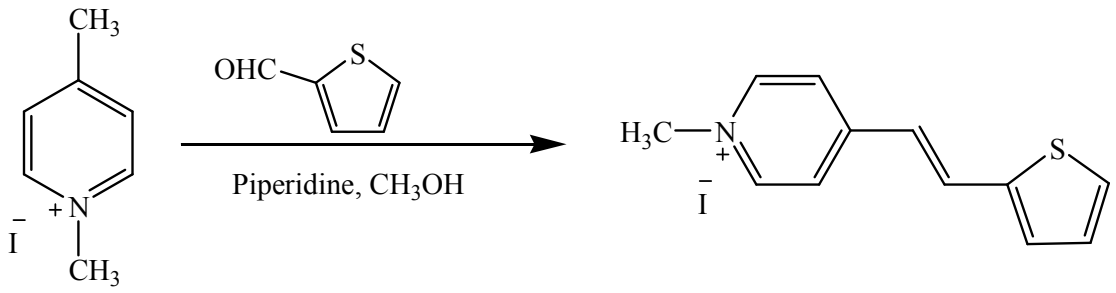

PM-S1 **PM-C1**

The mixture of 1,4-dimethylpyridinium iodide (3.00 g, 12.80 mmol), thiophene-2-carboxaldehyde (1.18 ml, 12.82 mmol) and piperidine (1.25 ml, 12.65 mmol) in methanol was refluxed under nitrogen atmosphere for 4 hrs. The solid formed was filtered off, washed with diethyl ether to give pale yellowish green solid of 4-[(*E*)-2-(2-Thienyl)ethenyl]-1-methylpyridinium iodide **(PM-C1)** (3.17 g, 75%), mp. 219-221 °C, UV (CH_3OH) λ_{max} (nm) (log ε): 218.6 (4.12), 250.6 (2.51),

389.7 (4.16), IR (KBr) ν(cm^{-1}): 1607 (C=C stretching), 1168 (C-O stretching), ^{1}H NMR (see **Table 1**).

2.3.2 2-[(*E*)-2-(4-Ethoxyphenyl)ethenyl]-1-methylquinolidinium iodide (PM-C2)

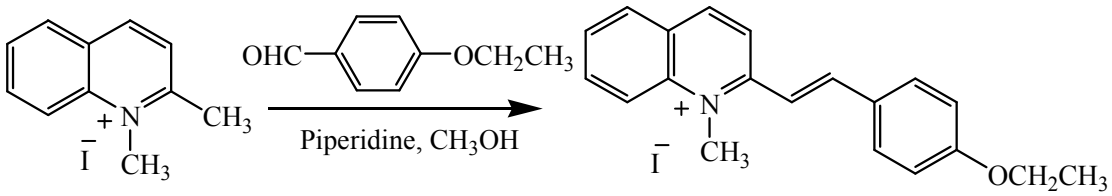

PM-S2 **PM-C2**

2-[(*E*)-2-(4-Ethoxyphenyl)ethenyl]-1-methylquinolinium iodide **(PM-C2)** was prepared to be employed as cationic part by refluxing a stirred solution of 1,2-dimethylquinolinium iodide (2.98 g, 10.05 mmol), 4-ethoxybenzaldehyde (1.46 ml, 10.05 mmol) and piperidine (1.00 ml, 10.00 mmol) in methanol (25 ml) for 3 hrs under nitrogen atmosphere. The solid was filtered, washed with diethyl ether to give brown-red solid of **PM-C2** (3.86 g, 92%), mp. 219-221 °C, UV (CH_3OH) λ_{max} (nm) (log ε): 217.5 (3.59), 252.8 (3.02), 314.1 (3.54), 416.2 (3.19), IR (KBr) ν(cm^{-1}): 1605 (C=C stretching), 1233 (C-O stretching), ^{1}H NMR (see **Table 2**).

2.3.3 2-[(*E*)-2-(3-Hydroxy-4-methoxyphenyl)ethenyl]-1-methylquinolinium iodide (PM-C3)

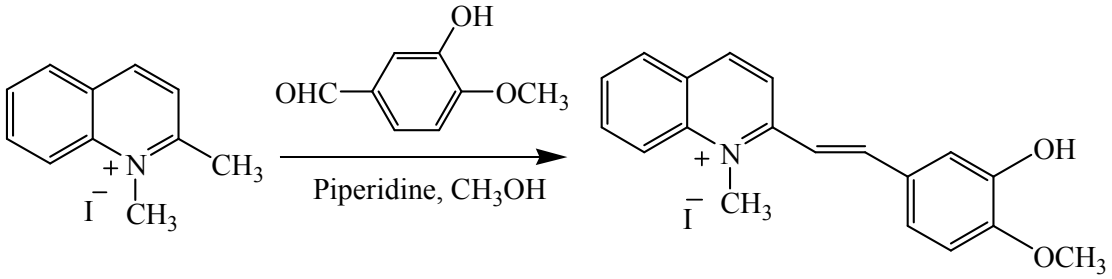

PM-S2 **PM-C3**

2-[(*E*)-2-(3-Hydroxy-4-methoxyphenyl)ethenyl]-1-methylquinolinium iodide **(PM-C3)** was prepared by condensation of 1,2-dimethylquinolinium iodide **(PM-S2)** (3.00 g, 10.05 mmol) and isovanillin (1.60 g, 10.05 mmol) in the presence of piperidine (1.00 ml, 10.00 mmol) as a catalyst. The reaction mixture was refluxed for 2 hrs under nitrogen atmosphere. The solid formed was filtered, washed with diethyl ether and re-crystallized from methanol to give red-brown crystals of **PM-C3** (2.80 g, 64%), mp. 218-220 °C, UV (CH_3OH) λ_{max} (nm) (log ε): 216.1 (4.12), 306.2 (3.59), 431.3 (4.06), IR (KBr) $\nu(cm^{-1})$: 3424 (O-H stretching), 1612, 1583 (C=C stretching), 1235 (C-O stretching), ^{1}H NMR (see **Table 3**).

2.3.4 4-[(*E*)-2-(4-Hydroxy-3-methoxyphenyl)ethenyl]-1-methylpyridinium iodide (PM-C4)

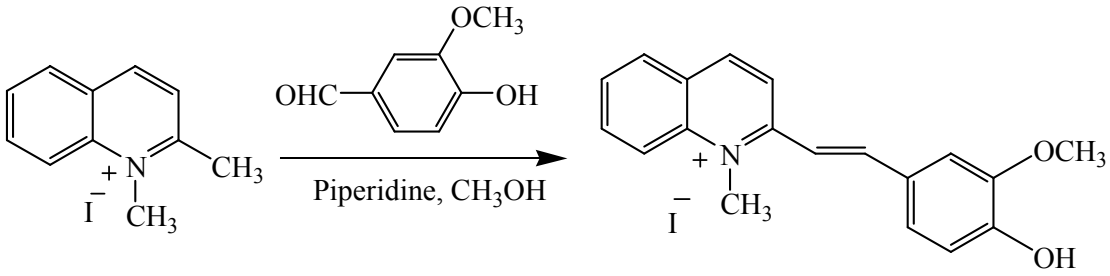

PM-S2 **PM-C4**

2-[(*E*)-2-(4-Hydroxy-3-methoxyphenyl)ethenyl]-1-methylquinolinium iodide **(PM-C4)** was prepared to be employed as cationic part by refluxing a stirred solution of 1,2-dimethylquinolinium iodide (2.98 g, 10.05 mmol), vanillin (1.60 g, 10.05 mmol) and piperidine (1.00 ml, 10.00 mmol) in methanol (25 ml) for 3 hrs under nitrogen atmosphere. The solid was filtered, washed with diethyl ether and crystallized from methanol to give dark red crystals of **PM-C4** (3.00 g, 68%), mp. 248-250 °C, UV (CH_3OH) λ_{max} (nm) (log ε): 215.3 (3.59), 308.9 (3.02), 440.1 (3.54), 576.5 (3.19), IR (KBr) $\nu(cm^{-1})$: 3439 (O-H stretching), 1609, 1580 (C=C stretching), 1233 (C-O stretching), ^{1}H NMR (see **Table 4**).

2.3.5 2-[(*E*)-2-(4-Hydroxyphenyl)ethenyl]-1-methylquinolidinium iodide (PM-C5)

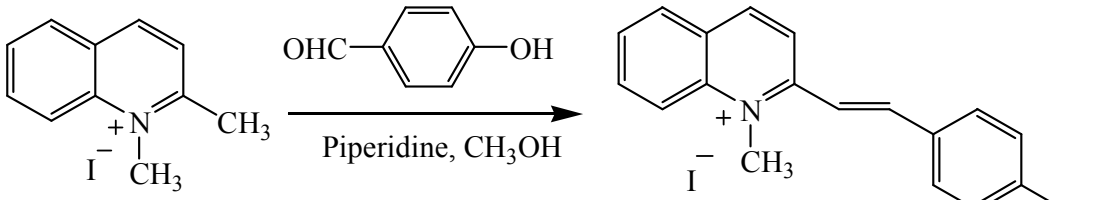

PM-S2 **PM-C5**

2-[(*E*)-2-(4-Hydroxyphenyl)ethenyl]-1-methylquinolinium iodide **(PM-C5)** was prepared by refluxing a stirred solution of 1,2-dimethylquinolinium iodide (2.00 g, 7.01 mmol), 4-hydroxybenzaldehyde (0.86 g, 7.01 mmol) and piperidine (0.69 ml, 7.01 mmol) in methanol (25 ml) for 3 hrs under nitrogen atmosphere. The solid was filtered, washed with diethyl ether to give purple solid of **PM-C5** (1.99 g, 73%), mp. 192-194 °C, UV (CH_3OH) λ_{max} (nm) (log ε): 218.3 (2.99), 258.9 (2.75), 425.1 (2.84), IR (KBr) ν(cm^{-1}): 3447 (O-H stretching), 1576 (C=C stretching), 1220 (C-O stretching), ^{1}H NMR (see **Table 5**).

2.3.6 2-[(*E*)-2-(4-Methoxyphenyl)ethenyl]-1-methylquinolidinium iodide (PM-C6)

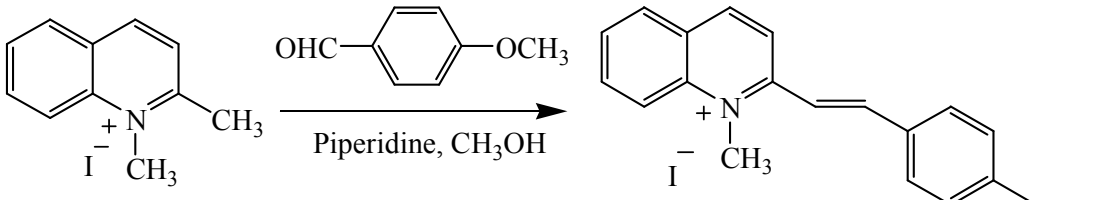

PM-S2 **PM-C6**

2-[(*E*)-2-(4-Methoxyphenyl)ethenyl]-1-methylquinolinium iodide **(PM-C6)** was prepared by refluxing a stirred solution of 1,2-dimethylquinolinium

iodide (1.00 g, 3.51 mmol), 4-methoxybenzaldehyde (0.43 g, 3.55 mmol) and piperidine (0.35 ml, 3.54 mmol) in methanol (25 ml) for 7 hrs under nitrogen atmosphere. The solid was filtered, washed with diethyl ether to give brown solid of **PM-C6** (0.95 g, 67%), mp. 225-226 °C, UV (CH_3OH) λ_{max} (nm) (log ε): 217.3 (2.99), 407.6 (2.66), IR (KBr) $\nu(cm^{-1})$: 1569-1595 (C=C stretching), 1221 (C-O stretching), ^{1}H NMR (see **Table 6**).

2.4 Synthesis of anions counter part

2.4.1 Silver (I) 4-methylbenzenesulfonate (An-CH_3)

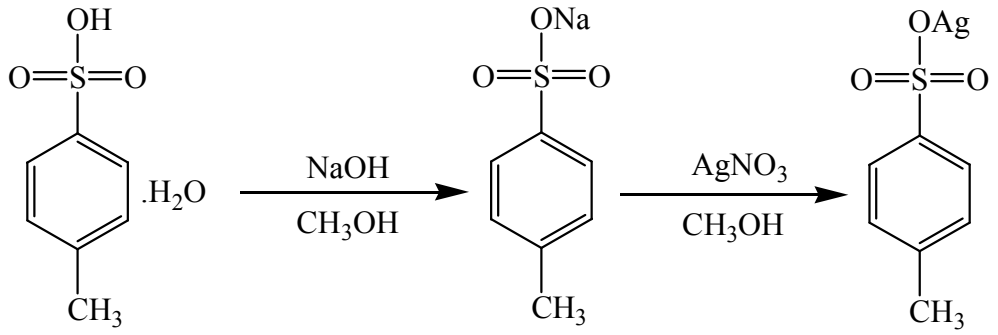

PM1C **An-CH_3**

A solution of 4-methylbenzenesulfonic acid monohydrate **(PM1C)** (5.00 g, 26.30 mmol) in hot methanol was added to a stirred solution of sodium hydroxide (1.05 g, 26.30 mmol) in hot methanol, followed by addition of a solution of silver nitrate (4.47 g, 26.30 mmol) in hot methanol. A solution mixed with a solid was obtained which was then filtered. The white crystalline solid of **An-CH_3** (5.20 g, 71%) was collected after allowing the filtrate to stand in air for a few days, mp. 264-266 °C (decomp.), ^{1}H NMR ($CDCl_3$ + DMSO-d_6) (δ ppm) (300 MHz): 7.74 (2H, *d*, *J* = 8.1 Hz), 7.17 (2H, *d*, *J* = 8.1 Hz), 2.38 (1H, *s*).

2.4.2 Silver (I) 4-methoxybenzenesulfonate (An-OCH_3)

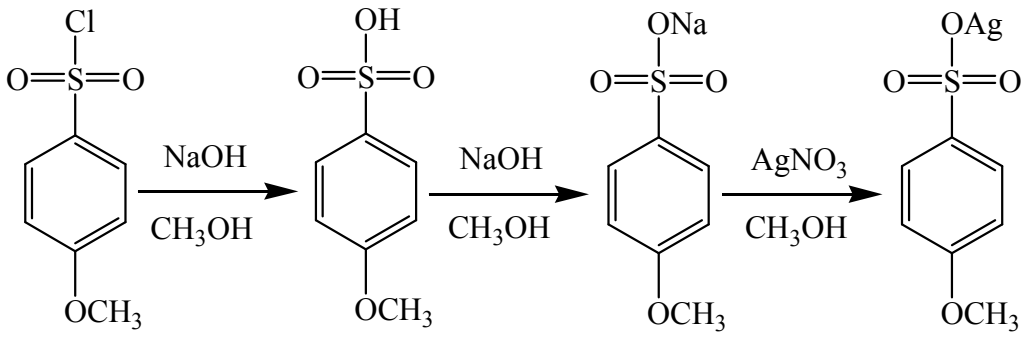

PM1D **An-OCH_3**

Silver (I) 4-methoxybenzenesulfonate **(An-OCH_3)** was prepared by mixing a solution of 4-methoxybenzenesulfonyl chloride **(PM1D)** (5.00 g, 24.20 mmol) and sodium hydroxide (0.97 g, 24.25 mmol) in hot methanol. A colorless solution mixed with a white solid of sodium chloride was obtained. The mixture was worked up by addition of water and extraction with dichloromethane. The dichloromethane part was evaporated and the resulting residue was dissolved in methanol, followed by addition of the solution of sodium hydroxide (0.96 g, 24.00 mmol) in hot methanol and a solution of silver nitrate (4.10 g, 24.14 mmol) in hot methanol. The colorless solution mixed with a solid of sodium nitrate was obtained, which was filtered and discarded. Compound **An-OCH_3** (4.53 g, 63%) was obtained after allowing the resulting filtrate to stand in air for a few days, mp. 240-242 °C (decomp.), ^{1}H NMR ($CDCl_3$ + DMSO-d_6) (δ ppm) (300 MHz): 7.78 (2H, *d*, *J* = 8.7), 6.86 (2H, *d*, *J* = 8.7 Hz), 3.82 (1H, *s*).

2.4.3 Silver (I) 4-chlorobenzenesulfonate (An-Cl)

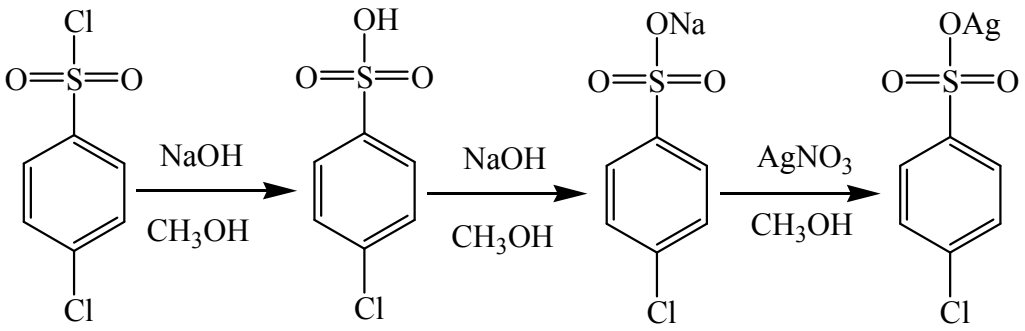

PM1E **An-Cl**

Silver (I) 4-chlorobenzenesulfonate **(An-Cl)** was prepared to be employed as anionic part by mixing a solution (1:1 molar ratio) of 4-chloro-benzenesulfonyl chloride **(PM1E)** (5.00 g, 19.57 mmol) and sodium hydroxide (0.78 g, 19.57 mmol) in hot methanol. A colorless solution mixed with a white solid of sodium chloride was obtained. The mixture was worked up by addition of water and extraction with dichloromethane. The dichloromethane part was evaporated and dissolved in methanol, followed by addition of the solution of sodium hydroxide (0.77 g, 19.32 mmol) in hot methanol and a solution of silver nitrate (3.32 g, 19.57 mmol) in hot methanol. The colorless solution mixed with a solid of sodium nitrate was obtained, which was filtered and discarded. Compound **An-Cl** (4.56 g, 68%) was obtained after allowing the resulting filtrate to stand in air for a few days, mp. 227-229 °C (decomp.), ^{1}H NMR ($CDCl_3$ + DMSO-d_6) (δ ppm) (300 MHz): 7.76 (2H, *d*, *J* = 7.8), 7.50 (2H, *d*, *J* = 7.8 Hz).

2.4.4 Silver (I) 4-bromobenzenesulfonate (An-Br)

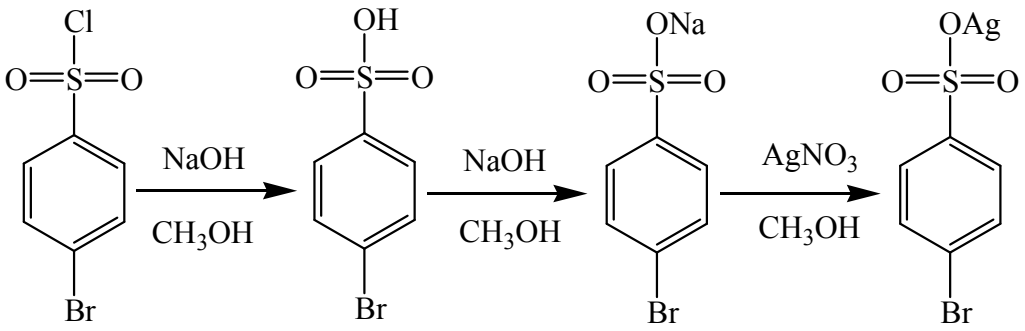

PM1F **An-Br**

Silver (I) 4-bromobenzenesulfonate **(An-Br)** was synthesized by mixing a solution of 4-bromobenzenesulfonyl chloride **(PM1F)** (5.00 g, 23.69 mmol) and sodium hydroxide (0.95 g, 23.69 mmol) in hot methanol. A colorless solution mixed with a white solid of sodium chloride was obtained. The mixture was worked up by addition of water and extraction with dichloromethane. The dichloromethane part was evaporated and dissolved in methanol, followed by addition of the solution of sodium hydroxide (0.96 g, 23.64 mmol) in hot methanol and a solution of silver nitrate (4.00 g, 23.57 mmol) in hot methanol. The colorless solution mixed with a solid of sodium nitrate was obtained, which was filtered and discarded. Compound **An-Br** (4.36 g, 61%) was obtained after allowing the resulting filtrate to stand in air for a few days, mp. 230-232 °C decomposed, ^{1}H NMR ($CDCl_3$ + DMSO-d_6) (δ ppm) (300 MHz): 7.81 (2H, *d*, *J* = 8.4), 7.34 (2H, *d*, *J* = 8.4 Hz).

2.5 Salt formations

2.5.1 4-[(*E*)-2-(2-Thienyl)ethenyl]-1-methylpyridinium 4-methylbenzenesulfonate (PM-C1Me)

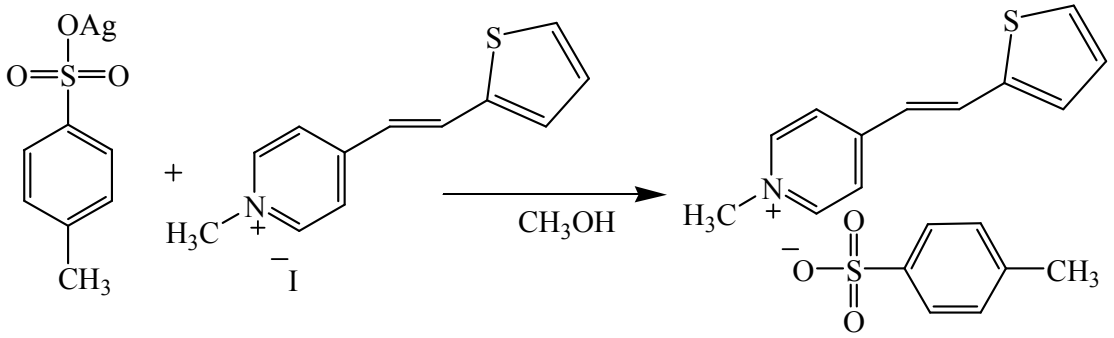

An-CH_3 **PM-C1** **PM-C1Me**

4-[(*E*)-2-(2-Thienyl)ethenyl]-1-methylpyridinium 4-methylbenzene-sulfonate **(PM-C1Me)**, was synthesized by addition of a solution of silver (I) 4-methylbenzenesulfonate (0.08 g, 0.30 mmol) in hot methanol (20 ml) to a solution of compound **PM-C1** (0.10 g, 0.30 mmol) in hot methanol (45 ml). Upon addition a yellow solid of silver iodide was immediately formed which was removed by filtration and the yellow filtrate was evaporated under reduced pressure to yield a brown solid. The brown solid was re-crystallized from methanol to give brown crystals of compound **PM-C1Me** (0.08 g, 75%), mp. 232-234 °C, UV (CH_3OH) λ_{max} (nm) (logε): 220.9 (4.04), 251.4 (3.58), 379.2 (3.95), IR (KBr) ν(cm^{-1}): 1523, (C=C stretching), 1186 (S=O stretching), ^{1}H NMR (see **Table 7**).

2.5.2 4-[(*E*)-2-(2-Thienyl)ethenyl]-1-methylpyridinium 4-methoxybenzenesulfonate (PM-C1OMe)

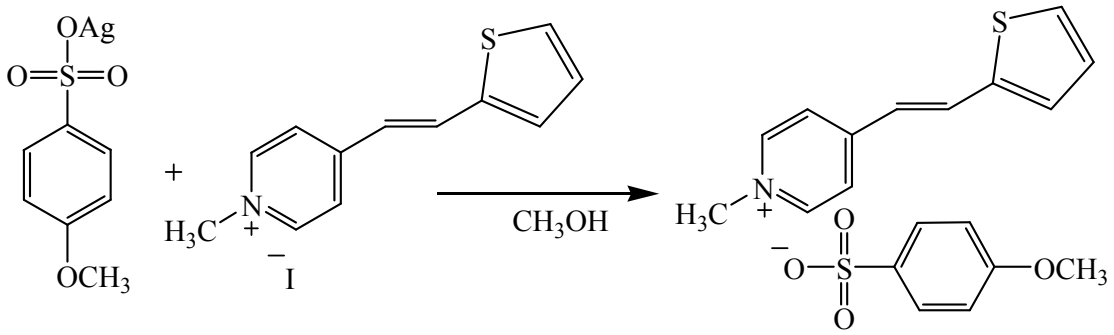

An-OCH$_3$ **PM-C1** **PM-C1OMe**

4-[(*E*)-2-(2-Thienyl)ethenyl]-1-methylpyridinium 4-methoxybenzene-sulfonate **(PM-C1OMe),** was synthesized by addition of a solution of silver (I) 4-methoxybenzenesulfonate (0.09 g, 0.30 mmol) in hot methanol (30 ml) to a solution of compound **PM-C1** (0.10 g, 0.30 mmol) in hot methanol (10 ml). Upon addition a yellow solid of silver iodide was immediately formed which was removed by filtration and the yellow filtrate was evaporated under reduced pressure to yield a yellow solid of compound **PM-C1OMe** (0.11 g, 87%)**,** mp. 234-236 °C, UV (CH_3OH) λ_{max} (nm) (logε): 230.2 (2.83), 381.1 (3.58), IR (KBr) ν(cm^{-1}): 1590 (C=C stretching), 1188 (S=O stretching), ^{1}H NMR (see **Table 11**).

2.5.3 4-[(*E*)-2-(2-Thienyl)ethenyl]-1-methylpyridinium 4-chlorobenzenesulfonate (PM-C1Cl)

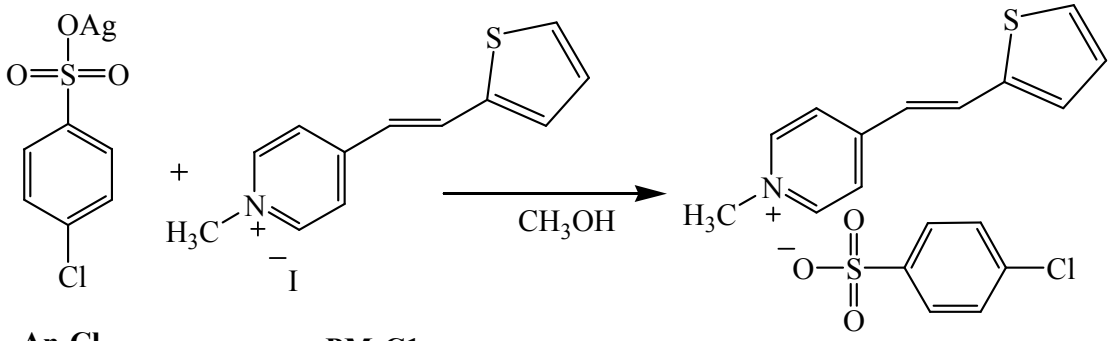

4-[(*E*)-2-(2-Thienyl)ethenyl]-1-methylpyridinium 4-chlorobenzene-sulfonate **(PM-C1Cl),** was synthesized by addition of a solution of silver (I) 4-chlorobenzenesulfonate (0.09 g, 0.30 mmol) in hot methanol (20 ml) to a solution of compound **PM-C1** (0.10 g, 0.30 mmol) in hot methanol (10 ml). Upon addition a yellow solid of silver iodide was immediately formed which was removed by filtration and the yellow filtrate was evaporated under reduced pressure to yield a brown solid. The brown solid was re-crystallized from methanol and ethanol (1:1) to give brown crystals of compound **PM-C1Cl** (0.11 g, 90%), mp. 230-232 °C, UV (CH_3OH) λ_{max} (nm) (logε): 220.9 (4.35), 251.4 (3.02) 379.2 (3.42), IR (KBr) $\nu(cm^{-1})$: 1523 (C=C stretching), 1210 (S=O stretching), ^{1}H NMR (see **Table 12**).

2.5.4 4-[(*E*)-2-(2-Thienyl)ethenyl]-1-methylpyridinium 4-bromobenzenesulfonate (PM-C1Br)

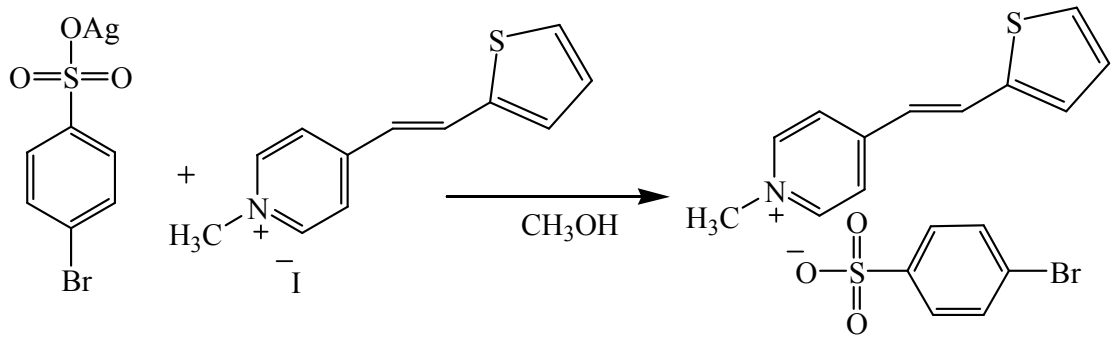

An-Br **PM-C1** **PM-C1Br**

4-[(*E*)-2-(2-Thienyl)ethenyl]-1-methylpyridinium 4-bromobenzene-sulfonate **(PM-C1Br),** was synthesized by addition of a solution of silver (I) 4-bromobenzenesulfonate (0.10 g, 0.30 mmol) in hot methanol (60 ml) to a solution of compound **PM-C1** (0.10 g, 0.30 mmol) in hot methanol (10 ml). Upon addition a yellow solid of silver iodide was immediately formed which was removed by filtration and the yellow filtrate was evaporated under reduced pressure to yield a brown solid of compound **PM-C1Br** (0.10 g, 70%)**,** mp. 231-233 °C, UV (CH_3OH) λ_{max} (nm) (logε): 222.3 (4.26), 258.0 (3.62), 381.8 (2.34), IR (KBr) $\nu(cm^{-1})$: 1577 (C=C stretching), 1208 (S=O stretching), ^{1}H NMR (see **Table 16**).

2.5.5 2-[(*E*)-2-(4-Ethoxyphenyl)ethenyl]-1-methylquinolinium 4-methylbenzenesulfonate (PM-C2Me)

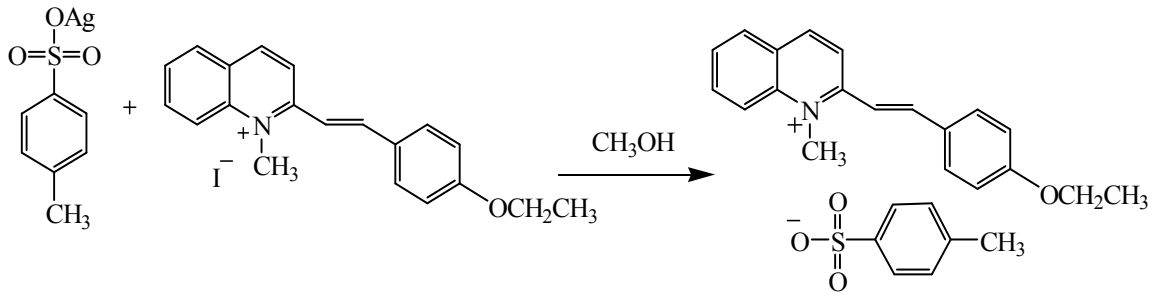

An-CH_3 **PM-C2** **PM-C2Me**

2-[(*E*)-2-(4-Ethoxyphenyl)ethenyl]-1-methylquinolinium 4-methyl-benzenesulfonate **(PM-C2Me)**, was synthesized by addition of a solution of silver (I) 4-methylbenzenesulfonate (0.07 g, 0.24 mmol) in hot methanol (10 ml) to a solution of compound **PM-C2** (0.10 g, 0.24 mmol) in hot methanol (70 ml). Upon addition a yellow solid of silver iodide was immediately formed which was removed by filtration and the yellow filtrate was evaporated under reduced pressure to yield a yellow solid of compound **PM-C2Me** (0.06 g, 54%), mp. 250-252 °C, UV (CH_3OH) λ_{max} (nm) (logε): 202.7 (4.68), 217.6 (4.88), 256.2 (3.45), 413.9 (3.75), IR (KBr) $\nu(cm^{-1})$: 1592 (C=C stretching), 1220 (C-O stretching), 1175 (S=O stretching), ^1H NMR (see **Table 17**).

2.5.6 2-[(*E*)-2-(4-Ethoxyphenyl)ethenyl]-1-methylquinolinium 4-methoxybenzenesulfonate (PM-C2OMe)

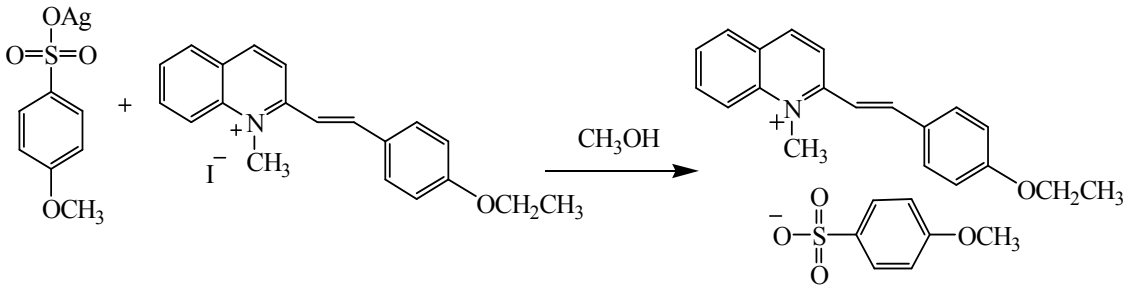

An-OCH3 **PM-C2** **PM-C2OMe**

2-[(*E*)-2-(4-Ethoxyphenyl)ethenyl]-1-methylquinolinium 4-methoxy-benzenesulfonate **(PM-C2OMe)**, was synthesized by addition of a solution of silver (I) 4-methoxybenzenesulfonate (0.07 g, 0.24 mmol) in hot methanol (20 ml) to a solution of compound **PM-C2** (0.10 g, 0.24 mmol) in hot methanol (70 ml). Upon addition a yellow solid of silver iodide was immediately formed which was removed by filtration and the yellow filtrate was evaporated under reduced pressure to yield a yellow solid of compound **PM-C2OMe** (0.07 g, 61%), mp. 256-257 °C, UV (CH_3OH) λ_{max} (nm) (logε): 330.3 (3.21), 413.1 (4.46), IR (KBr) $\nu(cm^{-1})$: 1572

(C=C stretching), 1220 (C-O stretching), 1164 (S=O stretching), ^{1}H NMR (see **Table 18**).

2.5.7 2-[(*E*)-2-(4-Ethoxyphenyl)ethenyl]-1-methylquinolinium 4-cholrobenzenesulfonate (PM-C2Cl)

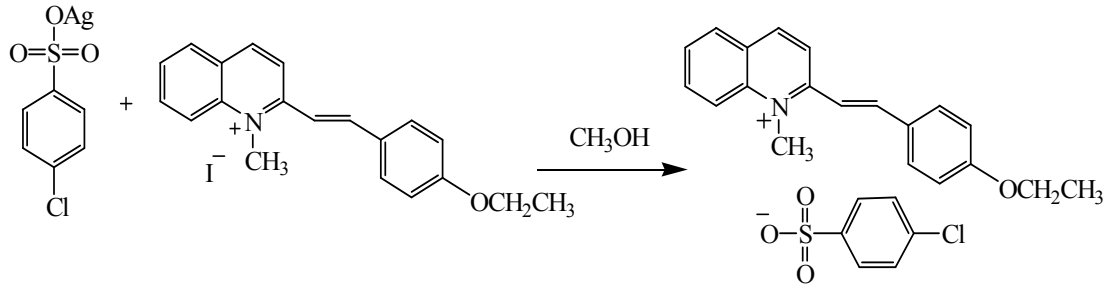

An-Cl **PM-C2** **PM-C2Cl**

2-[(*E*)-2-(4-Ethoxyphenyl)ethenyl]-1-methylquinolinium 4-chloro-benzenesulfonate **(PM-C2Cl),** was synthesized by addition of a solution of silver (I) 4-chlorobenzenesulfonate (0.07 g, 0.24 mmol) in hot methanol (20 ml) to a solution of compound **PM-C2** (0.10 g, 0.24 mmol) in hot methanol (70 ml). Upon addition a yellow solid of silver iodide was immediately formed which was removed by filtration and the yellow filtrate was evaporated under reduced pressure to yield a yellow-orange solid, The brown solid was re-crystallized from methanol to give yellow crystals of compound **PM-C2Cl** (0.07 g, 62%), (mp. 254-256 °C), UV (CH_3OH) λ_{max} (nm) (logε): 228.7 (3.86), 268.4 (3.12), 410.2 (4.37), IR (KBr) ν(cm^{-1}): 1590 (C=C stretching), 1225 (C-O stretching), 1153 (S=O stretching), ^{1}H NMR (see **Table 19**).

2.5.8 2-[(*E*)-2-(4-Ethoxyphenyl)ethenyl]-1-methylquinolinium 4-bromobenzenesulfonate (PM-C2Br)

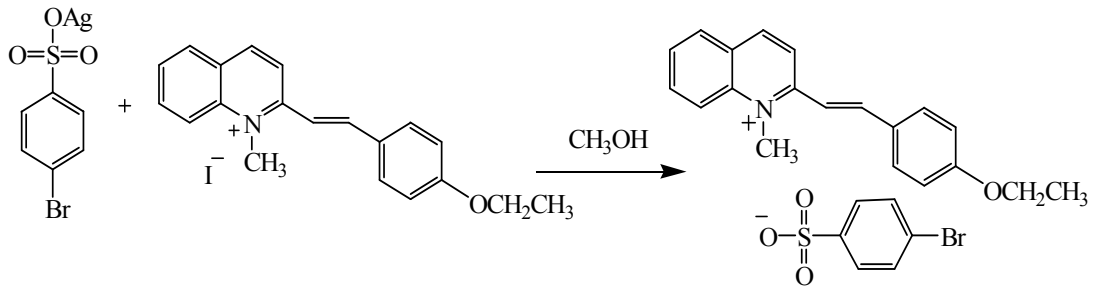

An-Br **PM-C2** **PM-C2Br**

2-[(*E*)-2-(4-Ethoxyphenyl)ethenyl]-1-methylquinolinium 4-bromobenzenesulfonate **(PM-C2Br)**, was synthesized by addition of a solution of silver (I) 4-Bromobenzenesulfonate (0.08 g, 0.24 mmol) in hot methanol (20 ml) to a solution of compound **PM-C2** (0.10 g, 0.24 mmol) in hot methanol (70 ml). Upon addition a yellow solid of silver iodide was immediately formed which was removed by filtration and the yellow filtrate was evaporated under reduced pressure to yield a yellow-orange solid of compound **PM-C2Br** (0.08 g, 72%), mp. 249-251 °C, UV (CH_3OH) λ_{max} (nm) (logε): 221.0 (4.20), 255.5 (3.69), 413.9 (2.68), IR (KBr) ν(cm^{-1}): 1592 (C=C stretching), 1224 (C-O stretching), 1169 (S=O stretching), ^{1}H NMR (see **Table 22**).

2.5.9 Bis[(*E*)-2-(3-hydroxy-4-methoxyphenyl)ethenyl]-1-methylquinolinium tetraiodidozincate(II) (PM-C3Zn)

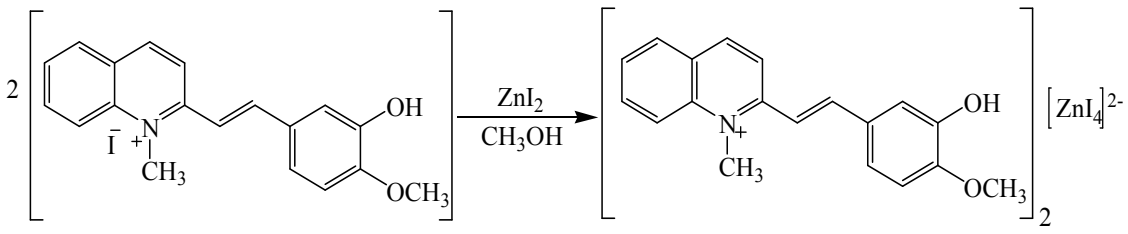

PM-C3 **PM-C3Zn**

Bis[(*E*)-2-(3-hydroxy-4-methoxyphenyl)ethenyl]-1-methylquinolinium tetraiodidozincate(II) **(PM-C3Zn),** was synthesized by addition 1:2 molar ratio of a solution of Zinc(II) iodide (0.15 g, 0.40 mmol) in hot methanol (10 ml) to a solution of compound **PM-C3** (0.40 g, 0.80 mmol) in hot methanol (15 ml). The mixture turned orange, stirring for 1 hr and was then evaporated to give a brown solid of compound **PM-C3Zn** (0.14 g, 40%), mp. 220-221 °C, UV (CH_3OH) λ_{max} (nm) (logε): 218.2 (5.24), 305.4 (4.51), 430.9 (4.99), IR (KBr) ν(cm^{-1}): 3436 (O-H stretching), 1585 (C=C stretching), 1221 (C-O stretching), ^{1}H NMR (see **Table 23**).

2.5.10 Bis[(*E*)-2-(4-hydroxy-3-methoxyphenyl)ethenyl]-1-methylquinolinium tetraiodidozincate(II) (PM-C4Zn)

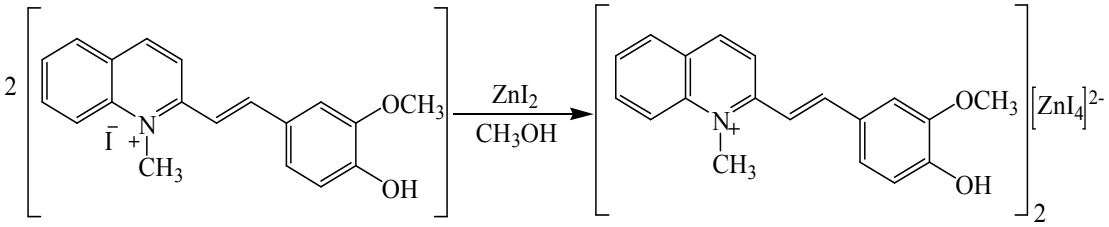

PM-C4 **PM-C4Zn**

Bis[(*E*)-2-(4-hydroxy-3-methoxyphenyl)ethenyl]-1-methylquinolinium tetraiodidozincate(II) **(PM-C4Zn),** was synthesized by addition 1:2 molar ratio of a solution of Zinc(II) iodide (0.15 g, 0.40 mmol) in hot methanol (10 ml) to a solution of compound **PM-C4** (0.40 g, 0.80 mmol) in hot methanol (15 ml). The mixture turned yellow, stirring for 1 hr and was then evaporated to give a brown solid of compound **PM-C4ZnBr** (0.14 g, 40%), mp. 225-226 °C, UV (CH_3OH) λ_{max} (nm) (logε): 217.3 (4.87), 311.6 (3.83), 440.9 (5.04), 561.8 (4.60), IR (KBr) ν(cm^{-1}): 3437 (O-H stretching), 1579 (C=C stretching), 1221 (C-O stretching), ^{1}H NMR (see **Table 27**).

2.5.11 Bis[(*E*)-2-(4-hydroxyphenyl)ethenyl]-1-methylquinolinium tetraiodidozincate(II) (PM-C5Zn)

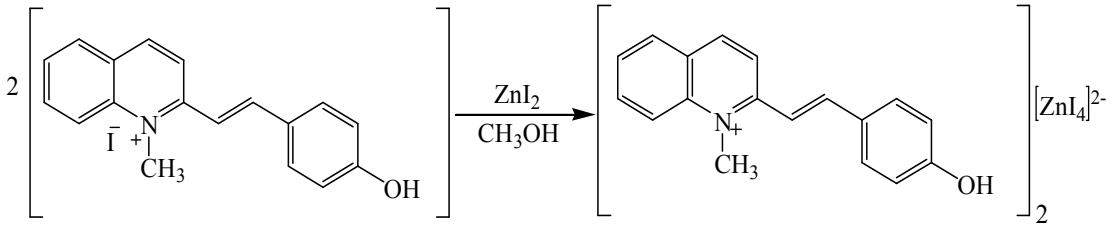

PM-C5 **PM-C5Zn**

Bis[(*E*)-2-(4-hydroxyphenyl)ethenyl]-1-methylquinolinium tetraiodidozincate(II) **(PM-C5Zn),** was synthesized by addition 1:2 molar ratio of a solution of Zinc(II) iodide (0.25 g, 0.77 mmol) in hot methanol (15 ml) to a solution of compound **PM-C5** (0.60 g, 1.54 mmol) in hot methanol (30 ml). The mixture turned dark red, stirring for 1 hr and was then evaporated to give a dark red solid of compound **PM-C5Zn** (0.37 g, 43%), mp. 234-236 °C, UV (CH_3OH) λ_{max} (nm) (logε): 220.9 (3.38), 260.6 (3.02), 312.2 (2.79), 426.8 (3.32), IR (KBr) $\nu(cm^{-1})$: 3421 (O-H stretching), 1586 (C=C stretching), ^{1}H NMR (see **Table 28**).

2.5.12 Bis[(*E*)-2-(4-methoxyphenyl)ethenyl]-1-methylquinolinium tetraiodidozincate(II) (PM-C6Zn)

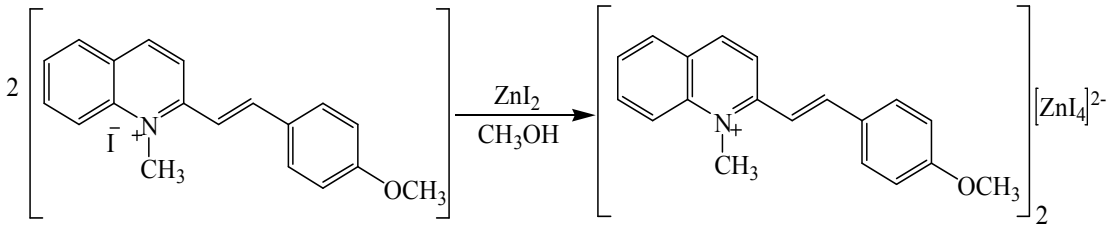

PM-C6 **PM-C6Zn**

Bis[(*E*)-2-(4-methoxyphenyl)ethenyl]-1-methylquinolinium tetraiodidozincate(II) **(PM-C6Zn),** was synthesized by addition 1:2 molar ratio of a solution of Zinc(II) iodide (0.24 g, 0.74 mmol) in hot methanol (35 ml) to a solution

of compound **PM-C6** (0.60 g, 1.48 mmol) in hot methanol (165 ml). The mixture turned brown, stirring for 0.5 hr and was then evaporated to give a brown solid of compound **PM-C6Zn** (0.4 g, 73%), mp. 229-231 °C, UV (CH_3OH) λ_{max} (nm) (logε): 219.1 (3.92), 249.2 (3.73), 407.2 (3.68), IR (KBr) $\nu(cm^{-1})$: 1,587 (C=C stretching) and C-O (1220 cm^{-1}). ^1H NMR (see **Table 29**).

CHAPTER 3
RESULTS AND DISCUSSION

3.1 Structural elucidations of the starting materials

3.1.1 1,4-Dimethylpyridinium iodide (PM-S1)

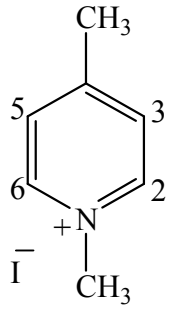

PM-S1

A pale yellow solid of **PM-S1** was received in 66% yield, mp. 140-142 °C. The UV-visible absorption spectra (**Fig. 15**) exhibited maximum bands at 219.7 and 255.3 nm. The IR spectrum (**Fig. 16**) revealed the presence of stretching vibration of C=C in aromatic ring at 1600-1500 cm^{-1}.

The ^{1}H NMR spectrum (**Fig. 17**) showed two *doublet* signals of equivalent protons H-2, H-6 and H-3, H-5 at δ 9.09 (2H, J = 6.6 Hz) and δ 7.92 (2H, J = 6.6 Hz), respectively. Two *singlet* signals of *N*-CH_3 and 4-CH_3 appeared at δ 4.55 and δ 2.71 ppm, respectively. **PM-S1** was assigned to be 1,4-dimethylpyridinium iodide.

3.1.2 1,2-dimethylquinolinium iodide (PM-S2)

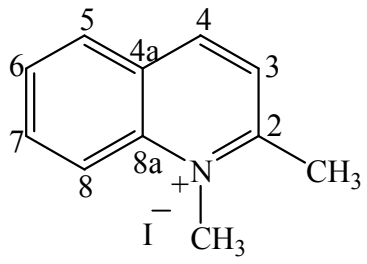

PM-S2

A yellow solid of **PM-S2** was obtained in 66% yield, mp. 172-174 °C. The UV-visible absorption spectra (**Fig. 18**) showed maximum bands at 204.8, 234.5 and 316.7 nm. The IR spectrum (**Fig. 19**) exhibited stretching vibration of C=C in aromatic ring at 1600-1500 cm^{-1}.

The ^{1}H NMR spectrum was shown in **Fig. 20**. The peak assigned to *N*-CH_3 and 2-CH_3 protons appeared at δ 4.57 (3H, *s*) and δ 3.20 (3H, *s*), respectively. Two *doublet* signals at δ 9.07 (1H, J = 8.7 Hz) and δ 8.09 (1H, J = 8.7 Hz) were assigned to H-4 and H-3, respectively. ^{1}H NMR spectrum also showed the signals of aromatic protons H-5 (δ 8.39), H-6 (δ 7.98), H-7 (δ 8.23) and H-8 (δ 8.55). From the above spectral data, **PM-S2** was assigned to be 1,2-dimethylquinolinium iodide.

3.2 Structural elucidations of cation parts

3.2.1 4-[(*E*)-2-(2-Thienyl)ethenyl]-1-methylpyridinium iodide (PM-C1)

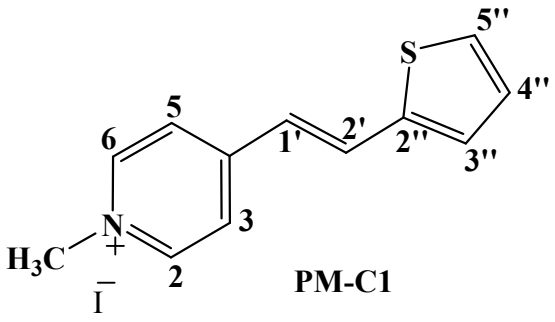

PM-C1

The pale yellowish green solid of **PM-C1** was prepared (75% yield), mp. 219-221 °C. The UV-visible spectrum (**Fig. 21**) showed maxima at 218.6, 250.6 and 389.7 nm. The C=C stretching vibration was observed in the IR spectrum (**Fig. 22**) at 1607 cm^{-1} and the C-O stretching vibration was observed at 1168 cm^{-1}.

The ^{1}H NMR spectrum (**Fig. 23,** see **Table 1**) consisted of *singlet* signals of *N*-CH_3 protons at δ 4.40 ppm (3H). Two *doublets* of H-1′ (δ 7.04, J = 15.6 Hz) and H-2′ (δ 8.08, J = 15.6 Hz) were assigned to be *trans*-disubstituted double bonds and two *doublets* at δ 8.89 (2H, J = 6.9 Hz) and δ 8.10 (2H, J = 6.9 Hz) were the signals of H-2, H-6 and H-3, H-5, respectively. Resonances of aromatic protons H-3″, H-4″ and H-5″ were also shown at δ 7.49 (*d*, J = 5.1 Hz), δ 7.16 (*t*, J = 5.1 Hz) and δ 7.57 (*d*, J = 5.1 Hz), respectively. Thus, these assignments clearly support the proposed structure.

Table 1 ^{1}H NMR of compound **PM-C1**

Position	**δ_H (ppm), *mult*, *J* (Hz)**
1-CH_3	4.40 (3H, *s*)
2	8.89 (2H, *d*, 6.9)
6	
3	8.10 (2H, *d*, 6.9)
5	
1′	7.04 (1H, *d*, 15.6)
2′	8.08 (1H, *d*, 15.6)
3″	7.49 (1H, *d*, 5.1)
4″	7.16 (1H, *t*, 5.1)
5″	7.57 (1H, *d*, 5.1)

3.2.2 2-[(*E*)-2-(4-Ethoxyphenyl)ethenyl]-1-methylquinolidinium iodide (PM-C2)

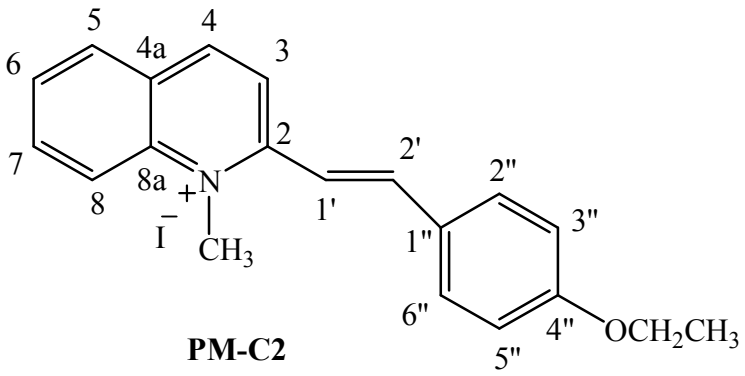

PM-C2

Compound **PM-C2** is a brown-red solid (92% yield), mp. 219-221 °C. The UV-visible spectrum (**Fig. 24**) showed maximum absorptions at 217.5, 252.8, 314.1 and 416.2 nm. The IR spectrum (**Fig. 25**) exhibited stretching vibrations of C=C (1605 cm^{-1}) and C-O (1233 cm^{-1}).

The ^{1}H NMR spectrum (**Fig. 26**, see **Table 2**) showed characteristic of *trans*-disubstituted double bonds at δ 7.74 (1H, *d*, *J* = 15.6 Hz, H-1′) and δ 8.09 (1H, *d*, *J* = 15.6 Hz, H-2′).The *singlet* signal at δ 4.62 (3H) was assigned as *N*-CH_3. The *triplet* and *quartet* signals at δ 1.42 (3H, *J* = 6.9 Hz) and δ 4.15 (2H, *J* = 6.9 Hz) were assigned as CH_3 and CH_2 of ethoxy, respectively. Two signals of 4-substituted benzene pattern at δ 7.89 (2H, *d*, *J* = 8.7 Hz) and δ 7.02 (2H, *d*, *J* = 8.7 Hz) were assigned to H-2″, H-6″, H-3″ and H-5″, respectively. Two *doublet* signals at δ 8.93 (1H, *J* = 9.0 Hz) and δ 8.50 (1H, *J* = 9.0 Hz) were the signals of H-4 and H-3, respectively. ^{1}H NMR spectrum also showed resonances of aromatic protons H-5 (δ 8.27), H-6 (δ 7.90), H-7 (δ 8.15) and H-8 (δ 8.45). Accordingly, compound **PM-C2** was assigned to be 2-[(*E*)-2-(4-ethoxyphenyl)ethenyl]-1-methylquinolidinium iodide.

Table 2 ^{1}H NMR of compound **PM-C2**

Position	**δ_H (ppm), *mult*, *J* (Hz)**
CH_3	1.42 (3H, *t,* 6.9)
OCH_2	4.15 (2H, *q,* 6.9)
1-CH_3	4.60 (1H, *s*)
3	8.50 (1H, *d*, 9.0)
4	8.93 (1H, *d*, 9.0)
5	8.27 (1H, *d*, 7.5)
6	7.90 (1H, *t*, 7.5)
7	8.15 (1H, *t*, 7.5)
8	8.45 (1H, *t*, 7.5)
1′	7.74 (1H, *d*, 15.6)
2′	8.09 (1H, *d*, 15.6)
2″ 6″	7.89 (2H, *d*, 8.7)
3″ 5″	7.02 (2H, *d*, 8.7)

3.2.3 2-[(*E*)-2-(3-Hydroxy-4-methoxyphenyl)ethenyl]-1-methylquinolinium iodide (PM-C3)

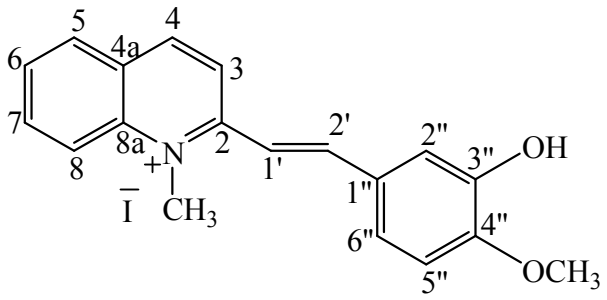

PM-C3

Compound **PM-C3** was synthesized as a red-brown crystal (64% yield), mp. 218-220 °C. The UV-Vis absorption bands (**Fig. 30**) appeared at 216.1, 306.2 and 431.3 nm. The IR spectrum (**Fig. 31**) displayed stretching vibrations of O-H (3424 cm^{-1}), C=C (1612 and 1583 cm^{-1}) and C-O (1235 cm^{-1}).

The ^{1}H NMR spectrum (**Fig. 29**, see **Table 3**) showed characteristic of *trans*-disubstituted double bonds at δ 7.69 (1H, *d*, *J* = 15.9 Hz, H-1′) and δ 8.09 (1H, *d*, *J* = 15.9 Hz, H-2′).Two *singlet* signals at δ 4.65 (3H) and δ 3.95 (3H) were assigned as *N*-CH_3 and *O*-CH_3, respectively. Three signals of 1,3,4-trisubstituted benzene pattern at δ 7.49 (1H, *d*, *J* = 2.1 Hz), δ 7.36 (1H, *d*, *J* = 8.4 Hz) and δ 7.41 (1H, *br d*, *J* = 8.4 Hz) were assigned to H-2″, H-5″ and H-6″, respectively. Two *doublet* signals at δ 8.95 (1H, *J* = 9.0 Hz) and δ 8.52 (1H, *J* = 9.0 Hz) were the signals of H-4 and H-3, respectively. ^{1}H NMR spectrum also further showed the signals of aromatic protons of H-5 (δ 8.32), H-6 (δ 7.93), H-7 (δ 8.18) and H-8 (δ 8.49). Accordingly, compound **PM-C3** was considered to be 2-[(*E*)-2-(3-hydroxy-4-methoxyphenyl)ethenyl]-1-methylquinolinium iodide.

Table 3 ^{1}H NMR of compound **PM-C3**

Position	**δ_H (ppm), *mult*, *J* (Hz)**
1-CH_3	4.65 (3H, *s*)
3	8.52 (1H, *d*, 9)
4	8.95 (1H, *d*, 9)
5	8.32 (1H, *d*, 7.5)
6	7.93 (1H, *t*, 7.5)
7	8.18 (1H, *dt*, 1.5, 7.5)
8	8.49 (1H, *d*, 7.5)
1′	7.69 (1H, *d*, 15.9)
2′	8.09 (1H, *d*, 15.9)
2″	7.49 (1H, *d*, 2.1)
4″-OCH_3	3.95 (3H, *s*)
5″	7.36 (1H, *d*, 8.4)
6″	7.41 (1H, *br d*, 8.4)

3.2.4 2-[(*E*)-2-(4-Hydroxy-3-methoxyphenyl)ethenyl]-1-methylquinolinium iodide (PM-C4)

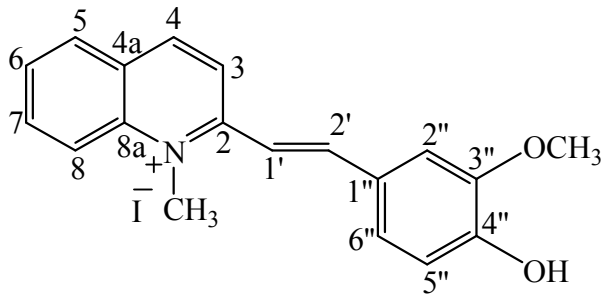

PM-C4

Compound **PM-C4** is a dark red crystal (68% yield), mp. 248-250 °C. The UV-visible spectrum (**Fig. 27**) showed maximum absorptions at 215.3, 308.9, 440.1 and 576.5 nm. The IR spectrum (**Fig. 28**) exhibited stretching vibrations of O-H (3439 cm^{-1}), C=C (1609 and 1580 cm^{-1}) and C-O (1233 cm^{-1}).

The ^{1}H NMR spectrum (**Fig. 32**, see **Table 4**) showed characteristic of *trans*-disubstituted double bonds at δ 7.73 (1H, *d*, *J* = 15.6 Hz, H-1′) and δ 8.17 (1H, *d*, *J* = 15.6 Hz, H-2′).Three *singlet* signals at δ 10.02 (1H), δ 4.62 (3H) and δ 3.95 (3H) were assigned as OH, *N*-CH_3 and *O*-CH_3. Three signals of 1,3,4-trisubstituted benzene pattern at δ 7.58 (1H, *d*, *J* = 1.8 Hz), δ 6.93 (1H, *d*, *J* = 8.1 Hz) and δ 7.41 (1H, *dd*, *J* = 1.8, 8.1 Hz) were assigned to H-2″, H-5″ and H-6″, respectively. Two *doublet* signals at δ 8.94 (1H, *J* = 9.0 Hz) and δ 8.53 (1H, *J* = 9.0 Hz) were the signals of H-4 and H-3, respectively. ^{1}H NMR spectrum also showed resonances of aromatic protons H-5 (δ 8.30), H-6 (δ 7.90), H-7 (δ 8.15) and H-8 (δ 8.50). Accordingly, compound **PM-C4** was assigned to be 2-[(*E*)-2-(4-hydroxy-3-methoxyphenyl)ethenyl]-1-methylquinolinium iodide.

Table 4 ^{1}H NMR of compound **PM-C4**

Position	**δ_H (ppm), *mult*, *J* (Hz)**
1-CH_3	4.62 (3H, *s*)
3	8.53 (1H, *d*, 9)
4	8.94 (1H, *d*, 9)
5	8.30 (1H, *dd*, 1.2, 7.5)
6	7.90 (1H, *t*, 7.5)
7	8.15 (1H, *dt*, 1.2, 7.5)
8	8.50 (1H, *d*, 7.5)
1′	7.73 (1H, *d*, 15.6)
2′	8.17 (1H, *d*, 15.6)
2″	7.58 (1H, *d*, 1.8)
3″-OCH_3	3.95 (3H, *s*)
4″- OH	10.02 (1H, *s*)
5″	6.93 (1H, *d*, 8.1)
6″	7.41 (1H, *dd*, 1.8, 8.1)

3.2.5 2-[(*E*)-2-(4-Hydroxyphenyl)ethenyl]-1-methylquinolinium iodide (PM-C5)

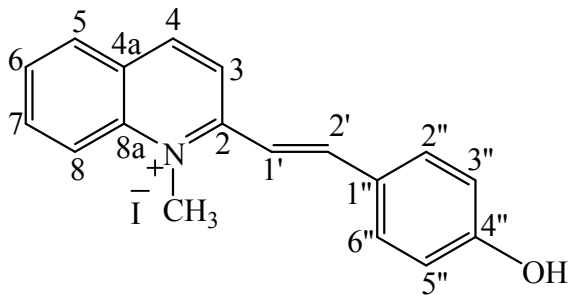

PM-C5

Compound **PM-C5** is a brown solid (73% yield), mp. 192-194 °C. The UV-visible spectrum (**Fig. 33**) showed maximum absorptions at 218.3, 258.9 and 425.1 nm. The IR spectrum (**Fig. 34**) exhibited stretching vibrations of O-H (3447 cm^{-1}), C=C (1576 cm^{-1}) and C-O (1220 cm^{-1}).

The ^{1}H NMR spectrum (**Fig. 35**, see **Table 5**) showed characteristic of *trans*-disubstituted double bonds at δ 7.02 (1H, *d*, *J* = 15.3 Hz, H-1′) and δ 7.98 (1H, *d*, *J* = 15.3 Hz, H-2′).The *singlet* signal at δ 4.35 (3H) was assigned as *N*-CH_3. Two signals of 4-substituted benzene pattern at δ 7.68 (2H, *d*, *J* = 9.0 Hz) and δ 6.72 (2H, *d*, *J* = 9.0 Hz) were assigned to H-2″, H-6″, H-3″ and H-5″, respectively. Two *doublet* signals at δ 8.47 (1H, *J* = 9.0 Hz) and δ 8.22 (1H, *J* = 9.0 Hz) were the signals of H-4 and H-3, respectively. ^{1}H NMR spectrum also showed resonances of aromatic protons H-5 (δ 8.05), H-6 (δ 7.72), H-7 (δ 8.01) and H-8 (δ 8.15). Accordingly, compound **PM-C5** was assigned to be 2-[(*E*)-2-(4-hydroxyphenyl)ethenyl]-1-methylquinolinium iodide.

Table 5 ^{1}H NMR of compound **PM-C5**

Position	**δ_H (ppm), *mult*, *J* (Hz)**
1-CH_3	4.35 (3H, *s*)
3	8.22 (1H, *d*, 9.0)
4	8.47 (1H, *d*, 9.0)
5	8.05 (1H, *br d*, 8.1)
6	7.72 (1H, *dd*, 7.2, 8.1)
7	8.01 (1H, *ddd*, 1.5, 7.2, 8.4)
8	8.15 (1H, *d*, 8.4)
1′	7.02 (1H, *d*, 15.3)
2′	7.98 (1H, *d*, 15.3)
2″ 6″	7.68 (2H, *d*, 9.0)
3″ 5″	6.72 (2H, *d*, 9.0)

3.2.6 2-[(*E*)-2-(4-Methoxyphenyl)ethenyl]-1-methylquinolinium iodide (PM-C6)

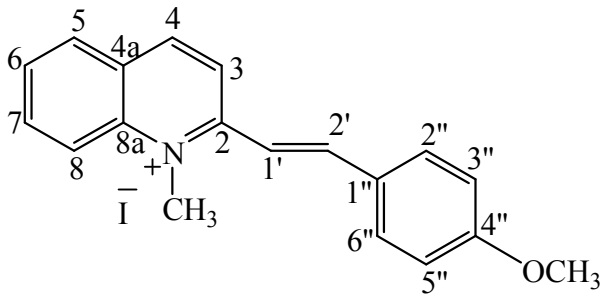

PM-C6

Compound **PM-C6** was synthesized as brown solid (67% yield), mp. 225-226 °C. The UV-Vis absorption bands (**Fig. 36**) appeared at 217.3 and 407.6 nm. The IR spectrum (**Fig. 37**) displayed stretching vibrations of C=C (1569-1595cm^{-1}) and C-O (1221 cm^{-1}).

The ^{1}H NMR spectrum (**Fig. 38**, see **Table 6**) showed characteristic of *trans*-disubstituted double bonds at δ 7.72 (1H, *d*, *J* = 15.6 Hz, H-1′) and δ 8.10 (1H, *d*, *J* = 15.6 Hz, H-2′).Two *singlet* signals at δ 4.62 (3H) and δ 3.91 (3H) were assigned as *N*-CH_3 and *O*-CH_3, respectively. Two signals of 4-substituted benzene pattern at δ 7.90 (2H, *d*, *J* = 8.7 Hz) and δ 7.04 (2H, *d*, *J* = 8.7 Hz) were assigned to H-2″, H-6″, H-3″ and H-5″, respectively. Two *doublet* signals at δ 8.91 (1H, *J* = 9.0 Hz) and δ 8.47 (1H, *J* = 9.0 Hz) were the signals of H-4 and H-3, respectively. ^{1}H NMR spectrum also further showed the signals of aromatic protons of H-5 (δ 8.27), H-6 (δ 7.92), H-7 (δ 8.17) and H-8 (δ 8.42). Accordingly, compound **PM-C6** was considered to be 2-[(*E*)-2-(4-methoxyphenyl)ethenyl]-1-methylquinolinium iodide.

Table 6 ^{1}H NMR of compound **PM-C6**

Position	**δ_H (ppm), *mult*, *J* (Hz)**
1-CH_3	4.62 (3H, *s*)
3	8.47 (1H, *d*, 9.0)
4	8.91 (1H, *d*, 9.0)
5	8.27 (1H, *br d*, 8.1)
6	7.92 (1H, *t*, 8.1)
7	8.17 (1H, *dt*, 1.5, 8.1)
8	8.42 (1H, *d*, 8.1)
1′	7.72 (1H, *d*, 15.6)
2′	8.10 (1H, *d*, 15.6)
2″ 6″	7.90 (2H, *d*, 8.7)
3″ 5″	7.04 (2H, *d*, 8.7)
4″-OCH_3	3.91 (3H, *s*)

3.3 Structural elucidations of anions counter parts

3.3.1 Silver (I) 4-methylbenzenesulfonate (An-CH_3)

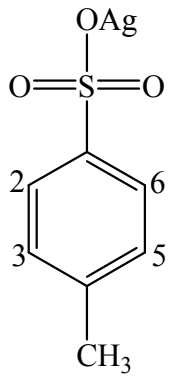

An-CH_3

A white solid of compound **An-CH_3** was obtained in 71% yield which decomposed at 264-266 °C. The ^{1}H NMR spectrum (**Fig.39**) showed equivalent protons of *p*-disubstituted aromatic at δ 7.74 (2H, *d*, *J* = 8.1 Hz, H-2, H-6) and 7.17 (2H, *d*, *J* = 8.1 Hz, H-3, H-5). A *singlet* signal of 4-CH_3 was observed at δ 2.38 ppm. Therefore, compound **An-CH_3** was identified to be silver (I) 4-methylbenzenesulfonate.

3.3.2 Silver (I) 4-methoxybenzenesulfonate (An-OCH_3)

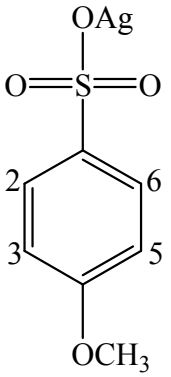

An-OCH_3

Compound **An-OCH_3** was obtained as a white solid, decomposed at 240-242°C. The ^{1}H NMR spectrum (**Fig. 40**) showed two *doublet* signals of H-2, H-6 and H-3, H-5 at δ 7.78 (2H, J = 8.7 Hz) and δ 6.86 (2H, J = 8.7 Hz) respectively. The *singlet* signal of 4-OCH_3 appeared at δ 3.82 (3H). Therefore, compound **An-OCH_3** was assigned to be silver (I) 4-methoxybenzenesulfonate.

3.3.3 Silver (I) 4-chlorobenzenesulfonate (An-Cl)

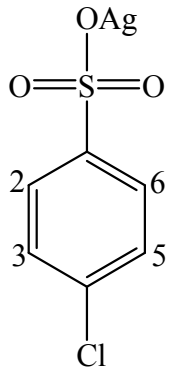

An-Cl

Compound **An-Cl** was synthesized as a white solid, decomposed at 227-229 °C. The ^{1}H NMR spectrum (**Fig. 41**) exhibited only two *doublet* signals of AA′ BB′ pattern at δ 7.76 (H-2, H-6) and δ 7.50 (H-3, H-5) with coupling constant of 7.8 Hz which indicated the location of Cl at C-4. Thus, compound **An-Cl** was considered to be silver (I) 4-chlorobenzenesulfonate.

3.3.4 Silver (I) 4-bromobenzenesulfonate (An-Br)

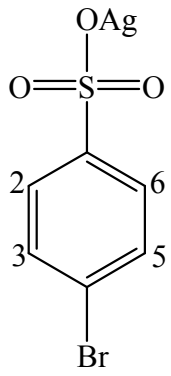

An-Br

Compound **An-Br** was received as a white solid, decomposed at 230-232 °C. The ^{1}H NMR spectrum (**Fig. 42**) exhibited only two *doublet*s of AA′ BB′ pattern at δ 7.81 (H-2, H-6) and δ 7.34 (H-3, H-5) with coupling constant of 8.4 Hz which indicated the location of Br at C-4. Accordingly, compound **An-Br** was assigned as silver (I) 4-bromobenzenesulfonate.

3.4 Structural elucidations of Salts

3.4.1 4-[(*E*)-2-(2-Thienyl)ethenyl]-1-methylpyridinium 4-methylbenzenesulfonate (PM-C1Me)

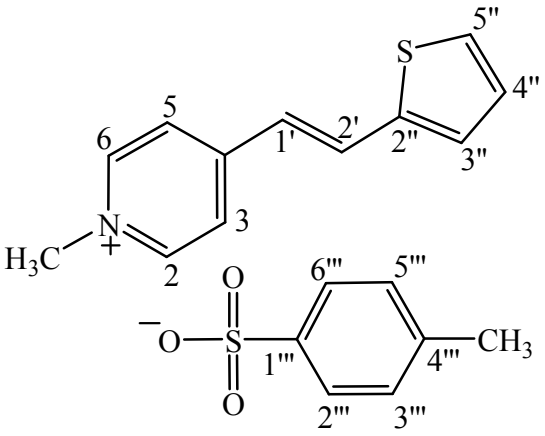

PM-C1Me

Compound **PM-C1Me** was obtained as a brown crystals (75% yield), mp. 232-234 °C. The UV-Vis absorption spectra (**Fig. 43**) showed maximum bands at 220.9, 251.4 and 379.2 nm. The IR spectrum (**Fig. 44**) exhibited stretching vibrations of C=C (1523 cm^{-1}) and S=O in sulfonates (1186 cm^{-1}).

The ^{1}H NMR spectrum (**Fig. 45,** see **Table 7**) showed two fragments of cationic and anionic parts. The former showed characteristic of *trans*-disubstituted double bonds at δ 6.91 (1H, *d*, *J* = 15.6 Hz, H-1′) and δ 7.94 (1H, *d*, *J* = 15.6 Hz, H-2′). The *singlet* signal at δ 4.22 (3H) was assigned as *N*-CH$_3$. Equivalent protons of *p*-disubstituted aromatic appeared as two *doublet* signals at δ 8.72 (2H, *J* = 6.9 Hz, H-2, H-6) and δ 7.93 (2H, *J* = 6.9 Hz, H-3, H-5). Three signals of thiophene ring at

δ 7.37 (1H, *d*, *J* = 5.1 Hz), δ 7.04 (1H, *t*, *J* = 5.1 Hz) and δ 7.49 (1H, *d*, *J* = 5.1 Hz) were assigned to H-3″, H-4″ and H-5″, respectively. ^{1}H NMR spectrum also showed resonances of aromatic protons of anionic part at δ 7.59 (2H, *d*, *J* = 8.4 Hz, H-2‴, H-6‴) and δ 7.01 (2H, *d*, *J* = 8.4 Hz, H-3‴, H-5‴). The *singlet* signal of 4‴-OCH_3 appeared at δ 3.95 (3H). These observations confirmed the structure of compound **PM-C1Me**.

The crystal structure of **PM-C1Me** is illustrated in **Fig. 7** and **Fig. 8** which show the packing diagram of **PM-C1Me** and intermolecular hydrogen bondings. The crystal and experiment data are given in **Table 8**. Bond lengths and angles are shown in **Table 9.** The X-ray study shows that **PM-C1Me** crystallized out in centrosymmetric space group ***P*$\bar{1}$.**

The asymmetric unit of the **PM-C1Me** compound consists of the $C_{12}H_{12}NS^+$ cation and the $C_7H_7O_3S^-$ anion. The cation exists in an *E* configuration with respect to the ethenyl C=C bond[C6=C7 = 1.346(3) Å]. The cation is essentially planar with a dihedral angle between the pyridinium and thiophene rings of 1.94(1)°. The orientation of the anion with respect to the cation can be indicated by the interplanar angles between the benzene ring [C13—C18] with the pyridinium [C1—C5/N1] and thiophene [C8—C11/S1] rings of 75.23(1) and 76.83(1)°, respectively. The ethenyl unit is nearly coplanar with the pyridinium and thiophene rings with the torsion angles C4—C5—C6—C7 = 3.0(3)° and C6—C7—C8—S1 = -3.7(3)°. The atom O3 of the sulfonate and the S1 atom of the thiophene contribute to the weak intramolecular C—H···O and C—H···S interactions (**Fig. 7** and **Table 10**), forming S(5) ring motifs (Bernstein *et al*., 1995).

All the O atoms of 4-methylbenzenesulfonate anion are involved in the C—H···O weak interaction (**Table 10**). In the crystal packing (**Fig. 8**), the cations and anions form alternate layers parallel to the *bc* plane. Within each layer both cations and anions are arranged into chains directed along the *b* axis. The cations and anions chains are interconnected by C—H···O weak interactions into a three dimensional network. The crystal structure is future stabilized by the C4—H4A···π and C10—H10A···π interactions (**Table 10**); Cg1 is the centroid of the C13—C18 benzene ring.

Table 7 ^{1}H NMR of compound **PM-C1Me**

Position	**δ_H (ppm), *mult*, *J* (Hz)**
1-CH_3	4.22 (3H, *s*)
2 6	8.72 (2H, *d*, 6.9)
3 5	7.93 (2H, *d*, 6.9)
1′	6.91 (1H, *d*, 15.6)
2′	7.94 (1H, *d*, 15.6)
3″	7.37 (1H, *d*, 5.1 Hz)
4″	7.04 (1H, *t*, 5.1 Hz)
5″	7.49 (1H, *d*, 5.1 Hz)
2‴ 6‴	7.59 (2H, *d*, 8.4)
3‴ 5‴	7.01 (2H, *d*, 8.4)
4‴-CH_3	3.95 (3H, *s*)

Table 8 Crystal data of **PM-C1Me**.

Identification code	**PM-C1Me**
Empirical formula	$C_{19}H_{19}NO_3S_2$
Formula weight	373.47
Temperature	100.0(1) K
Wavelength	0.71073 Å
Crystal system, space group	Triclinic, $P\bar{1}$
Unit cell dimensions	a = 9.2947(1) Å α = 87.817(1) °
	b = 9.6144(1) Å β = 64.702(1) °
	c = 10.779(1) Å γ = 88.712(1) °
Volume	870.214(15) $Å^3$
Z, Calculated density	2, 1.425 Mg/m^3
Absorption coefficient	0.324 mm^{-1}
F(000)	392
Crystal size	0.36 x 0.35 x 0.18 mm
Theta range for data collection	2.42 to 29.00 °
Limiting indices	-12<=h<=12, -13<=k<=13, -14<=l<=14
Reflections collected / unique	18024 / 4606 [R(int) = 0.0231]
Completeness to theta = 29.00	99.6 %
Max. and min. transmission	0.9451 and 0.8927
Refinement method	Full-matrix least-squares on F^2
Data / restraints / parameters	4606 / 0 / 228
Goodness-of-fit on F^2	1.044
Final R indices [I>2σ(I)]	*R1* = 0.0514, *wR2* = 0.1439
R indices (all data)	*R1* = 0.0565, *wR2* = 0.1485
Largest diff. peak and hole	0.291 and -0.253 e.$Å^3$

Table 9 Bond lengths [Å] and angles [°] for **PM-C1Me**

S1-C11	1.707(2)	C9-C10	1.484(3)
S1-C8	1.715(2)	C9-H9A	0.9300
S2-O2	1.4569(15)	C10-C11	1.362(3)
S2-O3	1.4574(14)	C10-H10A	0.93
S2-O1	1.4587(14)	C11-H11A	0.93
S2-C16	1.7769(18)	C12-H12A	0.96
N1-C3	1.351(2)	C12-H12B	0.96
N1-C2	1.352(3)	C12-H12C	0.96
N1-C12	1.479(3)	C13-C18	1.394(3)
C1-C2	1.367(3)	C13-C14	1.398(3)
C1-C5	1.400(3)	C13-C19	1.504(3)
C1-H1A	0.93	C14-C15	1.391(3)
C2-H2A	0.93	C14-H14A	0.93
C3-C4	1.371(3)	C15-C16	1.393(3)
C3-H3A	0.93	C15-H15A	0.93
C4-C5	1.403(3)	C16-C17	1.393(3)
C4-H4A	0.93	C17-C18	1.393(3)
C5-C6	1.458(3)	C17-H17A	0.93
C6-C7	1.346(3)	C18-H18A	0.93
C6-H6A	0.9300	C19-H19A	0.96
C7-C8	1.447(3)	C19-H19B	0.96
C7-H7A	0.93	C19-H19C	0.96
C8-C9	1.357(3)		
O2-S2-O3	112.96(8)	C11-S1-C8	92.72(11)
O2-S2-O1	113.06(9)	C3-N1-C12	118.95(17)
O3-S2-O1	113.19(9)	C2-N1-C12	120.41(17)
O2-S2-C16	105.46(9)	C2-C1-C5	120.85(18)
O3-S2-C16	105.73(9)	C2-C1-H1A	119.6
O1-S2-C16	105.54(8)	C5-C1-H1A	119.6

Table 9 (Continued)

C3-N1-C2	120.63(17)	N1-C12-H12A	109.5
N1-C2-C1	120.52(18)	N1-C12-H12B	109.5
N1-C2-H2A	119.7	H12A-C12-H12B	109.5
C1-C2-H2A	119.7	N1-C12-H12C	109.5
N1-C3-C4	120.49(18)	H12A-C12-H12C	109.5
N1-C3-H3A	119.8	H12B-C12-H12C	109.5
C4-C3-H3A	119.8	C18-C13-C14	118.08(18)
C3-C4-C5	120.62(18)	C18-C13-C19	121.03(18)
C3-C4-H4A	119.7	C14-C13-C19	120.87(18)
C5-C4-H4A	119.7	C15-C14-C13	121.46(18)
C1-C5-C4	116.87(18)	C15-C14-H14A	119.3
C1-C5-C6	117.82(18)	C13-C14-H14A	119.3
C4-C5-C6	125.3(19)	C14-C15-C16	119.38(17)
C7-C6-C5	123.75(19)	C14-C15-H15A	120.3
C7-C6-H6A	118.1	C16-C15-H15A	120.3
C5-C6-H6A	118.1	C15-C16-C17	120.27(17)
C6-C7-C8	126.6(2)	C15-C16-S2	119.07(14)
C6-C7-H7A	116.7	C17-C16-S2	120.61(14)
C8-C7-H7A	116.7	C16-C17-C18	119.45(17)
C9-C8-C7	122.8(2)	C16-C17-H17A	120.3
C9-C8-S1	112.58(16)	C18-C17-H17A	120.3
C7-C8-S1	124.57(17)	C17-C18-C13	121.35(18)
C8-C9-C10	110.76(17)	C17-C18-H18A	119.3
C8-C9-H9A	124.6	C13-C18-H18A	119.3
C10-C9-H9A	124.6	C13-C19-H19A	109.5
C11-C10-C9	112.07(19)	C13-C19-H19B	109.5
C11-C10-H10A	124.	H19A-C19-H19B	109.5
C9-C10-H10A	124.	C13-C19-H19C	109.5
C10-C11-S1	111.84(17)	H19A-C19-H19C	109.5
C10-C11-H11A	124.1	H19B-C19-H19C	109.5
S1-C11-H11A	124.1		

Table 10 Hydrogen-bond geometry (Å, °)

D—H···*A*	D—H	H···*A*	D···*A*	D—H···*A*
C2—H2A···O3^{i}	0.93	2.31	3.219(3)	166
C3—H3A···O1^{ii}	0.93	2.49	3.168(2)	130
C6—H6A···O2	0.93	2.56	3.378(3)	147
C11—H11A···O1^{iii}	0.93	2.54	3.303(3)	139
C12—H12A···O1^{i}	0.96	2.52	3.455(3)	165
C12—H12A···O1^{ii}	0.96	2.47	3.341(3)	151
C15—H15A···O2^{iv}	0.93	2.42	3.272(2)	152
C17—H17A···O3^{i}	0.93	2.43	3.202(2)	141
C4—H4A···Cg1^{v}	0.93	2.62	3.431(2)	145
C10—H10A···Cg1^{vi}	0.93	2.95	3.666(3)	135

Symmetry codes: (i) –x+1, -y+1, -z+1; (ii) x-1, y, z+1; (iii) –x+1, -y+2, -z; (iv) -x+1, -y+1, -z; (v) –x, -y+1, -z+1; (vi) x-1, y+1, z. Cg1 is the centroid of the C13—C18 benzene ring.

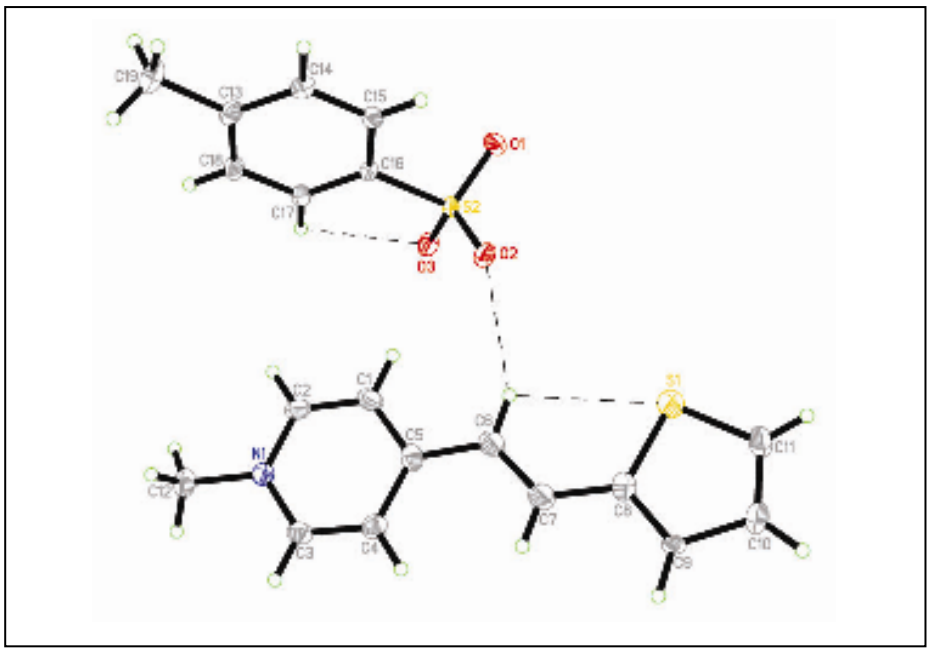

Figure 7 X-ray ORTEP diagram of the compound **PM-C1Me**

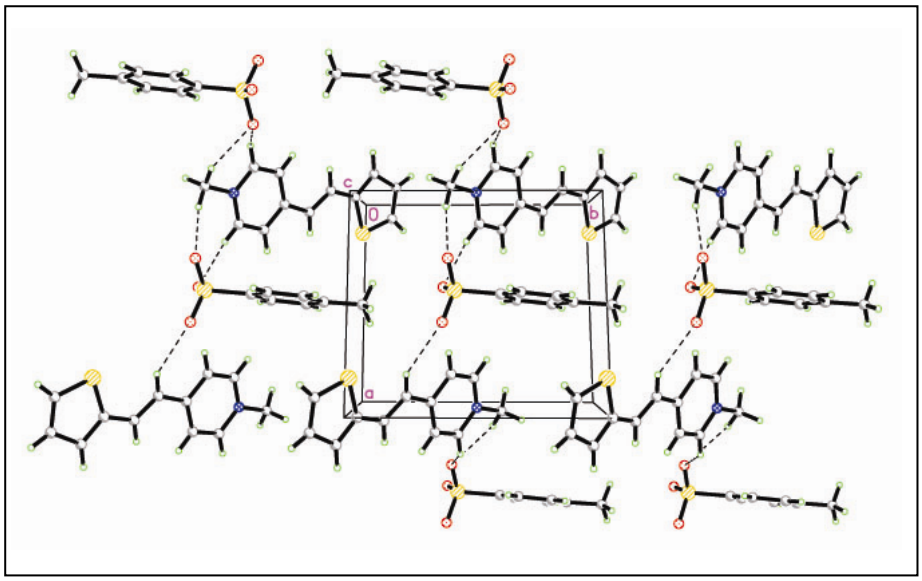

Figure 8 Packing diagram of **PM-C1Me** viewed down the *a* axis with H-bonds shown as dashed lines.

3.4.2 4-[(*E*)-2-(2-Thienyl)ethenyl]-1-methylpyridinium 4-methoxybenzenesulfonate (PM-C1OMe)

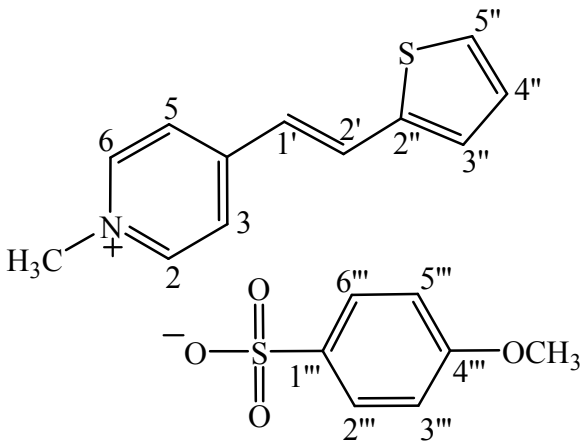

PM-C1OMe

Compound **PM-C1OMe** was obtained as a yellow solid (87% yield), mp. 234-236 °C. The UV-Vis absorption spectra (**Fig. 46**) showed maximum bands at 230.2 and 381.1 nm. The IR spectrum (**Fig. 47**) exhibited stretching vibrations of C=C (1590 cm^{-1}) and S=O in sulfonates (1188 cm^{-1}).

The ^{1}H NMR spectrum (**Fig. 48,** see **Table 11**) showed two fragments of cationic and anionic parts. The former showed characteristic of *trans*-disubstituted double bonds at δ 6.99 (1H, *d*, *J* = 15.6 Hz, H-1′) and δ 8.01 (1H, *d*, *J* = 15.6 Hz, H-2′). The *singlet* signal at δ 4.43 (3H) was assigned as *N*-CH_3. Equivalent protons of *p*-disubstituted aromatic appeared as two *doublet* signals at δ 8.82 (2H, *J* = 6.9 Hz, H-2, H-6) and δ 7.98 (2H, *J* = 6.9 Hz, H-3, H-5). Three signals of thiophene ring at δ 7.46 (1H, *d*, *J* = 5.1 Hz), δ 7.16 (1H, *t*, *J* = 5.1 Hz) and δ 7.57 (1H, *d*, *J* = 5.1 Hz) were assigned to H-3″, H-4″ and H-5″, respectively. ^{1}H NMR spectrum also showed resonances of aromatic protons of anionic part at δ 7.77 (2H, *d*, *J* = 8.4 Hz, H-2‴, H-6‴) and δ 6.81 (2H, *d*, *J* = 8.4 Hz, H-3‴, H-5‴). The *singlet* signal of 4‴-OCH_3 appeared at δ 3.79 (3H). These observations confirmed that **PM-C1OMe** is 4-[(*E*)-2-(2-thienyl)ethenyl]-1-methylpyridinium 4-methoxybenzenesulfonate.

Table 11 ^{1}H NMR of compound **PM-C1OMe**

Position	**δ_H (ppm), *mult*, *J* (Hz)**
1-CH_3	4.43 (3H, *s*)
2 6	8.82 (2H, *d*, 6.9)
3 5	7.98 (2H, *d*, 6.9)
1′	6.99 (1H, *d*, 15.6)
2′	8.01 (1H, *d*, 15.6)
3″	7.46 (1H, *d*, 5.1 Hz)
4″	7.16 (1H, *t*, 5.1 Hz)
5″	7.57 (1H, *d*, 5.1 Hz)
2‴ 6‴	7.77 (2H, *d*, 8.4)
3‴ 5‴	6.81 (2H, *d*, 8.4)
4‴-OCH_3	3.79 (3H, *s*)

3.4.3 4-[(*E*)-2-(2-Thienyl)ethenyl]-1-methylpyridinium 4-chlorobenzenesulfonate (PM-C1Cl)

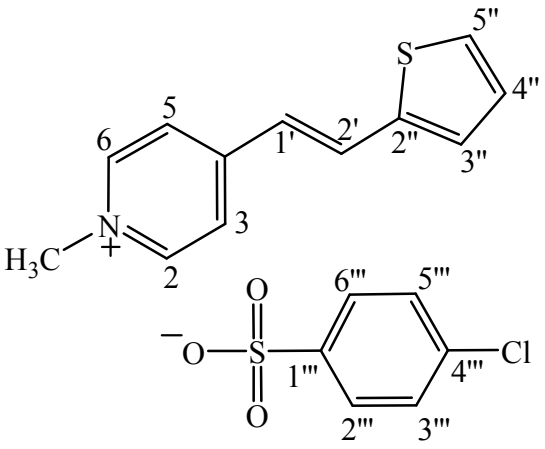

PM-C1Cl

Compound **PM-C1Cl** was obtained as a brown crystals (90% yield), mp. 230-232 °C. The UV-Vis absorption spectra (**Fig. 49**) showed maximum bands at 220.9, 251.4 and 379.2 nm. The IR spectrum (**Fig. 50**) exhibited stretching vibrations of C=C (1523 cm^{-1}) and S=O in sulfonates (1210 cm^{-1}).

The ^{1}H NMR spectrum (**Fig. 51,** see **Table 12**) showed two fragments of cationic and anionic parts. The former showed characteristic of *trans*-disubstituted double bonds at δ 6.99 (1H, *d*, *J* = 15.6 Hz, H-1′) and δ 8.02 (1H, *d*, *J* = 15.6 Hz, H-2′). The *singlet* signal at δ 4.34 (3H) was assigned as *N*-CH_3. Equivalent protons of *p*-disubstituted aromatic appeared as two *doublet* signals at δ 8.79 (2H, *J* = 6.9 Hz, H-2, H-6) and δ 8.01 (2H, *J* = 6.9 Hz, H-3, H-5). Three signals of thiophene ring at δ 7.47 (1H, *d*, *J* = 5.1 Hz), δ 7.14 (1H, *t*, *J* = 5.1 Hz) and δ 7.58 (1H, *d*, *J* = 5.1 Hz) were assigned to H-3″, H-4″ and H-5″, respectively. ^{1}H NMR spectrum also showed resonances of aromatic protons of anionic part at δ 7.79 (2H, *d*, *J* = 8.4 Hz, H-2‴, H-6‴) and δ 7.30 (2H, *d*, *J* = 8.4 Hz, H-3‴, H-5‴). These observations confirmed that **PM-C1Cl** is 4-[(*E*)-2-(2-thienyl)ethenyl]-1-methylpyridinium 4-chlorobenzene-sulfonate.

The crystal structure of **PM-C1Cl** is illustrated in **Fig. 9** and **Fig. 10** which show the packing diagram of **PM-C1Cl** and intermolecular hydrogen bondings. The crystal and experiment data are given in **Table 12**. Bond lengths and angles are shown in **Table 13.** The X-ray study shows that **PM-C1Cl** crystallized out in centrosymmetric space group $\boldsymbol{P2_1/c}$**.**

The asymmetric unit of the **PM-C1Cl** compound consists of the $C_{12}H_{12}NS^+$ cation and the $C_6H_4ClO_3S^-$ anion. The cation is almost planar and exists in the *E* configuration with respect to the C6=C7 double bond [1.334(3) Å]. The cation is almost perpendicular to the anion as is indicated by the angles between the mean planes of the chlorophenyl ring to the pyridinium as well as to the thiophene ring being 87.64(9)° and 86.73(9)°, respectively. The dihedral angle between the pyridinium and the thiophene rings is 5.74(10)°. The ethenyl unit is nearly planar. The torsion angles C4—C5—C6—C7 = -4.3(3)° and C6—C7—C8—S1 = -1.5(3)°.

The atom O3 of the sulfonate and the S atom of the thiophene contribute to the C—H···O and C—H···S intramolecular weak interactions (**Fig. 9** and **Table 15**) forming S(5) ring motifs (Bernstein *et al*., 1995).

All the O atoms of 4-chlorobenzenesulfonate anion are involved in the C—H···O weak interaction (**Table 15**). The cations and anions form alternate layers parallel to the *ab* plane. Within each respective layer, the ions are interconnected by C—H···O weak ineractions and in each respective layer can be distinguished chains directed along the *b* axis. The alternating layers are separated by 4.282(2) Å and are future linked into a three dimensional network by C—H···O weak interaction (**Table 15**). The sulfonate as well as the thiophene are involved in C—H···O and C—H···S intramolecular weak interactions, respectively. These weak hydrogen bonds participate in S(5) ring motifs.The crystal structure is future stabilized by the C12—H12B···π interaction to the thiophene ring C8—C11/S1: C12—H12B = 0.96; H12B···Cg1^{i} = 2.692; C12—Cg1^{i} = 3.515(2) Å; C12—H12B···Cg1^{i} = 144°. [Cg1^{i} is the centroid of the S1/C8—C11 thiophene ring (symmetry code: (i): 2-x, 2-y, 1-z).]

Table 12 ^{1}H NMR of compound **PM-C1Cl**

Position	**δ_H (ppm), *mult*, *J* (Hz)**
1-CH_3	4.34 (3H, *s*)
2 6	8.79 (2H, *d*, 6.9)
3 5	8.01 (2H, *d*, 6.9)
1′	6.99 (1H, *d*, 15.6)
2′	8.02 (1H, *d*, 15.6)
3″	7.47 (1H, *d*, 5.1 Hz)
4″	7.14 (1H, *t*, 5.1 Hz)
5″	7.58 (1H, *d*, 5.1 Hz)
2‴ 6‴	7.79 (2H, *d*, 8.4)
3‴ 5‴	7.3 (2H, *d*, 8.4)

Table 13 Crystal data of **PM-C1Cl**.

Identification code	**PM-C1Cl**
Empirical formula	$C_{18}H_{16}ClNO_3S_2$
Formula weight	393.89
Temperature	100.0(1) K
Wavelength	0.71073 Å
Crystal system, space group	Monoclinic, $P2_1/c$
Unit cell dimensions	a = 7.3532(1) Å α = 90°
	b = 14.025(2) Å β = 111.232(1)°
	c = 18.3755(2) Å γ = 90°
Volume	1766.41(4) $Å^3$
Z, Calculated density	1, 1.481 Mg/m^3
Absorption coefficient	0.470 mm^{-1}
F(000)	816
Crystal size	0.49 x 0.22 x 0.18 mm
Theta range for data collection	1.88 to 29.00 °
Limiting indices	-10<=h<=10, -19<=k<=19, -21<=l<=25
Reflections collected / unique	23692 / 4688 [R(int) = 0.0371]
Completeness to theta = 29.00	99.9 %
Max. and min. transmission	0.9206 and 0.8013
Refinement method	Full-matrix least-squares on F^2
Data / restraints / parameters	4688 / 0 / 227
Goodness-of-fit on F^2	1.057
Final R indices [I>2σ(I)]	*R1* = 0.0371, *wR2* = 0.0893
R indices (all data)	*R1* = 0.0469, *wR2* = 0.0944
Largest diff. peak and hole	0.567 and -0.424 $e.Å^3$

Table 14 Bond lengths [Å] and angles [°] for **PM-C1Cl**

S1-C11	1.7105(19)	C7-C8	1.443(3)
S1-C8	1.7335(18)	C7-H7A	0.93
S2-O1	1.4541(12)	C8-C9	1.366(2)
S2-O3	1.4550(12)	C9-C10	1.443(2)
S2-O2	1.4560(12)	C9-H9A	0.93
S2-C13	1.7806(16)	C10-C11	1.367(3)
Cl1-C1	1.7428(16)	C10-H10A	0.93
N1-C2	1.346(2)	C11-H11A	0.93
N1-C3	1.352(2)	C12-H12A	0.96
N1-C12	1.479(2)	C12-H12B	0.96
C1-C2	1.363(3)	C12-H12C	0.96
C1-C5	1.395(3)	C13-C18	1.388(2)
C1-H1A	0.93	C13-C14	1.393(2)
C2-H2A	0.93	C14-C15	1.390(2)
C3-C4	1.369(3)	C14-H14A	0.93
C3-H3A	0.93	C15-C16	1.393(2)
C4-C5	1.404(3)	C15-H15A	0.93
C4-H4A	0.93	C16-C17	1.381(2)
C5-C6	1.455(3)	C17-C18	1.393(2)
C6-C7	1.334(3)	C17-H17A	0.93
C6-H6A	0.93	C18-H18A	0.93
C11-S1-C8	91.87(9)	C2-N1-C12	120.78(16)
O1-S2-O3	113.77(7)	C3-N1-C12	119.34(16)
O1-S2-O2	112.64(7)	C2-C1-C5	120.86(18)
O3-S2-O2	112.86(7)	C2-C1-H1A	119.6
O1-S2-C13	105.32(7)	C5-C1-H1A	119.6
O3-S2-C13	105.65(7)	N1-C2-C1	121.28(17)
O2-S2-C13	105.68(7)	N1-C2-H2A	119.4
C2-N1-C3	119.87(16)	C1-C2-H2A	119.4

Table 14 (Continued)

N1-C3-C4	120.76(17)	S1-C11-H11A	123.9
N1-C3-H3A	119.6	N1-C12-H12A	109.5
C4-C3-H3A	119.6	N1-C12-H12B	109.5
C3-C4-C5	120.70(17)	H12A-C12-H12B	109.5
C3-C4-H4A	119.6	N1-C12-H12C	109.5
C5-C4-H4A	119.6	H12A-C12-H12C	109.5
C1-C5-C4	116.51(17)	H12B-C12-H12C	109.5
C1-C5-C6	119.63(17)	C18-C13-C14	120.17(15)
C4-C5-C6	123.86(17)	C18-C13-S2	120.39(13)
C7-C6-C5	124.26(17)	C14-C13-S2	119.44(12)
C7-C6-H6A	117.9	C15-C14-C13	120.28(15)
C5-C6-H6A	117.9	C15-C14-H14A	119.9
C6-C7-C8	126.54(17)	C13-C14-H14A	119.9
C6-C7-H7A	116.7	C14-C15-C16	118.36(15)
C8-C7-H7A	116.7	C14-C15-H15A	120.8
C9-C8-C7	124.44(16)	C16-C15-H15A	120.8
C9-C8-S1	111.55(13)	C17-C16-C15	122.2(15)
C7-C8-S1	124.01(14)	C17-C16-Cl1	118.91(12)
C8-C9-C10	112.16(15)	C15-C16-Cl1	118.89(13)
C8-C9-H9A	123.9	C16-C17-C18	118.65(15)
C10-C9-H9A	123.9	C16-C17-H17A	120.7
C11-C10-C9	112.22(16)	C18-C17-H17A	120.7
C11-C10-H10A	123.9	C13-C18-C17	120.27(15)
C9-C10-H10A	123.9	C13-C18-H18A	119.9
C10-C11-S1	112.19(14)	C17-C18-H18A	119.9
C10-C11-H11A	123.9		

Table 15 Hydrogen-bond geometry (Å, °)

D—H···*A*	D—H	H···*A*	D···*A*	D—H···*A*
C3—H3A···O3^{i}	0.93	2.31	3.211(2)	164
C6—H6A···S1	0.93	2.84	3.228(2)	106
C7—H7A···O1^{ii}	0.93	2.39	3.266(2)	157
C9—H9A···O3^{ii}	0.93	2.58	3.495(2)	166
C10—H10A···O2^{iii}	0.93	2.39	3.302(2)	167
C11—H11A···O2^{iv}	0.93	2.55	3.063(2)	115
C12—H12C···O2^{i}	0.96	2.39	3.344(2)	168
C17—H17A···O2^{iv}	0.93	2.41	3.318(2)	166
C18—H18A···O3	0.93	2.51	2.892(2)	105
C12—H12B···Cg1^{i}	0.96	2.69	3.515(2)	144

Symmetry codes: (i) –x+2, -y+2, -z+1; (ii) x, -y+3/2, z+1/2;
(iii) –x+2, -y+1, -z+1; (iv) x-1, y, z. Cg1 is the centroid of the S1/C8—C11 thiophene ring.

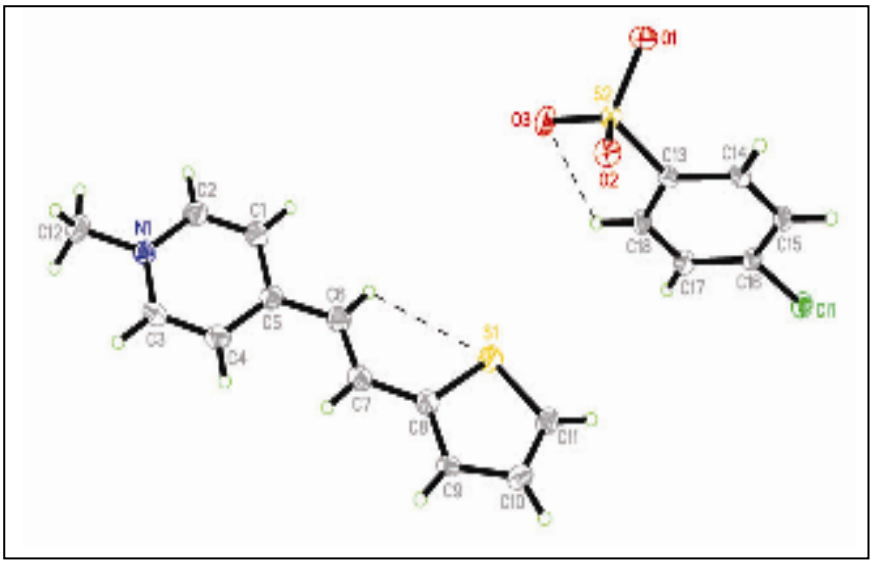

Figure 9 X-ray ORTEP diagram of the compound **PM-C1Cl**

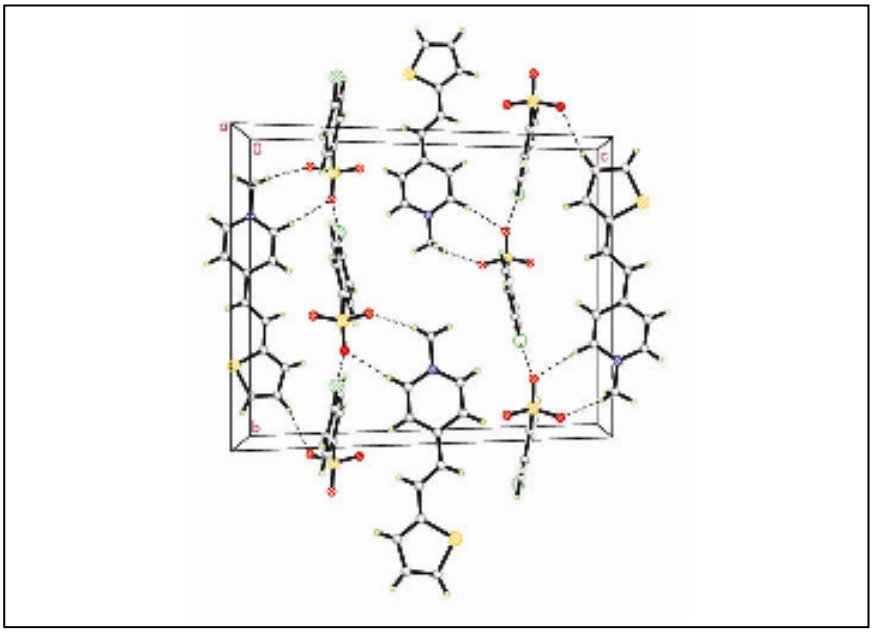

Figure 10 Packing diagram of **PM-C1Cl** viewed down the a axis with H-bonds shown as dashed lines.

3.4.4 4-[(*E*)-2-(2-Thienyl)ethenyl]-1-methylpyridinium 4-bromobenzenesulfonate (PM-C1Br)

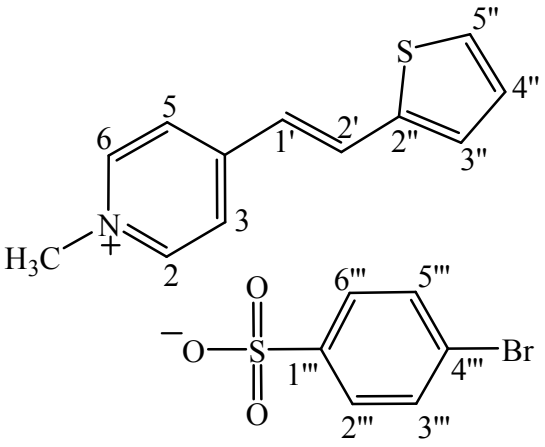

PM-C1Br

Compound **PM-C1Br** was obtained as a brown solid (70% yield), mp. 231-233 °C. The UV-Vis absorption spectra (**Fig. 52**) showed maximum bands at 222.3, 258.0 and 381.8 nm. The IR spectrum (**Fig. 53**) exhibited stretching vibrations of C=C (1577 cm^{-1}) and S=O in sulfonates (1208 cm^{-1}).

The ^{1}H NMR spectrum (**Fig. 54,** see **Table 16**) showed two fragments of cationic and anionic parts. The former showed characteristic of *trans*-disubstituted double bonds at δ 7.10 (1H, *d*, *J* = 15.6 Hz, H-1′) and δ 8.14 (1H, *d*, *J* = 15.6 Hz, H-2′). The *singlet* signal at δ 4.29 (3H) was assigned as *N*-CH_3. Equivalent protons of *p*-disubstituted aromatic appeared as two *doublet* signals at δ 8.82 (2H, *J* = 6.9 Hz, H-2, H-6) and δ 8.15 (2H, *J* = 6.9 Hz, H-3, H-5). Three signals of thiophene ring at δ 7.43 (1H, *d*, *J* = 5.1 Hz), δ 7.16 (1H, *t*, *J* = 5.1 Hz) and δ 7.62 (1H, *d*, *J* = 5.1 Hz) were assigned to H-3″, H-4″ and H-5″, respectively. ^{1}H NMR spectrum also showed resonances of aromatic protons of anionic part at δ 7.62 (2H, *d*, *J* = 8.4 Hz, H-2‴, H-6‴) and δ 7.43 (2H, *d*, *J* = 8.4 Hz, H-3‴, H-5‴). These observations confirmed that **PM-C1Br** is 4-[(*E*)-2-(2-thienyl)ethenyl]-1-methylpyridinium 4-bromobenzene-sulfonate.

Table 16 ^{1}H NMR of compound **PM-C1Br**

Position	**δ_H (ppm), *mult*, *J* (Hz)**
1-CH_3	4.29 (3H, *s*)
2 6	8.82 (2H, *d*, 6.9)
3 5	8.15 (2H, *d*, 6.9)
1′	8.14 (1H, *d*, 15.6)
2′	7.10 (1H, *d*, 15.6)
3″	7.43 (1H, *d*, 5.1 Hz)
4″	7.16 (1H, *t*, 5.1 Hz)
5″	7.62 (1H, *d*, 5.1 Hz)
2‴ 6‴	7.62 (2H, *d*, 8.4)
3‴ 5‴	7.43 (2H, *d*, 8.4)

3.4.5 2-[(*E*)-2-(4-Ethoxyphenyl)ethenyl]-1-methylquinolinium 4-methylbenzenesulfonate (PM-C2Me)

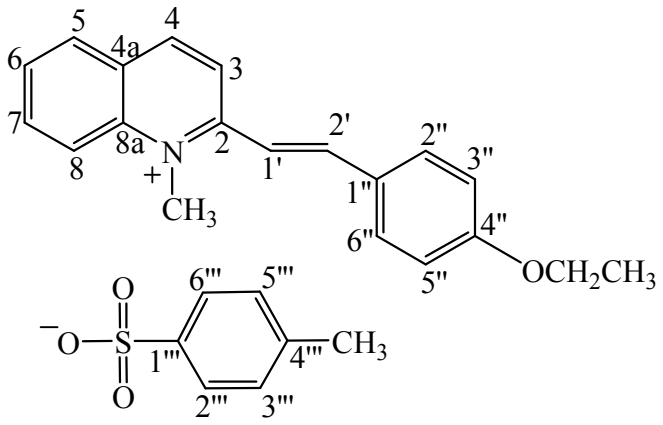

PM-C2Me

Compound **PM-C2Me** was obtained as a yellow solid (54% yield), mp. 250-252 °C. The UV-Vis absorption bands (**Fig. 55**) were shown at 202.7, 217.6, 256.2 and 413.9nm. The IR spectrum (**Fig. 56**) exhibited stretching vibrations of C=C (1592 cm^{-1}), C-O (1220 cm^{-1}) and S=O in sulfonates (1175 cm^{-1}).

The ^{1}H NMR spectrum (**Fig. 57,** see **Table 17**) showed two fragments of cationic and anionic parts. The former showed characteristic of *trans*-disubstituted double bonds at δ 7.69 (1H, *d*, *J* = 15.9 Hz, H-1′) and δ 8.09 (1H, *d*, *J* = 15.9 Hz, H-2′). The *singlet* signals at δ 4.53 (3H) was assigned as *N*-CH_3. The *triplet* and *quartet* signals at δ 1.49 (3H, *J* = 6.9 Hz) and δ 4.08 (2H, *J* = 6.9 Hz) were assigned as CH_3 and CH_2 of ethoxy, respectively. Two signals of 4-substituted benzene pattern at δ 7.83 (2H, *d*, *J* = 8.7 Hz) and δ 6.96 (2H, *d*, *J* = 8.7 Hz) were assigned to H-2″, H-6″, H-3″ and H-5″, respectively. Two *doublets* of H-3 and H-4 were observed at δ 8.43 (1H, *J* = 9.0 Hz) and δ 8.85 (1H, *J* = 9.0 Hz), respectively. Resonances of aromatic protons H-5, H-6, H-7 and H-8 were also shown at δ 8.22 (*d*, *J* = 7.5 Hz), δ 7.84 (*t*, *J* = 7.5 Hz), δ 8.09 (*t*, *J* = 7.5 Hz) and δ 8.39 (*d*, *J* = 7.5 Hz), respectively. ^{1}H NMR spectrum showed signals of anionic part. Equivalent protons of *p*-disubstituted aromatic appeared as two *doublets* at δ 7.57 (2H, *J* = 8.1 Hz, H-2‴, H-6‴) and δ 7.03 (2H, *J* = 8.1 Hz, H-3‴, H-5‴). The *singlet* signal of 4‴-CH_3 was observed

at δ 2.27 (3H). These spectroscopic data confirmed that **PM-C2Me** is 2-[(*E*)-2-(4-ethoxyphenyl)ethenyl]-1-methylquinolinium 4-methylbenzenesulfonate .

Table 17 ^{1}H NMR of compound **PM-C2Me**

Position	**δ_H (ppm), *mult*, *J* (Hz)**
1-CH_3	4.53 (3H, *s*)
CH_3	1.49 (3H, 6.9 Hz)
O-CH_2	4.08 (2H, 6.9 Hz)
3	8.43 (1H, 9.0 Hz)
4	8.85 (1H, 9.0 Hz)
5	8.22 (1H, *d*, 7.5 Hz)
6	7.84 (1H, *t*, 7.5 Hz)
7	8.09 (1H, *t*, 7.5 Hz)
8	8.39 (1H, *d*, 7.5 Hz)
1′	7.69 (1H, *d*, 15.9)
2′	8.09 (1H, *d*, 15.9)
2″ 6″	7.83 (2H, *d*, 8.7)
3″ 5″	6.96 (2H, *d*, 8.7)
2‴ 6‴	7.57 (2H, *d*, 8.1)
3‴ 5‴	7.03 (2H, *d*, 8.1)
4‴-CH_3	2.27 (3H, *s*)

3.4.6 2-[(*E*)-2-(4-Ethoxyphenyl)ethenyl]-1-methylquinolinium 4-methoxybenzenesulfonate (PM-C2OMe)

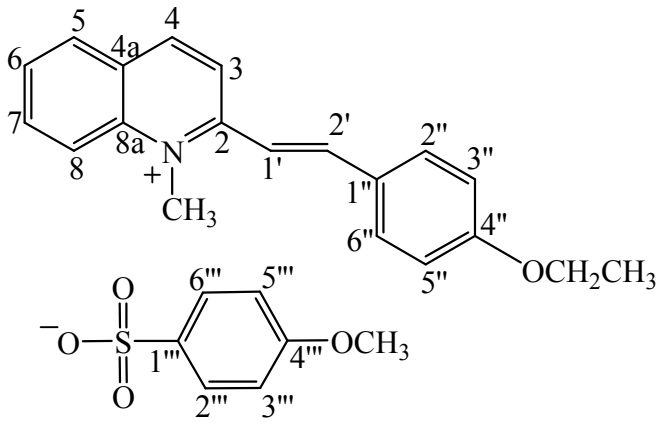

PM-C2OMe

Compound **PM-C2OMe** was obtained as a yellow solid (61% yield), mp. 256-257 °C. The UV-Vis absorption bands (**Fig. 58**) were shown at 330.3 and 413.1 nm. The IR spectrum (**Fig. 59**) exhibited stretching vibrations of C=C (1572 cm^{-1}), C-O (1220 cm^{-1}) and S=O in sulfonates (1164 cm^{-1}).

The ^{1}H NMR spectrum (**Fig. 60,** see **Table 18**) showed two fragments of cationic and anionic parts. The former showed characteristic of *trans*-disubstituted double bonds at δ 7.70 (1H, *d*, *J* = 15.8 Hz, H-1′) and δ 8.09 (1H, *d*, *J* = 15.8 Hz, H-2′). The *singlet* signals at δ 4.60 (3H) was assigned as *N*-CH_3. The *triplet* and *quartet* signals at δ 1.45 (3H, *J* = 6.9 Hz) and δ 4.13 (2H, *J* = 6.9 Hz) were assigned as CH_3 and CH_2 of ethoxy, respectively. Two signals of 4-substituted benzene pattern at δ 7.85 (2H, *d*, *J* = 8.7 Hz) and δ 6.80 (2H, *d*, *J* = 8.7 Hz) were assigned to H-2″, H-6″, H-3″ and H-5″, respectively. Two *doublets* of H-3 and H-4 were observed at δ 8.47 (1H, *J* = 9.0 Hz) and δ 8.89 (1H, *J* = 9.0 Hz), respectively. Resonances of aromatic protons H-5, H-6, H-7 and H-8 were also shown at δ 8.25 (*d*, *J* = 7.5 Hz), δ 7.89 (*t*, *J* = 7.5 Hz), δ 8.18 (*t*, *J* = 7.5 Hz) and δ 8.40 (*d*, *J* = 7.5 Hz), respectively. ^{1}H NMR spectrum showed signals of anionic part. Equivalent protons of *p*-disubstituted aromatic appeared as two *doublets* at δ 7.60 (2H, *J* = 8.7 Hz, H-2‴, H-6‴) and δ 7.01 (2H, *J* = 8.7 Hz, H-3‴, H-5‴). The *singlet* signal of 4‴-OCH□□3

was observed at δ 3.78 (3H). From these spectroscopic data **PM-C2OMe** was assigned to be 2-[(*E*)-2-(4-ethoxyphenyl)ethenyl]-1-methylquinolinium 4-methoxybenzene-sulfonate.

Table 18 ^{1}H NMR of compound **PM-C2OMe**

Position	**δ_H (ppm), *mult*, *J* (Hz)**
1-CH_3	4.60 (3H, *s*)
CH_3	1.45 (3H, 6.9 Hz)
O-CH_2	4.13 (2H, 6.9 Hz)
3	8.47 (1H, 9.0 Hz)
4	8.89 (1H, 9.0 Hz)
5	8.25 (1H, *d*, 7.5 Hz)
6	7.89 (1H, *t*, 7.5 Hz)
7	8.18 (1H, *t*, 7.5 Hz)
8	8.40 (1H, *d*, 7.5 Hz)
1′	7.70 (1H, *d*, 15.8)
2′	8.09 (1H, *d*, 15.8)
2″	7.85 (2H, *d*, 8.7)
6″	
3″	6.80 (2H, *d*, 8.7)
2‴	7.60 (2H, *d*, 8.1)
6‴	
3‴	7.01 (2H, *d*, 8.1)
5‴	
4‴-CH_3	3.78 (3H, *s*)

3.4.7 2-[(*E*)-2-(4-Ethoxyphenyl)ethenyl]-1-methylquinolinium 4-cholrobenzenesulfonate (PM-C2Cl)

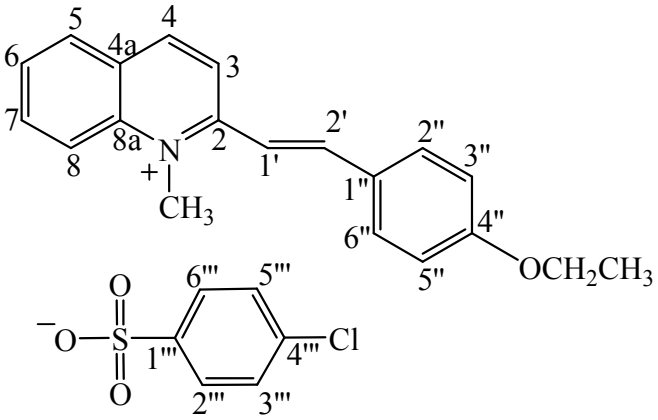

PM-C2Cl

Compound **PM-C2Cl** was obtained as a yellow crystals (62% yield), mp. 254-256 °C. The UV-Vis absorption bands (**Fig. 61**) were shown at 228.7, 268.4 and 410.2 nm. The IR spectrum (**Fig. 62**) exhibited stretching vibrations of C=C (15920 cm^{-1}), C-O (1225 cm^{-1}) and S=O in sulfonates (1153 cm^{-1}).

The ^{1}H NMR spectrum (**Fig. 63,** see **Table 19**) showed two fragments of cationic and anionic parts. The former showed characteristic of *trans*-disubstituted double bonds at δ 7.72 (1H, *d*, *J* = 15.9 Hz, H-1′) and δ 8.09 (1H, *d*, *J* = 15.9 Hz, H-2′). The *singlet* signals at δ 4.60 (3H) was assigned as *N*-CH_3. The *triplet* and *quartet* signals at δ 1.46 (3H, *J* = 6.9 Hz) and δ 4.18 (2H, *J* = 6.9 Hz) were assigned as CH_3 and CH_2 of ethoxy, respectively. Two signals of 4-substituted benzene pattern at δ 7.88 (2H, *d*, *J* = 8.7 Hz) and δ 7.05 (2H, *d*, *J* = 8.7 Hz) were assigned to H-2″, H-6″, H-3″ and H-5″, respectively. Two *doublets* of H-3 and H-4 were observed at δ 8.45 (1H, *J* = 9.0 Hz) and δ 8.90 (1H, *J* = 9.0 Hz), respectively. Resonances of aromatic protons H-5, H-6, H-7 and H-8 were also shown at δ 8.35 (*d*, *J* = 7.5 Hz), δ 7.91 (*t*, *J* = 7.5 Hz), δ 8.12 (*t*, *J* = 7.5 Hz) and δ 8.41 (*d*, *J* = 7.5 Hz), respectively. ^{1}H NMR spectrum showed signals of anionic part. Equivalent protons of *p*-disubstituted aromatic appeared as two *doublets* at δ 7.74 (2H, *J* = 8.1 Hz, H-2‴, H-6‴) and δ 7.30 (2H, *J* = 8.1 Hz, H-3‴, H-5‴). The *singlet* signal of 4‴-CH_3 was observed at δ 2.27 (3H). From these spectroscopic data **PM-C2Cl** was assigned

to be 2-[(*E*)-2-(4-ethoxyphenyl)ethenyl]-1-methylquinolinium 4-chlorobenzenesulfonate.

The crystal structure of **PM-C2Cl** is illustrated in **Fig. 11** and **Fig. 12** which show the packing diagram of **PM-C2Cl** and intermolecular hydrogen bondings. The crystal and experiment data are given in **Table 18**. Bond lengths and angles are shown in **Table 19.** It was found that **PM-C2Cl** crystallized out in non-centrosymmetric $\boldsymbol{P2_1}$ space group.

Table 19 ^{1}H NMR of compound **PM-C2Cl**

Position	$\boldsymbol{\delta_H}$ **(ppm),** ***mult*****,** ***J*** **(Hz)**
1-CH_3	4.60 (3H, *s*)
CH_3	1.46 (3H, 6.9 Hz)
O-CH_2	4.18 (2H, 6.9 Hz)
3	8.45 (1H, 9.0 Hz)
4	8.90 (1H, 9.0 Hz)
5	8.35 (1H, *d*, 7.5 Hz)
6	7.91 (1H, *t*, 7.5 Hz)
7	8.12 (1H, *t*, 7.5 Hz)
8	8.41 (1H, *d*, 7.5 Hz)
1′	7.72 (1H, *d*, 15.9)
2′	8.09 (1H, *d*, 15.9)
2″ 6″	7.78 (2H, *d*, 8.7)
3″ 5″	7.05 (2H, *d*, 8.7)
2‴ 6‴	7.74 (2H, *d*, 8.1)

3‴ 5‴	7.30 (2H, *d*, 8.1)

Table 20 Crystal data of **PM-C2Cl**.

Identification code	**PM-C2Cl**
Empirical formula	$C_{26}H_{28}ClNO_6S$
Formula weight	518.00
Temperature	100.0(1) K
Wavelength	0.71073 Å
Crystal system, space group	Monoclinic, $P2_1$
Unit cell dimensions	a = 9.8072(9) Å α = 90°
	b = 6.4848(5) Å β = 103.421(5) °
	c = 19.4405(16) Å γ = 90°
Volume	1202.61(17) $Å^3$
Z, Calculated density	2, 1.431 Mg/m^3
Absorption coefficient	0.290 mm^{-1}
F(000)	544
Crystal size	0.58 x 0.26 x 0.06 mm
Theta range for data collection	2.13 to 30.00 °
Limiting indices	-13<=h<=13, -9<=k<=9, -27<=l<=27
Reflections collected / unique	12272 / 6192 [R(int) = 0.0603]
Completeness to theta = 30.00	99.7 %
Max. and min. transmission	0.9820 and 0.8505
Refinement method	Full-matrix least-squares on F^2
Data / restraints / parameters	6192 / 1 / 316
Goodness-of-fit on F^2	1.035
Final R indices [I>2σ(I)]	*R1* = 0.0705, *wR2* = 0.1501
R indices (all data)	*R1* = 0.0907, *wR2* = 0.1592
Largest diff. peak and hole	0.750 and -0.592 $e.Å^3$

Table 21 Bond lengths [Å] and angles [°] for **PM-C2Cl**

S1-O2	1.445(3)	C12-C17	1.390(5)
S1-O4	1.454(3)	C13-C14	1.379(6)
S1-O3	1.455(3)	C13-H13A	0.93
S1-C24	1.770(4)	C14-C15	1.378(5)
Cl1-C21	1.745(4)	C14-H14A	0.93
O1-C15	1.365(4)	C15-C16	.404(5)
O1-C18	1.443(5)	C16-C17	1.385(6)
C1-C6	1.403(5)	C16-H16A	0.93
C1-C2	1.405(5)	C17-H17A	0.93
C1-N1	1.414(5)	C18-C19	1.506(5)
C2-C3	1.370(6)	C18-H18A	0.97
C2-H2A	0.93	C18-H18B	0.97
C3-C4	1.388(6)	C19-H19A	0.96
C3-H3A	0.93	C19-H19B	0.96
C4-C5	1.360(6)	C19-H19C	0.96
C4-H4A	0.93	C20-N1	1.47(5)
C5-C6	1.421(5)	C20-H20A	0.96
C5-H5A	0.93	C20-H20B	0.96
C6-C7	1.411(5)	C20-H20C	0.96
C7-C8	1.348(6)	C21-C26	1.365(6)
C7-H7A	0.93	C21-C22	1.396(6)
C8-C9	1.424(5)	C22-C23	1.381(6)
C8-H8A	0.93	C22-H22A	0.93
C9-N1	1.345(5)	C23-C24	1.388(5)
C9-C10	1.459(5)	C23-H23A	0.93
C10-C11	1.341(5)	C24-C25	1.400(6)
C10-H10A	0.93	C25-C26	1.381(6)

C11-C12	1.454(6)	C25-H25A	0.93
C11-H11A	0.93	C26-H26A	0.93
C12-C13	1.389(5)	O1W-H1W1	0.9845

Table 21 (Continued)

O1W-H2W1	1.2162	O2W-H1W2	0.8918
O2W-H2W2	0.9862		
O2-S1-O4	113.1(2)	C7-C8-C9	121.5(3)
O2-S1-O3	113.01(19)	C7-C8-H8A	119.2
O4-S1-O3	112.68(18)	C9-C8-H8A	119.2
O2-S1-C24	105.87(17)	N1-C9-C8	118.2(3)
O4-S1-C24	105.46(19)	N1-C9-C10	121.1(3)
O3-S1-C24	105.84(17)	C8-C9-C10	120.7(3)
C15-O1-C18	118.8(3)	C11-C10-C9	123.7(3)
C6-C1-C2	119.5(4)	C11-C10-H10A	118.1
C6-C1-N1	119.2(3)	C9-C10-H10A	118.1
C2-C1-N1	121.3(3)	C10-C11-C12	127.3(3)
C3-C2-C1	119.5(4)	C10-C11-H11A	116.4
C3-C2-H2A	120.2	C12-C11-H11A	116.4
C1-C2-H2A	120.2	C13-C12-C17	117.6(4)
C2-C3-C4	121.1(4)	C13-C12-C11	118.6(3)
C2-C3-H3A	119.4	C17-C12-C11	123.8(3)
C4-C3-H3A	119.4	C14-C13-C12	121.4(4)
C5-C4-C3	120.9(4)	C14-C13-H13A	119.3
C5-C4-H4A	119.5	C12-C13-H13A	119.3
C3-C4-H4A	119.5	C15-C14-C13	120.2(3)
C4-C5-C6	119.4(4)	C15-C14-H14A	119.9
C4-C5-H5A	120.3	C13-C14-H14A	119.9
C6-C5-H5A	120.3	O1-C15-C14	115.8(3)
C1-C6-C7	118.5(4)	O1-C15-C16	124.1(3)
C1-C6-C5	119.6(3)	C14-C15-C16	120.1(3)

C7-C6-C5	122.0(3)	C17-C16-C15	118.3(3)
C8-C7-C6	120.6(3)	C17-C16-H16A	120.9
C8-C7-H7A	119.7	C15-C16-H16A	120.9
C6-C7-H7A	119.7	C16-C17-C12	122.4(4)

Table 21 (Continued)

C16-C17-H17A	118.8	C22-C21-Cl1	118.4(3)
C12-C17-H17A	118.8	C23-C22-C21	117.8(4)
O1-C18-C19	106.2(3)	C23-C22-H22A	121.1
O1-C18-H18A	110.5	C21-C22-H22A	121.1
C19-C18-H18A	110.5	C22-C23-C24	121.7(4)
O1-C18-H18B	110.5	C22-C23-H23A	119.2
C19-C18-H18B	110.5	C24-C23-H23A	119.2
H18A-C18-H18B	108.7	C23-C24-C25	119.1(4)
C18-C19-H19A	109.5	C23-C24-S1	120.4(3)
C18-C19-H19B	109.5	C25-C24-S1	120.5(3)
H19A-C19-H19B	109.5	C26-C25-C24	119.4(4)
C18-C19-H19C	109.5	C26-C25-H25A	120.3
H19A-C19-H19C	109.5	C24-C25-H25A	120.3
H19B-C19-H19C	109.5	C21-C26-C25	120.4(4)
N1-C20-H20A	109.5	C21-C26-H26A	119.8
N1-C20-H20B	109.5	C25-C26-H26A	119.8
H20A-C20-H20B	109.5	C9-N1-C1	121.9(3)
N1-C20-H20C	109.5	C9-N1-C20	121.8(3)
H20A-C20-H20C	109.5	C1-N1-C20	116.3(3)
H20B-C20-H20C	109.5	H1W1-O1W-H2W1	109.3
C26-C21-C22	121.6(4)	H2W2-O2W-H1W2	101.8
C26-C21-Cl1	120.0(3)		

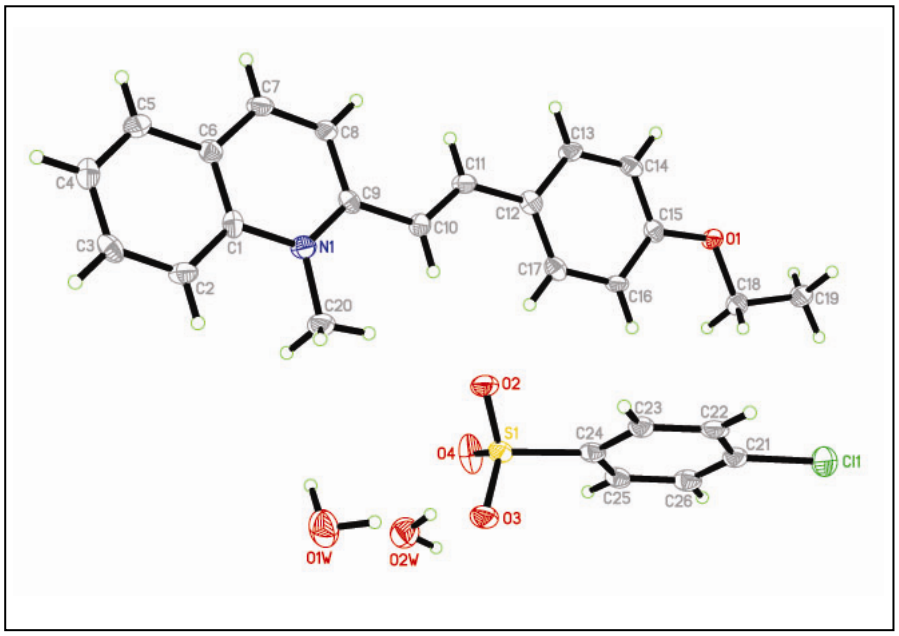

Figure 11 X-ray ORTEP diagram of the compound **PM-C2Cl.**

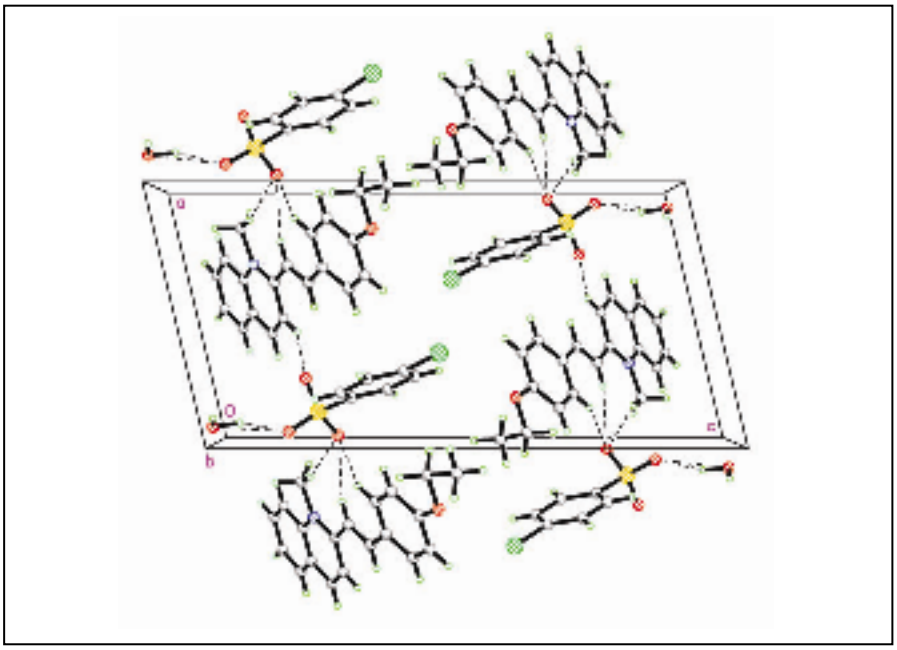

Figure 12 Packing diagram of **PM-C2Cl** viewed down the a axis with H-bonds shown as dashed lines.

3.4.8 2-[(*E*)-2-(4-Ethoxyphenyl)ethenyl]-1-methylquinolinium 4-bromobenzenesulfonate (PM-C2Br)

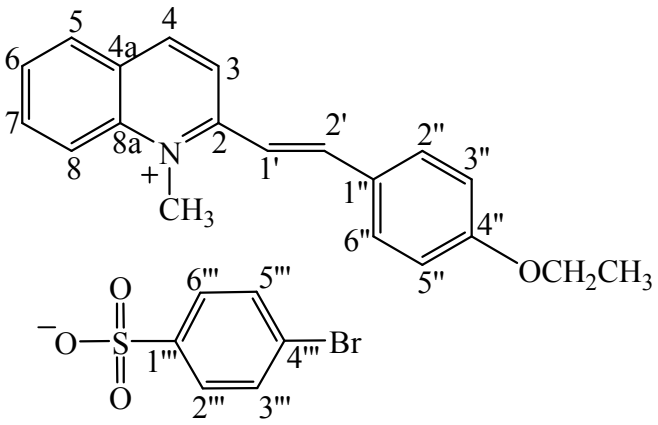

PM-C2Br

Compound **PM-C2Br** was obtained as a yellow-orange solid (72% yield), mp. 249-251 °C. The UV-Vis absorption bands (**Fig. 64**) were shown at 221.0, 255.5 and 413.9 nm. The IR spectrum (**Fig. 65**) exhibited stretching vibrations of C=C (1592 cm^{-1}), C-O (1224 cm^{-1}) and S=O in sulfonates (1169 cm^{-1}).

The ^{1}H NMR spectrum (**Fig. 66,** see **Table 22**) showed two fragments of cationic and anionic parts. The former showed characteristic of *trans*-disubstituted double bonds at δ 7.72 (1H, *d*, *J* = 15.6 Hz, H-1′) and δ 8.00 (1H, *d*, *J* = 15.6 Hz, H-2′). The *singlet* signals at δ 4.55 (3H) was assigned as *N*-CH_3. The *triplet* and *quartet* signals at δ 1.40 (3H, *J* = 6.9 Hz) and δ 4.10 (2H, *J* = 6.9 Hz) were assigned as CH_3 and CH_2 of ethoxy, respectively. Two signals of 4-substituted benzene pattern at δ 7.84 (2H, *d*, *J* = 8.7 Hz) and δ 6.98 (2H, *d*, *J* = 8.7 Hz) were assigned to H-2″, H-6″, H-3″ and H-5″, respectively. Two *doublets* of H-3 and H-4 were observed at δ 8.48 (1H, *J* = 9.0 Hz) and δ 8.89 (1H, *J* = 9.0 Hz), respectively. Resonances of aromatic protons H-5, H-6, H-7 and H-8 were also shown at δ 8.25 (*d*, *J* = 7.5 Hz), δ 7.87 (*t*, *J* = 7.5 Hz), δ 8.09 (*t*, *J* = 7.5 Hz) and δ 8.44 (*d*, *J* = 7.5 Hz), respectively. ^{1}H NMR spectrum showed signals of anionic part. Equivalent protons of

p-disubstituted aromatic appeared as two *doublets* at δ 7.60 (2H, J = 8.1 Hz, H-2‴, H-6‴) and δ 7.41 (2H, J = 8.1 Hz, H-3‴, H-5‴). The *singlet* signal of 4‴-CH□□3 was observed at δ 2.27 (3H). From these spectroscopic data **PM-C2Br** was assigned to be 2-[(*E*)-2-(4-ethoxyphenyl)ethenyl]-1-methylquinolinium 4-bromobenzenesulfonate.

Table 22 ^{1}H NMR of compound **PM-C2Br**

Position	**δ_H (ppm), *mult*, *J* (Hz)**
1-CH_3	4.55 (3H, *s*)
CH_3	1.40 (3H, 6.9 Hz)
O-CH_2	4.10 (2H, 6.9 Hz)
3	8.48 (1H, 9.0 Hz)
4	8.89 (1H, 9.0 Hz)
5	8.25 (1H, *d*, 7.5 Hz)
6	7.87 (1H, *t*, 7.5 Hz)
7	8.09 (1H, *t*, 7.5 Hz)
8	8.44 (1H, *d*, 7.5 Hz)
1′	7.72 (1H, *d*, 15.9)
2′	8.00 (1H, *d*, 15.9)
2″ 6″	7.84 (2H, *d*, 8.7)
3″ 5″	6.98 (2H, *d*, 8.7)
2‴ 6‴	7.60 (2H, *d*, 8.1)
3‴ 5‴	7.41 (2H, *d*, 8.1)

3.4.9 Bis[(*E*)-2-(3-hydroxy-4-methoxyphenyl)ethenyl]-1-methylquinolinium tetraiodidozincate(II) (PM-C3Zn)

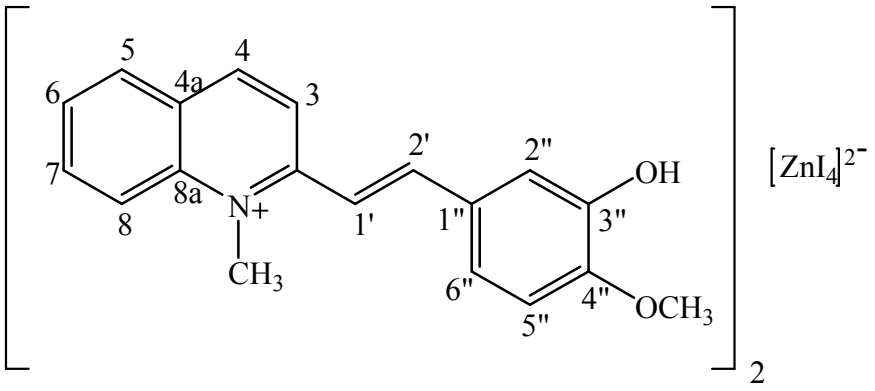

PM-C3Zn

Compound **PM-C3Zn** was obtained as a brown solid (40% yield), mp. 220-221 °C. The UV-Vis absorption bands (**Fig. 67**) were shown at 218.2, 249.4, 305.4, 403.9 and 574.8 nm. The IR spectrum (**Fig. 68**) exhibited stretching vibrations of O-H (3436 cm^{-1}), C=C (1585 cm^{-1}) and C-O (1221 cm^{-1}).

The ^{1}H NMR spectrum (**Fig. 69,** see **Table 23**) showed characteristic of *trans*-disubstituted double bonds at δ 7.70 (1H, *d*, *J* = 15.9 Hz, H-1′) and δ 8.11 (1H, *d*, *J* = 15.9 Hz, H-2′). Three *singlet* signals at δ 9.31 (3H), δ 4.57 (3H) and δ 3.92 (3H) were assigned as OH, *N*-CH_3 and *O*-CH_3, respectively. Three signals of 1,3,4-trisubstituted benzene pattern at δ 7.47 (1H, *d*, *J* = 2.1 Hz), δ 7.04 (1H, *d*, *J* = 8.4 Hz) and δ 7.41 (1H, *br d*, *J* = 8.4 Hz) were assigned to H-2″, H-5″ and H-6″, respectively. Two *doublets* of H-3 and H-4 were observed at δ 8.54 (1H, *J* = 9.0 Hz) and δ 8.97 (1H, *J* = 9.0 Hz), respectively. Resonances of aromatic protons H-5, H-6, H-7 and H-8 were also shown at δ 8.31 (*d*, *J* = 7.5 Hz), δ 7.91 (*t*, *J* = 7.5 Hz), δ 8.15 (*dt*, *J* = 1.5, 7.5 Hz) and δ 8.50 (*d*, *J* = 7.5 Hz), respectively. From these spectroscopic data **PM-C3Zn** was assigned to be Bis[(*E*)-2-(3-hydroxy-4-methoxyphenyl)ethenyl]-1-methylquinolinium tetraiodidozincate(II).

The crystal structure of **PM-C3Zn** is illustrated in **Fig. 13** and **Fig. 14** which show the packing diagram of **PM-C3Zn** and intermolecular hydrogen bondings. The crystal and experiment data are given in **Table 22**. Bond lengths and angles are shown in **Table 23.** It was found that **PM-C3Zn** crystallized out in centrosymmetric $\mathbf{P2_1/}\boldsymbol{c}$ space group

The asymmetric unit of the **PM-C3Zn** compound consists of two $C_{19}H_{18}NO_2^+$ cations, a ZnI_4^{2-} anion and a methanol solvate molecule (**Fig. 13**)**.** Each cation is nearly planar as indicated by the dihedral angle between the quinolinium planes and the benzene rings in each cation being 1.78(1) and 5.44(1)°, respectively. The H atoms attached to the alkene C atoms C10 and C11 and C29 and C30 are mutually *trans***;** torsion angles C9—C10—C11—C12 = 179.1(2)° and C28—C29—C30—C31 = -179.3(2)°. Both the hydroxyl and methoxy groups are reasonably coplanar with the benzene rings to which they are attached with torsion angles C19—O2—C15—C16 = -0.4(4)° and C38—O4—C34—C35 = 1.2(4)°. Both cations form intramolecular O—H···O hydrogen bonds between the hydroxyl and methoxy groups whch generate S(5) ring motifs (Bernstein *et al.*, 1995). The two cations are approximately parallel to one another with dihedral angles 7.55(7)° between two the quinolinium planes (C1—C9/N1 and C20—C28/N2) and 12.28(12)° between the two benzene rings (C12—C17 and C31—C36). The ZnI_4^{2-} anion shows only small distortions from a regular tetrahedron as was found previously (Glavcheva *et al*., 2004). Zn—I bond distances are in the range 2.6035(3)-2.6409(3) Å, and I—Zn—I bond angles lie in the range 106.583(11)-114.187(11)°.

In the crystal packing, the cations are linked together through O—H···O hydrogen bond and weak C—H···O interactions (**Table 26**). The cations are also linked to the ZnI_4^{2-} anions through weak C27—H27A···I4 interactions (symmetry code: -1+x, y, -1+z). The methanol molecule links with the cation by an O3—H1O3···O5 hydrogen bond (symmetry code: 1-x, -1/2+y, ½-z) and with the ZnI_4^{2-} anion by an O5—H1O5···I1 hydrogen bond (symmetry code: 1-x, 1-y, 1-z). The cations are arranged in an antiparallel manner and stacked along the *a* axis in such a way that the centroid-centroid distance between the C1—C6 (Cg1) and C12—C17 (Cg2) rings is 3.6054(15) Å (symmetry code: 1-x, 1-y, 1-z) and that between the C20—C25 (Cg3) and C31—C36 (Cg4) rings is 3.6057(15) Å (symmetry code: 1-x,

1-y, -z), indicating π—π interactions. The crystal further stabilized by C—H···π interactions (**Table 26**); Cg2 and Cg4 are the centroids of the C12—C17 and C31—C36 benzene rings, respectively.

Table 23 ^{1}H NMR of compound **PM-C3Zn**

Position	**δ_H (ppm), *mult*, *J* (Hz)**
1-CH_3	4.57 (3H, *s*)
3	8.54 (1H, *d*, 9)
4	8.97 (1H, *d*, 9)
5	8.31 (1H, *d*, 7.5)
6	7.91 (1H, *t*, 7.5)
7	8.15 (1H, *dt*, 1.5, 7.5)
8	8.50 (1H, *d*, 7.5)
1′	7.70 (1H, *d*, 15.9)
2′	8.11 (1H, *d*, 15.9)
2″	7.47 (1H, *d*, 2.1)
3″-OH	9.31 (3H, *s*)
4″-OCH_3	3.92 (3H, *s*)
5″	7.04 (1H, *d*, 8.4)
6″	7.41 (1H, *br d*, 8.4)

Table 24 Crystal data of **PM-C3Zn**.

Identification code	**PM-C3Zn**
Empirical formula	$C_{39}H_{40}I_4N_2O_5Zn$
Formula weight	1189.70
Temperature	100.0(1) K
Wavelength	0.71073 Å
Crystal system, space group	Monoclinic, $P2_1/c$
Unit cell dimensions	a = 8.6449(1) Å α = 90°
	b = 23.4312(4) Å β = 91.724(1)°
	c = 19.7763(3) Å γ = 90°
Volume	4004.08(10) $Å^3$
Z, Calculated density	4, 1.974 Mg/m^3
Absorption coefficient	3.742 mm^{-1}
F(000)	2280
Crystal size	0.43 x 0.28 x 0.13 mm
Theta range for data collection	1.35 to 36.00 °
Limiting indices	-14<=h<=14, -38<=k<=38, -32<=l<=32
Reflections collected / unique	100181 / 18959 [R(int) = 0.0327]
Completeness to theta = 36.00	99.9 %
Max. and min. transmission	0.6459 and 0.2948
Refinement method	Full-matrix least-squares on F^2
Data / restraints / parameters	18959 / 0 / 465
Goodness-of-fit on F^2	1.096
Final R indices [I>2σ(I)]	*R1* = 0.0352, *wR2* = 0.0811
R indices (all data)	*R1* = 0.0492, *wR2* = 0.0912
Largest diff. peak and hole	4.980 and -1.460 e.$Å^3$

Table 25 Bond lengths [Å] and angles [°] for **PM-C3Zn**

Zn1-I3	2.6035(3)	C11-H11A	0.93
Zn1-I2	2.6135(3)	C12-C17	1.397(3)
Zn1-I1	2.6406(3)	C12-C13	1.408(3)
Zn1-I4	2.6409(3)	C13-C14	1.383(3)
O1-C14	1.364(3)	C13-H13A	0.93
O1-H1O1	0.82	C14-C15	1.405(3)
O2-C15	1.356(3)	C15-C16	1.389(3)
O2-C19	1.426(3)	C16-C17	1.393(3)
N1-C9	1.347(3)	C16-H16A	0.93
N1-C1	1.401(3)	C17-H17A	0.93
N1-C18	1.478(3)	C18-H18A	0.96
C1-C2	1.405(3)	C18-H18B	0.96
C1-C6	1.413(3)	C18-H18C	0.96
C2-C3	1.380(3)	C19-H19A	0.96
C2-H2A	0.93	C19-H19B	0.96
C3-C4	1.399(4)	C19-H19C	0.96
C3-H3A	0.93	O3-C33	1.353(3)
C4-C5	1.366(4)	O3-H1O3	0.82
C4-H4A	0.93	O4-C34	1.351(3)
C5-C6	1.420(3)	O4-C38	1.434(3)
C5-H5A	0.93	N2-C28	1.354(3)
C6-C7	1.413(4)	N2-C20	1.403(3)
C7-C8	1.359(4)	N2-C37	1.480(3)
C7-H7A	0.93	C20-C21	1.408(3)
C8-C9	1.422(3)	C20-C25	1.415(3)
C8-H8A	0.93	C21-C22	1.375(3)
C9-C10	1.455(3)	C21-H21A	0.93
C10-C11	1.344(3)	C22-C23	1.407(4)

C10-H10A	0.93	C22-H22A	0.93
C11-C12	1.459(3)	C23-C24	1.368(4)

Table 25 (Continued)

C23-H23A	0.93	C33-C34	1.412(3)
C24-C25	1.412(3)	C34-C35	1.389(3)
C24-H24A	0.93	C35-C36	1.393(3)
C25-C26	1.404(4)	C35-H35A	0.93
C26-C27	1.370(3)	C36-H36A	0.93
C26-H26A	0.93	C37-H37A	0.96
C27-C28	1.415(3)	C37-H37B	0.96
C27-H27A	0.93	C37-H37C	0.96
C28-C29	1.450(3)	C38-H38A	0.96
C29-C30	1.351(3)	C38-H38B	0.96
C29-H29A	0.93	C38-H38C	0.96
C30-C31	1.450(3)	O5-C39	1.429(4)
C30-H30A	0.93	O5-H1O5	0.82
C31-C36	1.398(3)	C39-H39A	0.96
C31-C32	1.409(3)	C39-H39B	0.96
C32-C33	1.384(3)	C39-H39C	0.96
C32-H32A	0.93		
I3-Zn1-I2	106.804(12)	C2-C1-C6	119.8(2)
I3-Zn1-I1	111.295(11)	C3-C2-C1	119.0(2)
I2-Zn1-I1	106.985(11)	C3-C2-H2A	120.5
I3-Zn1-I4	110.977(11)	C1-C2-H2A	120.5
I2-Zn1-I4	114.187(11)	C2-C3-C4	121.9(3)
I1-Zn1-I4	106.583(11)	C2-C3-H3A	119.0
C14-O1-H1O1	109.5	C4-C3-H3A	119.0
C15-O2-C19	118.2(2)	C5-C4-C3	119.6(2)
C9-N1-C1	122.09(19)	C5-C4-H4A	120.2
C9-N1-C18	119.8(2)	C3-C4-H4A	120.2

C1-N1-C18	118.1(2)	C4-C5-C6	120.4(2)
N1-C1-C2	121.6(2)	C4-C5-H5A	119.8
N1-C1-C6	118.6(2)	C6-C5-H5A	119.8

Table 25 (Continued)

C1-C6-C7	119.3(2)	C15-C16-H16A	120.3
C1-C6-C5	119.1(2)	C17-C16-H16A	120.3
C7-C6-C5	121.5(2)	C16-C17-C12	121.1(2)
C8-C7-C6	119.9(2)	C16-C17-H17A	119.4
C8-C7-H7A	120.0	C12-C17-H17A	119.4
C6-C7-H7A	120.0	N1-C18-H18A	109.5
C7-C8-C9	120.9(2)	N1-C18-H18B	109.5
C7-C8-H8A	119.6	H18A-C18-H18B	109.5
C9-C8-H8A	119.6	N1-C18-H18C	109.5
N1-C9-C8	119.1(2)	H18A-C18-H18C	109.5
N1-C9-C10	119.9(2)	H18B-C18-H18C	109.5
C8-C9-C10	121.0(2)	O2-C19-H19A	109.5
C11-C10-C9	125.2(2)	O2-C19-H19B	109.5
C11-C10-H10A	117.4	H19A-C19-H19B	109.5
C9-C10-H10A	117.4	O2-C19-H19C	109.5
C10-C11-C12	125.0(2)	H19A-C19-H19C	109.5
C10-C11-H11A	117.5	H19B-C19-H19C	109.5
C12-C11-H11A	117.5	C33-O3-H1O3	109.5
C17-C12-C13	119.0(2)	C34-O4-C38	118.0(2)
C17-C12-C11	122.4(2)	C28-N2-C20	122.0(2)
C13-C12-C11	118.5(2)	C28-N2-C37	120.7(2)
C14-C13-C12	120.0(2)	C20-N2-C37	117.3(2)
C14-C13-H13A	120.0	N2-C20-C21	121.8(2)
C12-C13-H13A	120.0	N2-C20-C25	118.4(2)
O1-C14-C13	120.5(2)	C21-C20-C25	119.8(2)
O1-C14-C15	119.3(2)	C22-C21-C20	119.1(2)
C13-C14-C15	120.2(2)	C22-C21-H21A	120.4
O2-C15-C16	126.4(2)	C20-C21-H21A	120.4

O2-C15-C14	113.4(2)	C21-C22-C23	121.8(2)
C16-C15-C14	120.2(2)	C21-C22-H22A	119.1
C15-C16-C17	119.4(2)	C23-C22-H22A	119.1

Table 25 (Continued)

C24-C23-C22	119.2(2)	O3-C33-C32	119.5(2)
C24-C23-H23A	120.4	O3-C33-C34	121.2(2)
C22-C23-H23A	120.4	C32-C33-C34	119.3(2)
C23-C24-C25	120.9(2)	O4-C34-C35	125.3(2)
C23-C24-H24A	119.5	O4-C34-C33	114.5(2)
C25-C24-H24A	119.5	C35-C34-C33	120.2(2)
C26-C25-C24	121.5(2)	C34-C35-C36	119.9(2)
C26-C25-C20	119.5(2)	C34-C35-H35A	120.0
C24-C25-C20	119.0(2)	C36-C35-H35A	120.0
C27-C26-C25	119.8(2)	C35-C36-C31	120.8(2)
C27-C26-H26A	120.1	C35-C36-H36A	119.6
C25-C26-H26A	120.1	C31-C36-H36A	119.6
C26-C27-C28	121.0(2)	N2-C37-H37A	109.5
C26-C27-H27A	119.5	N2-C37-H37B	109.5
C28-C27-H27A	119.5	H37A-C37-H37B	109.5
N2-C28-C27	118.9(2)	N2-C37-H37C	109.5
N2-C28-C29	120.1(2)	H37A-C37-H37C	109.5
C27-C28-C29	121.0(2)	H37B-C37-H37C	109.5
C30-C29-C28	124.5(2)	O4-C38-H38A	109.5
C30-C29-H29A	117.7	O4-C38-H38B	109.5
C28-C29-H29A	117.7	H38A-C38-H38B	109.5
C29-C30-C31	124.6(2)	O4-C38-H38C	109.5
C29-C30-H30A	117.7	H38A-C38-H38C	109.5
C31-C30-H30A	117.7	H38B-C38-H38C	109.5
C36-C31-C32	118.7(2)	C39-O5-H1O5	109.5
C36-C31-C30	122.2(2)	O5-C39-H39A	109.5
C32-C31-C30	119.1(2)	O5-C39-H39B	109.5
C33-C32-C31	121.1(2)	H39A-C39-H39B	109.5

C33-C32-H32A	119.4	O5-C39-H39C	109.5
C31-C32-H32A	119.4	C1-C6-C5	119.1(2)

Table 25 (Continued)

C7-C6-C5	121.5(2)	C16-C17-C12	121.1(2)
C8-C7-C6	119.9(2)	C16-C17-H17A	119.4
C8-C7-H7A	120.0	C12-C17-H17A	119.4
C6-C7-H7A	120.0	N1-C18-H18A	109.5
C7-C8-C9	120.9(2)	N1-C18-H18B	109.5
C7-C8-H8A	119.6	H18A-C18-H18B	109.5
C9-C8-H8A	119.6	N1-C18-H18C	109.5
N1-C9-C8	119.1(2)	H18A-C18-H18C	109.5
N1-C9-C10	119.9(2)	H18B-C18-H18C	109.5
C8-C9-C10	121.0(2)	O2-C19-H19A	109.5
C11-C10-C9	125.2(2)	O2-C19-H19B	109.5
C11-C10-H10A	117.4	H19A-C19-H19B	109.5
C9-C10-H10A	117.4	O2-C19-H19C	109.5
C10-C11-C12	125.0(2)	H19A-C19-H19C	109.5
C10-C11-H11A	117.5	H19B-C19-H19C	109.5
C12-C11-H11A	117.5	C33-O3-H1O3	109.5
C17-C12-C13	119.0(2)	C34-O4-C38	118.0(2)
C17-C12-C11	122.4(2)	C28-N2-C20	122.0(2)
C13-C12-C11	118.5(2)	C28-N2-C37	120.7(2)
C14-C13-C12	120.0(2)	C20-N2-C37	117.3(2)
C14-C13-H13A	120.0	N2-C20-C21	121.8(2)
C12-C13-H13A	120.0	N2-C20-C25	118.4(2)
O1-C14-C13	120.5(2)	C21-C20-C25	119.8(2)
O1-C14-C15	119.3(2)	C22-C21-C20	119.1(2)
C13-C14-C15	120.2(2)	C22-C21-H21A	120.4
O2-C15-C16	126.4(2)	C20-C21-H21A	120.4
O2-C15-C14	113.4(2)	C21-C22-C23	121.8(2)
C16-C15-C14	120.2(2)	C21-C22-H22A	119.1

C15-C16-C17	119.4(2)	H39A-C39-H39C	109.5
C15-C16-H16A	120.3	H39B-C39-H39C	109.5
C17-C16-H16A	120.3		

Table 26 Hydrogen-bond geometry (Å, °)

D—H···*A*	D—H	H···*A*	D···*A*	D—H···*A*
O1—H1O1···O2	0.82	2.15	2.611(3)	116
O3—H1O3···O4	0.82	2.23	2.673(3)	114
O3—H1O3···O5^{i}	0.82	1.92	2.693(3)	156
O5—H1O5···I1^{ii}	0.82	2.82	3.6161(17)	163
C2—H2A···O3^{iii}	0.93	2.56	3.476(3)	167
C18—H18B··· O3^{iii}	0.96	2.60	3.355(3)	136
C27—H27A···I4^{iv}	0.93	3.02	3.899(3)	158
C19—H19B···Cg4	0.96	2.99	3.944(3)	172
C38—H38B···Cg2	0.96	2.94	3.871(3)	165

Symmetry codes: (i) –x+1, y-1/2, -z+1/2; (ii) –x+1, -y+1, -z+1;
(iii) –x+1, -y+1/2, -z+1/2; (iv) –x-1, y, z-1.

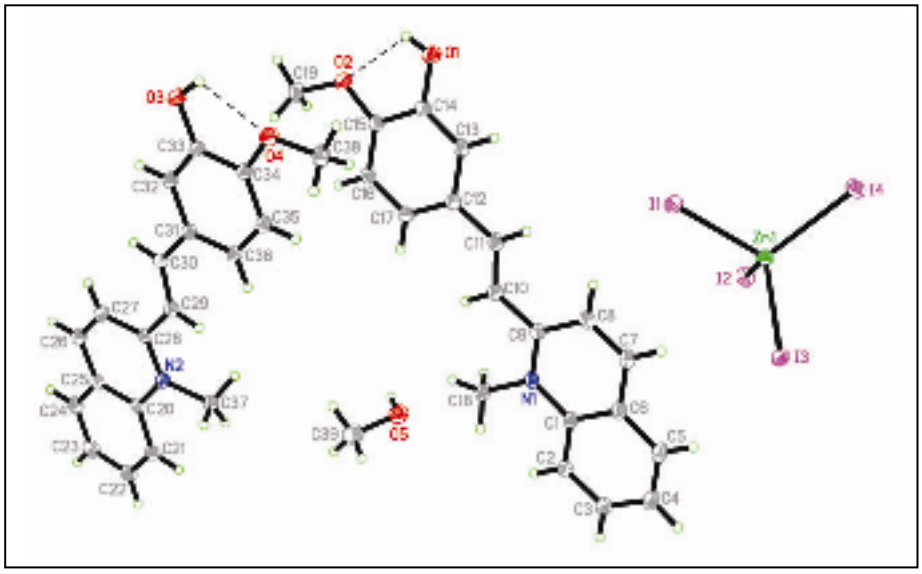

Figure 13 X-ray ORTEP diagram of the compound **PM-C3Zn.**

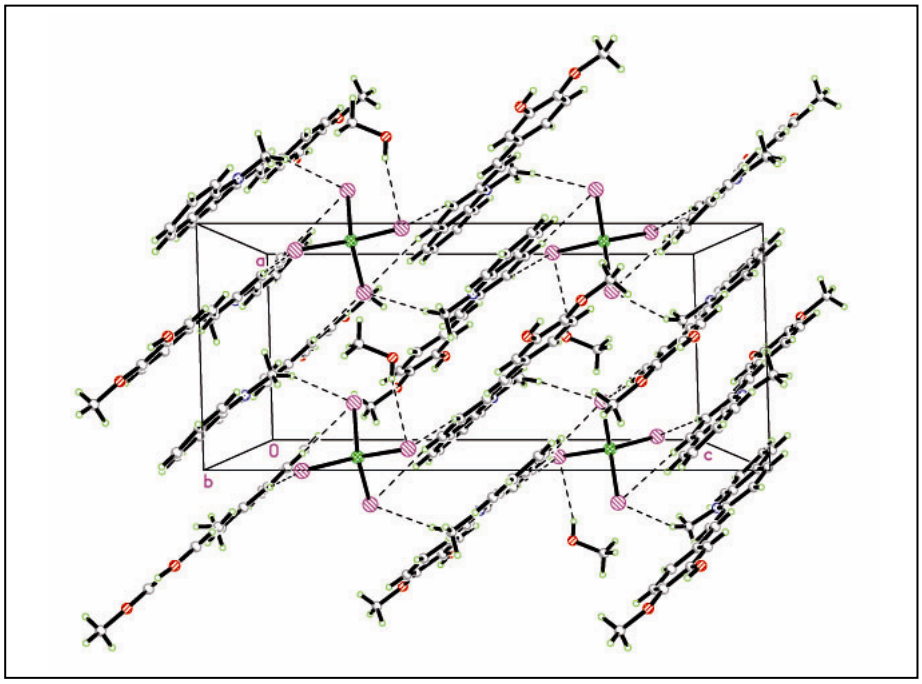

Figure 14 Packing diagram of **PM-C3Zn** viewed down the a axis with H-bonds shown as dashed lines.

3.4.10 Bis[(*E*)-2-(4-hydroxy-3-methoxyphenyl)ethenyl]-1-methylquinolinium tetraiodidozincate(II) (PM-C4Zn)

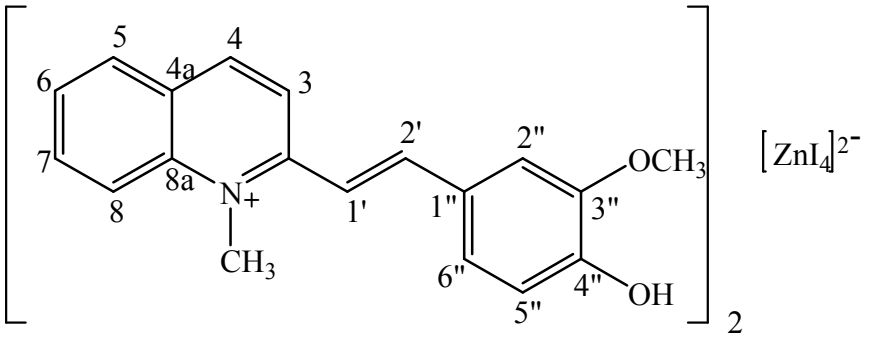

PM-C4Zn

Compound **PM-C4Zn** was obtained as a brown solid (40% yield), mp. 225-226 °C. The UV-Vis absorption bands (**Fig. 70**) were shown at 217.3, 311.6, 440.9 and 561.8 nm The IR spectrum (**Fig. 71**) exhibited stretching vibrations of O-H (3437 cm^{-1}), C=C (1579 cm^{-1}) and C-O (1221 cm^{-1}).

The ^{1}H NMR spectrum (**Fig. 72,** see **Table 27**) showed characteristic of *trans*-disubstituted double bonds at δ 7.70 (1H, *d*, *J* = 15.6 Hz, H-1′) and δ 7.92 (1H, *d*, *J* = 15.6 Hz, H-2′). Two *singlet* signals at δ 4.62 (3H) and δ 4.00 (3H) were assigned as *N*-CH_3 and *O*-CH_3, respectively. Three signals of 1,3,4-trisubstituted benzene pattern at δ 7.52 (1H, *d*, *J* = 1.8 Hz), δ 6.95 (1H, *d*, *J* = 8.1 Hz) and δ 7.39 (1H, *d d*, *J* = 1.8, 8.1 Hz) were assigned to H-2″, H-5″ and H-6″, respectively. Two *doublets* of H-3 and H-4 were observed at δ 8.48 (1H, *J* = 9.0 Hz) and δ 8.89 (1H, *J* = 9.0 Hz), respectively. Resonances of aromatic protons H-5, H-6, H-7 and H-8 were also shown at δ 8.27 (*dd*, *J* = 1.2, 7.5 Hz), δ 7.90 (*t*, *J* = 7.5 Hz), δ 8.14 (*dt*, *J* = 1.2, 7.5 Hz) and δ 8.45 (*d*, *J* = 7.5 Hz), respectively. From these spectroscopic data **PM-C4Zn** was assigned to be Bis[(*E*)-2-(4-hydroxy-3-methoxyphenyl)ethenyl]-1-methylquinolinium tetraiodidozincate(II).

Table 27 ^{1}H NMR of compound **PM-C4Zn**

Position	**δ_H (ppm), *mult*, *J* (Hz)**
1-CH_3	4.62 (3H, *s*)
3	8.48 (1H, *d*, 9.0)
4	8.89 (1H, *d*, 9.0)
5	8.27 (1H,*d d*, 1.2, 7.5)
6	7.90 (1H, *t*, 7.5)
7	8.14 (1H, *dt*, 1.2, 7.5)
8	8.45 (1H, *d*, 7.5)
1′	7.70 (1H, *d*, 15.9)
2′	7.92 (1H, *d*, 15.9)
2″	7.52 (1H, *d*, 1.8)
3″-OCH_3	4.00 (3H, *s*)
5″	6.95 (1H, *d*, 8.1)
6″	7. 39 (1H, *dd*, 1.8, 8.1)

2.5.11 Bis[(*E*)-2-(4-hydroxyphenyl)ethenyl]-1-methylquinolinium tetraiodidozincate(II) (PM-C5Zn)

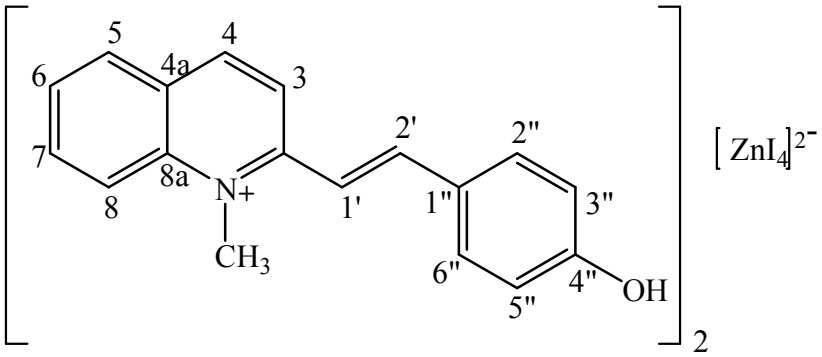

PM-C5Zn

Compound **PM-C5Zn** was obtained as a dark red solid (43% yield), mp. 234-236 °C. The UV-Vis absorption bands (**Fig. 73**) were shown at 220.9, 260.6, 312.2 and 426.8 nm. The IR spectrum (**Fig. 74**) exhibited stretching vibrations of O-H (3421 cm^{-1}) and C=C (1586 cm^{-1}).

The ^{1}H NMR spectrum (**Fig. 75,** see **Table 28**) showed characteristic of *trans*-disubstituted double bonds at δ 7.64 (1H, *d*, *J* = 15.3 Hz, H-1′) and δ 8.10 (1H, *d*, *J* = 15.3 Hz, H-2′). The *singlet* signal at δ 4.48 (3H) was assigned as *N*-CH_3. Two signals of 4-substituted benzene pattern at δ 7.78 (2H, *d*, *J* = 9.0 Hz) and δ 6.92 (2H, *d*, *J* = 9.0 Hz) were assigned to H-2″, H-6″, H-3″ and H-5″ respectively. Two *doublets* of H-3 and H-4 were observed at δ 8.46 (1H, *J* = 9.0 Hz) and δ 8.86 (1H, *J* = 9.0 Hz) respectively. Resonances of aromatic protons H-5, H-6, H-7 and H-8 were also shown at δ 8.25 (*br d*, *J* = 8.1 Hz), δ 7.87 (*t*, *J* = 8.1 Hz), δ 8.12 (*dt*, *J* = 1.5, 8.1 Hz) and δ 8.41 (*d*, *J* = 8.1 Hz) respectively. From these spectroscopic data **PM-C5Zn** was assigned to be Bis[(*E*)-2-(4-hydroxyphenyl)ethenyl]-1-methylquinolinium tetraiodidozincate(II).

Table 28 ^{1}H NMR of compound **PM-C5Zn**

Position	**δ_H (ppm), *mult*, *J* (Hz)**
1-CH_3	4.48(3H, *s*)
3	8.46 (1H, *d*, 9.0)
4	8.86 (1H, *d*, 9.0)
5	8.25 (1H, *br d*, 8.1)
6	7.87 (1H, *t*, 8.1)
7	8.12 (1H, *dt*, 1.5, 8.1)
8	8.41 (1H, *d*, 8.1)
1′	7.64 (1H, *d*, 15.3)
2′	8.10 (1H, *d*, 15.3)
2″	7.78 (2H, *d*, 9.0)
6″	
3″	6.92 (2H, *d*, 9.0)
5″	

3.4.12 Bis[(*E*)-2-(4-methoxyphenyl)ethenyl]-1-methylquinolinium tetraiodidozincate(II) (PM-C6Zn)

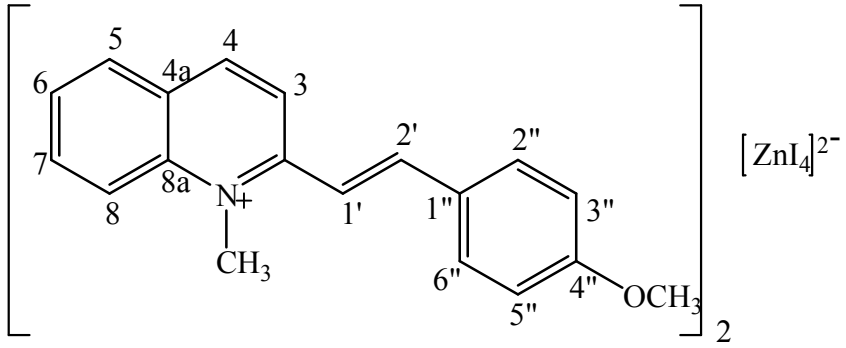

PM-C6Zn

Compound **PM-C6Zn** was obtained as a brown solid (73% yield), mp. 229-231 °C. UV-Vis absorption bands (**Fig. 76**) were shown at 204.1, 237.1, 306.4 and 442.2 nm. The IR spectrum (**Fig. 77**) exhibited stretching vibrations of C=C (1587 cm^{-1}) and C-O (1220 cm^{-1}).

The ^{1}H NMR spectrum (**Fig. 78,** see **Table 29**) showed characteristic of *trans*-disubstituted double bonds at δ 7.79 (1H, *d*, *J* = 15.9 Hz, H-1′) and δ 8.20 (1H, *d*, *J* = 15.9 Hz, H-2′). Two *singlet* signals at δ 4.57 (3H) and 3.59 (3H) were assigned as *N*-CH_3 and *O*-CH_3, respectively. Two signals of 4-substituted benzene pattern at δ 7.95 (2H, *d*, *J* = 8.7 Hz) and δ 7.08 (2H, *d*, *J* = 8.7 Hz) were assigned to H-2″, H-6″, H-3″ and H-5″, respectively. Two d*oublets* of H-3 and H-4 were observed at δ 8.53 (1H, *J* = 8.7 Hz) and δ 8.97 (1H, *J* = 8.7 Hz), respectively. Resonances of aromatic protons H-5, H-6, H-7 and H-8 were also shown at δ 8.32 (*d*, *J* = 7.2 Hz), δ 8.02-7.90 (1H, *m*), δ 8.25-8.14 (1H, *m*) and δ 8.51 (1H, *d*, *J* = 7.2 Hz), respectively. From these spectroscopic data **PM-C6Zn** was assigned to be Bis[(*E*)-2-(4-methoxyphenyl)ethenyl]-1-methylquinolinium tetraiodidozincate(II).

Table 29 ^{1}H NMR of compound **PM-C6Zn**

Position	**δ_H (ppm), *mult*, *J* (Hz)**
1-CH_3	4.57 (3H, *s*)
3	8.53 (1H, *d*, 8.7)
4	8.97 (1H, *d*, 8.7)
5	8.32 (1H, *d*, 7.2)
6	8.02-7.90 (1H, *m*)
7	8.25-8.14 (1H, *m*)
8	8.51 (1H, *d*, 7.2)
1′	7.79 (1H, *d*, 15.9)
2′	8.20 (1H, *d*, 15.9)
2″ 6″	7.95 (1H, *d*, 8.7)
3″ 5″	7.08 (1H, *d*, 8.7)
4″-OCH_3	3.59 (3H, *s*)

Table 30 UV-Vis absorption spectra of compounds **PM-S1**, **PM-S2**, **PM-C1**, **PM-C2, PM-C3**, **PM-C4, PM-C5** and **PM-C6**

Compounds	λ_{max} (nm)			
PM-S1	219.7	255.3		
PM-S2	234.5	316.7		
PM-C1	218.6	250.6	389.7	
PM-C2	217.5	252.8	314.1	416.2
PM-C3	216.1	306.2	431.3	
PM-C4	215.3	308.9	440.1	576.5
PM-C5	218.3	258.9	425.1	
PM-C6	217.3	407.6		

The λ_{max} (nm) of compounds **PM-S1**, **PM-S2**, **PM-C1**, **PM-C2, PM-C3**, **PM-C4, PM-C5** and **PM-C6** are listed in **Table 30** for comparision. It can be seen that when π-conjugation system was extended (**PM-S1** to **PM-C1** and **PM-S2** to **PM-C2** – **PM-C6**) the position of λ_{max} were shifted to the longer wavelength position (red-shift). In addition, the wavelength of the molecule which has stronger electron donor and electron acceptor (**PM-C4** > **PM-C3** > **PM-C5** > **PM-C2** > **PM-C6** > **PM-C1**) also tend to have a red-shift too which correspond to the polarizability of the compounds.

CHAPTER 4
CONCLUSION

Eight new ionic-organic compounds and four organic-inorganic compounds consist of four pyridine and eight quinoline derivatives were successfully synthesized. Their structures were elucidated by spectroscopic techniques. Four structures of these compounds namely:

4-[(*E*)-2-(2-thienyl)ethenyl]-1-methylpyridinium 4-methylbenzenesulfonate **(PM-C1Me),**

4-[(*E*)-2-(2-thienyl)ethenyl]-1-methylpyridinium 4-chlorobenzenesulfonate **(PM-C1Cl),**

2-[(*E*)-2-(4-ethoxyphenyl)ethenyl]-1-methylquinolinium 4-cholrobenzenesulfonate **(PM-C2Cl)** and

Bis[(*E*)-2-(3-hydroxy-4-methoxyphenyl)ethenyl]-1-methylquinolinium tetraiodidozincate(II) **(PM-C3Zn)** were also determined by the single crystal X-ray crystallography. It was found that **PM-C1Me**, **PM-C1Cl** and **PM-C3Zn** were crystallized out in centrosymmetric space group $\bar{P}\mathbf{1}$ (for **PM-C1Me**) and $P2_1/c$ (for **PM-C1Cl** and **PM-C3Zn**), thus they do not exhibit the second-order nonlinear optic properties. On the other hand, **PM-C2Cl** was crystallized out in non-centrosymmetric space group, $P2_1$ meaning that this compound showed NLO properties.

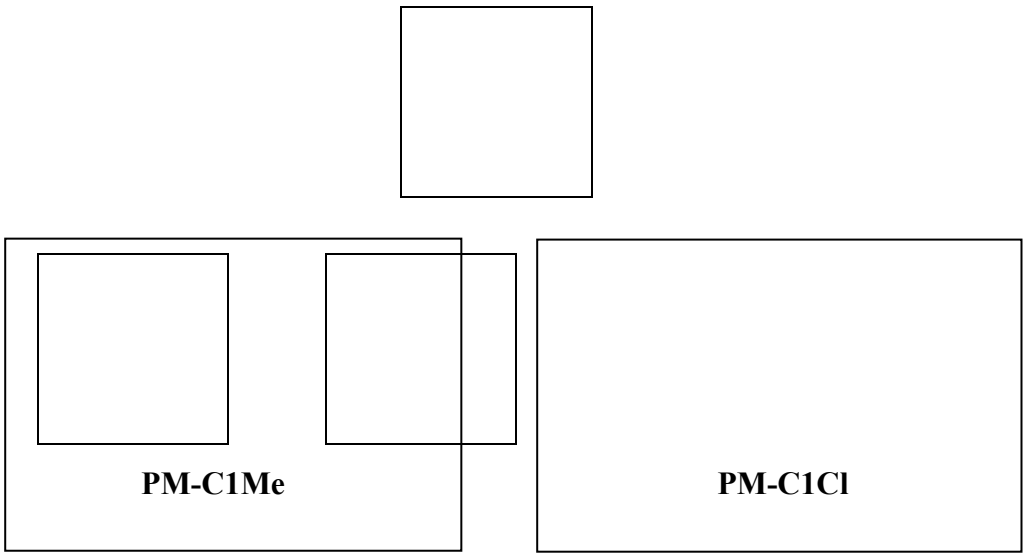
PM-C1Me
PM-C1Cl

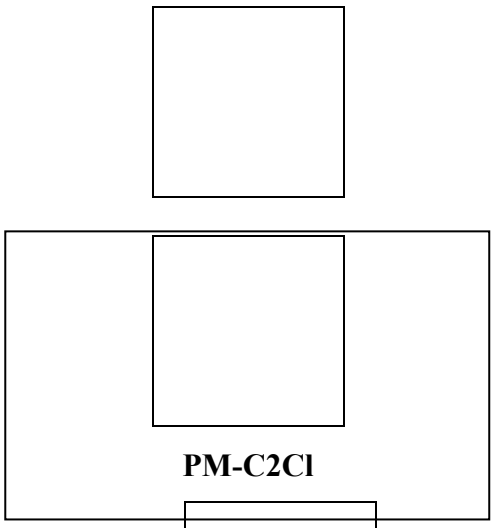
PM-C2Cl

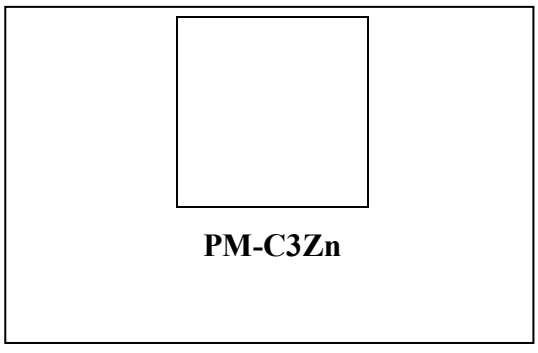
PM-C3Zn

REFERENCES

Anwar, A.; Komatsu, K.; Okada, S.; Oikawa, H.; Matsuda, H.; Nakanishi, H. 1999. "Synthesis, crystal structures, and second-order nonlinear optical properties of new colorless 4-carbamoylpyridinium benzenesulfonate salts", *Pro. SPIE.,* **3796**, 219-228.

Anwar; Duan, X-M.; Komatsu, K.; Okada, S.; Matsuda, H.; Oikawa, H.; Nakanishi, H. 1997. "Second-order hyperpolarizability of pyridinium cations", *Chem. Lett.,* **3**, 247-248.

Anwar; Duan, X-M.; Komatsu, K.; Okada, S.; Oikawa, H.; Matsuda, H.; Nakanishi, H. 1999. "Synthesis of substituted pyridinium-benzenesulfonates crystals for second-harmonic generation", *Nonlinear Optics*, **22**, 251-254.

Anwar; Duan, X-M.; Okada, S.; Matsuda, H.; Oikawa, H.; Nakanishi, H. 1998. "First hyperpolarizability of benzoate anions and esters"**,** *J. Chem. Soc., Perkin Trans.,* 2, **11**, 2451-2457.

Anwar; Kosuge, H.; Okada, S.; Oikawa, H.; Nakanishi, H. 2001. "4-(Dimethyl-amino)-1-ethylpyridinium iodide: a new colorless organic ionic crystal for second-order nonlinear optics", *Jpn. J. Appl. Phys*., **40**, 4213-4216.

Anwar; Okada, S.; Oikawa, H.; Nakanishi, H. 2000. "Preparation and Crystal Structures of New Colorless 4-Amino-1-methylpyridinium Benzenesulfonate Salts for Second-Order Nonlinear Optics", *Chem. Mater.*, **12**, 1162-1170.

Bass, M.; Franken, P. A.; Ward, J. F.; Weinreich, G. 1962. "Optical rectification", *Phys. Rev. Lett*., **9**, 446-448.

Bernstein, J., Davis, R. E., Shimoni, L., Chamg, N-L. 1995. "Patterns in hydrogen bonding: functionality and graph set analysis in crystals", *Angew. Chem. Int. Ed. Engl.*, **34**, 1555-1573.

Bourgogne, C.; Masson, P.; Nicoud, J-F.; Brasselet, S.; Zyss, J. 2001. "Investigation of new push-pull pyridine-1-oxide derivatives as 1D NLO chromophores with vanishing dipole moment", *Synthetic Metals*, **124**, 213-216.

Boomadevi, S.; Mittal, H.P.; Dhansekaran, R. 2004. "Synthesis, crystal growth and characterization of 3-methyl 4-nitropyridine 1-oxide (POM) single crystals", *J. Cryst. Growth*, **261**, 55-62.

Bruker 2005. *APEX*2, *SAINT* and *SADABS*. Bruker AXS Inc., Madison, Wisconsin, USA.

Chantrapromma, S.; Jindawong, B.; Fun, H-K.; Patil, P.S.; Karalai, C. 2007. "4-(4′-Hydroxy-3′-methoxystyryl)-1-methylpyridini 4-chlorobenzene-sulfonate", *Acta Cryst.*, **E61**, o2096-o2098.

Chantrapromma, S.; Jindawong, B.; Fun, H-K.; Anjum, S.; Karalai, C. 2005. " Synthesis, Characterization and Crystal Structure of 2-[(E)-2-(4-Hydroxy-3-methoxyphenyl)ethenyl]-1-methylquinolinium 4-chlorobenzenesulfonate", *Anal. Science.,* **23**, x27-x28.

Chemla, D. S.; Zyss, J. 1987. "Nonlinear Optical Properties of Organic Molecules and Crystals", Vol. 2, Academic press, Orlando, 275 pp.

Chou, S-S. P.; Sun, D-J.; Huang, J-Y.; Yang, P-K.; Lin, H-C. 1996. "Synthesis of sulfone-substituted thiophene chromophores for second-order nonlinear optics", *Tet. Lett.*, **37**, 7279-7282.

Cox, S. D.; Gier, T. E.; Stucky, G. D.; Bierlein, J. D. 1988. "Inclusion tuning of nonlinear optical materials: switching the SHG of p-nitroaniline and 2-methyl-*p*-nitroaniline with molecular sieve hosts", *J. Am. Chem. Soc*., **110**, 2986-2987.

Crasta, V.; Ravindrachary, V.; Bhajantri, R. F.; Gonsalves, R. 2004. "Growth and characterization of an organic NLO crystal: 1-(4-methylphenyl)-3-(4-methoxyphenyl)-2-propen-1-one", *J. Cryst. Growth*, **267**, 129-133.

Crasta, V.; Ravindrachary, V.; Lakshmi, S.; Pramod, S. N.; Shridar, M. A.; Prasad, J. S. 2005. "Growth, Characterization and Crystal structure analysis of 1-(4-chlorophenyl)-3-(4-chlorophenyl)-2-propen-1-one", *J. Cryst. Growth*, **275**, e329-e335.

Desiraju, G. R. 1995. "Supramolecular synthons in crystal engineering-a new organic synthesis", *Angew. Chem. Int. Ed. Engl*., **34**, 2311-2327.

Duan, X.-M.; Konami, H.; Okada, S.; Oikawa, H.; Matsuda, H.; Nakanishi, H. 2000. "Influence of counter anion on geometries, electronic structures and nonlinear optical properties of dimethylaminostilbazolium cation: an investigation by semiempirical calculation", *Journal of Molecular Structure*, **531**, 65-77.

Dulcic, A.; Sauteret, C. 1978. "The regularities observed in the second order hyperpolarizabilities of variously disubstituted benzenes", *J. Chem. Phys.*, **69**, 3453-3457.

Etter, M. C.; Frankenbach, G. M. 1989. "Hydrogen-bond directed cocrystallization as a tool for designing acentric organic solids", *Chemistry of materials*, **1**, 10-12.

Franken, P. A.; Hill, A. E.; Peters, C. W.; Weinrich, G. 1961. "Generation of optical harmonics", *Phys. Rev. Lett*. **7**, 118-119.

Glavcheva, Z.; Umezawa, H.; Okada, S., Nakanishi, H. 2004. "New pyridinium-metal iodide complexes toward nonlinear optical materials", *Materials Letters*, **58**, 2466-2471.

Huang, K-S.; Britton, D.; Etter, M. C.; Byrn, S. R. 1997. "A novel class of phenol-pyridine co-crystals for second harmonic generation" *J. Matter. Chem*., **7**, 713-720.

Jones, A. M.; Coleman, J. J. 1997. "Integrated optoelectronic devices by selective-area epitaxy", *Pro. SPIE.,The international Society for Optical Engineering*, **2918**, 146-154.

Lakshmanaperumal, C. K.; Arulchakkaravarthi, A.; Balamurugan, N.; Santhanaraghavan, P.; Ramasamy, P. 2004. "Synthesis, Crystal growth and Characterization of novel NLO material: 4-hydroxy benzaldehyde-*N*-methyl-4-stilbazolium tosylate", *J. Cryst. Growth,* **265**, 260-265.

Lakshmanaperumal, C. K.; Arulchakkaravarthi, A.; Rajesh, N. P.; Raghavan, P. S.; Huang, Y. C.; Ichimura, M.; Ramasamy, P. 2002. "Synthesis, Crystal growth and FTIR, NMR, SHG studies of 4-methoxy benzaldehyde-*N*-methyl-4-stilbazolium tosylate (MBST)", *J. Cryst. Growth,* **240**, 212-217.

Levine, B. F. 1975. "Conjugated electron contributions to the second order hyperpolarizability of substituted benzene molecules", *J. Chem. Phys*., **63**, 115-117.

Marder, S. R.; Beratan, D. N.; Cheng, L. T. 1991. “Approaches for optimizing the first electronic hyperpolarizability of conjugated organic molecules”, *Science(Washington, DC, United States)*, **252**, 103-106.

Marder, S. R.; Perry, J. W. 1993. “Molecular materials for second-order nonlinear optical applications”, *Adv. Mater.,* **5**, 804-815.

Marder, S. R.; Perry, J. W.; Schaefer, W. P. 1989. “Synthesis of organic salts with large second-order optical nonlinearities”, *Science*, **245**, 626-628.

Mitzi, D.B.; Chondroudis, K.; Kagan, C.R. 2001. “Organic-inorganic electronics”, *Org. Electron*., **45**, 29-45.

Nie, W. 1993. “Optical nonlinearity: phenomena, applications, and materials”, *Adv. Mater.*, **5**, 520-545.

Nogi, K.; Anwar; Tsuji, K.; Duan, X-M. 2000. “Preparation of polyene analogues of stilbazolium”, *Nonlinear Optics*, **24**, 35-40.

Okada, S.; Matsuda, H.; Nakanishi, H.; Kato, M. 1990. “Preparation and nonlinear optical property of polydiacetylenes from dialkyltetraacetylene compound”, *Molecular Crystals and Liquid Crystals*, **189**, 57-63.

Oudar, J. L.; Chemla, D. S. 1977. “Hyperpolarizabilities of the nitroanilines and their relations to the excited state dipole moment”, *J. Chem. Phys.,* **66**, 2664-2668.

Oudar, J. L.; Le Person, H. 1975. “Second-order polarizabilities of some aromatic molecules”, *Opt. Commun.*, **15**, 258-262.

Sheldrick, G. M. 2008. “A short history of SHELX”, *Acta Cryst*., **A64**, 112-122.

Terhune, R.; Maker, P.; Savage, C. 1963. “Observation of saturation effects in optical harmonic generation”, *Phys. Rev. Lett.* **2**, 54-55.

Umezawa, H.; Tsuji, K.; Anwar; Duan, X-M.; Okada, S.; Oikawa, H.; Matsuda, H. 2000. “Synthesis of stilbazolium derivatives having 2-(6-dimethylamino)-naphthyl group for nonlinear optics”, *Nonlinear Optics*, **24**, 73-78.

Williams, D. J. 1984. “Organic polymeric and Non-polymeric Materials with large optical nonlinearities”, *Angew. Chem. Int. Ed. Engl*., **23**, 690-703.

Zelichenok, A.; Burtman, V.; Zenou, N.; Yitzchaik, S.; Bella, S. D.; Meshulam. G.; Kotler, Z. 1999. “Quinolinium-derived acentric crystals for second-order NLO applications with transparency in the blue”, *J. Phys. Chem. B*, **103**, 8702-8705.

Zyss, J.; Nicoud, J. F.; Coquillay, M. 1984. “Chirality and hydrogen bonding in molecular crystals for phase-matched second-harmonic generation: *N*-(4-nitrophenyl)-(L)-prolinol (NPP)”, *J. Chem. Phys.*, **81**, 4160-4167.